



# A 19 to 17 Ma amagmatic extension event at the Mid-Atlantic Ridge: Ultramafic mylonites from the Vema Lithospheric Section

**Anna Cipriani**

*Lamont-Doherty Earth Observatory of Columbia University, Palisades, New York 10964, USA*  
(anka@ldeo.columbia.edu)

**Enrico Bonatti**

*Lamont-Doherty Earth Observatory of Columbia University, Palisades, New York 10964, USA*

*Dipartimento di Scienze della Terra, Università "La Sapienza," P.le Aldo Moro 5, I-00187 Rome, Italy*

*Istituto di Scienze Marine, Geologia Marina, CNR, Via Gobetti 101, I-40129 Bologna, Italy*

**Monique Seyler**

*UFR Sciences de la Terre, UMR8157, CNRS, Université Lille 1, F-59655 Villeneuve d'Acq CEDEX, France*

**Hannes K. Brueckner**

*School of Earth and Environmental Sciences, Queens College, and the Graduate Center of the City University of New York, New York, New York 11367, USA*

*Lamont-Doherty Earth Observatory of Columbia University, Palisades, New York 10964, USA*

**Daniele Brunelli**

*Dipartimento di Scienze della Terra, Università degli Studi di Modena e Reggio Emilia, I-41100 Modena, Italy*

*Istituto di Scienze Marine, Geologia Marina, CNR, Via Gobetti 101, I-40129 Bologna, Italy*

**Luigi Dallai**

*Istituto di Geoscienze e Georisorse, CNR, Via Moruzzi 1, I-56124 Pisa, Italy*

**Sidney R. Hemming**

*Lamont-Doherty Earth Observatory of Columbia University, Palisades, New York 10964, USA*

**Marco Ligi**

*Istituto di Scienze Marine, Geologia Marina, CNR, Via Gobetti 101, I-40129 Bologna, Italy*

**Luisa Ottolini**

*Istituto di Geoscienze e Georisorse, CNR, Via Ferrata 1, I-27100, Pavia, Italy*

**Brent D. Turrin**

*Lamont-Doherty Earth Observatory of Columbia University, Palisades, New York 10964, USA*

*Department of Earth and Planetary Sciences, Rutgers University, Wright-Rieman Labs, Piscataway, New Jersey 08854, USA*

[1] A >300 km long lithospheric section (Vema Lithospheric Section or VLS) is exposed south of the Vema transform at 11°N in the Atlantic. It is oriented along a seafloor spreading flow line and represents ~26 Ma of accretion at a single 80 km long segment (EMAR) of the Mid-Atlantic Ridge. The basal part of the VLS exposes a mantle unit made mostly of relatively undeformed coarse-grained/porphyroclastic peridotites that were sampled at close intervals. Strongly deformed mylonitic peridotites were found at 14 contiguous sites within a ~80 km stretch (~4.7 Ma interval); they are dominant in a time interval of 1.4 Ma, from crustal ages of 16.8 to 18.2 Ma (mylonitic stretch). Some of the mylonites are “dry,” showing anhydrous high-T deformation, but most contain amphibole. The mylonitic peridotites tend to be less depleted than the porphyroclastic peridotites on the basis of mineral major and trace elements composition, suggesting that the mylonites parent was a subridge mantle that underwent a relatively low degree of melting. The Sr, Nd, and O isotopic composition of the amphiboles is MORB-like and suggests either that seawater did not contribute to their isotopic signature or that their isotopic ratios re-equilibrated during fluid circulation in the upper mantle. Four  $^{40}\text{Ar}/^{39}\text{Ar}$  ages, on three amphiboles separated from the peridotites, are close to crustal ages predicted from magnetic anomalies, confirming that the amphiboles formed close to ridge axis. We propose that crustal accretion at the EMAR segment has been mostly symmetrical for the 26 Ma of its recorded history, except for the ~1.4 Ma interval of prevalent ultramafic mylonites (mylonitic stretch) that may record a period of quasi-amagmatic asymmetric accretion of oceanic lithosphere close to the ridge–Vema transform intersection, possibly with development of detachment faults. This interval may correspond to a thermal minimum of the subridge upwelling mantle, marking the transition from a period of decreasing to one of increasing mantle melting below the EMAR segment.

**Components:** 38,169 words, 13 figures, 21 tables.

**Keywords:** peridotite; mylonite; mantle melting; amagmatic event; mid-ocean ridge; petrology.

**Index Terms:** 1025 Geochemistry: Composition of the mantle; 3035 Marine Geology and Geophysics: Midocean ridge processes; 1038 Geochemistry: Mantle processes (3621).

**Received** 6 April 2009; **Revised** 22 July 2009; **Accepted** 29 July 2009; **Published** 23 October 2009.

Cipriani, A., E. Bonatti, M. Seyler, H. K. Brueckner, D. Brunelli, L. Dallai, S. R. Hemming, M. Ligi, L. Ottolini, and B. D. Turrin (2009), A 19 to 17 Ma amagmatic extension event at the Mid-Atlantic Ridge: Ultramafic mylonites from the Vema Lithospheric Section, *Geochim. Geophys. Geosyst.*, 10, Q10011, doi:10.1029/2009GC002534.

## 1. Introduction

[2] Mantle peridotites crop out at or near the ocean floor along portions of slow spreading mid-ocean ridges with low thermal regimes, and close to their intersection with major transform offsets [Bonatti, 1968; Dick et al., 1981; Cannat, 1993]. Moreover, the creation of oceanic crust is not a steady state process but proceeds in alternating cycles of magmatic and nearly amagmatic extension, particularly at slow spreading ridges [Kappel and Ryan, 1986; Pockalny et al., 1988; Cannat, 1993]. One asymmetric mechanism of accretion, that may lead to mantle denudation, involves low-angle detachment faults, observed at the inside corner of several Atlantic ridge-transform intersections (RTI) (i.e., Kane, 15°20'N, Atlantis) possibly because of a melt deficit near the tip of ridge segments [Tucholke and Lin, 1994; Cannat et al., 1995;

Tucholke et al., 1997, 1998; Blackman et al., 1998; Escartín et al., 2008; Smith et al., 2006, 2008]. However, some recent observations from gabbroic rocks drilled at oceanic core complexes, suggest that exhumation along detachment faults is not necessarily associated with periods of amagmatic extension [Dick et al., 2000; Kelemen et al., 2004, 2007; Ildefonse et al., 2007; Tucholke et al., 2008]. Mylonitic deformation and slip related corrugations or mullions may affect the upper mantle and lower crustal rock units at shear zones near the fault plane during quasi-amagmatic emplacement of the lithosphere at ridge axis, when tectonic extension becomes dominant [Honnerez et al., 1984; Cannat and Seyler, 1995; Jaroslow et al., 1996; Escartín et al., 2003, 2008; Smith et al., 2006, 2008]. In contrast, some Atlantic RTIs, for instance the Vema at 11°N, show symmetrical accretion, with no evidence of detachment faulting

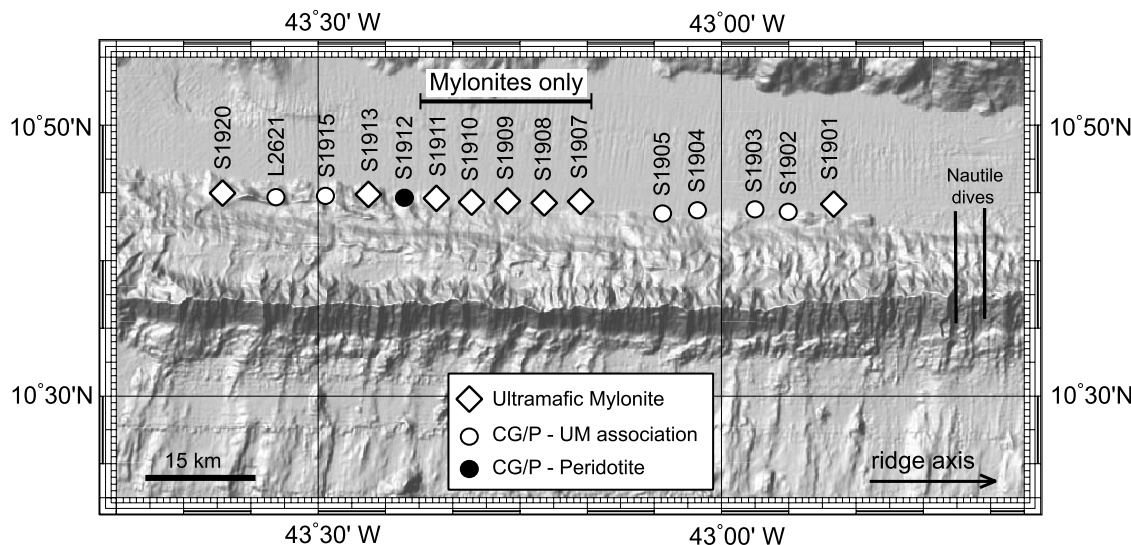


**Figure 1.** Location of the mylonitic stretch along the VLS and distribution of the peridotitic lithologies for each dredged site. UM, ultramafic mylonite; CG/P, coarse-grained/porphyroclastic.

[Bonatti et al., 2003, 2005; Lissenberg et al., 2009].

[3] Several km-thick shear zones with strongly deformed mantle rocks have been observed also in ophiolitic and massif peridotites [Drury et al., 1991; Vissers et al., 1991; Hoogerduijn Strating et al., 1993]. For instance, Nicolas et al. [1999] observed strongly deformed amphibole-bearing ultramafic units associated with thin basaltic crust in the Albanian Mirdita Ophiolites, where they alternate with less deformed ultramafic units overlain by thicker crust.

[4] We present here the results of a study of ultramafic mylonites found along the Vema Lithospheric Section (VLS) (Figure 1), a flexured and uplifted lithospheric block that exposes crustal and upper mantle units generated at a single 80 km long segment of Mid-Atlantic Ridge (EMAR segment) from ~26 Ma to present [Bonatti et al., 2003, 2005; Cipriani et al., 2004, 2009; Brunelli et al., 2006]. Crustal ages along the VLS cited in this paper are based on Africa-South America Euler vectors of Cande et al. [1988] and the geomagnetic time scale of Cande and Kent [1995]. The geochemistry of the mylonites, together with crustal thickness reconstructions from shipboard and satellite gravity data, suggest that they formed during a ~4.7 Ma long interval (from 14.9 to 19.6 Ma) of probably prevalent amagmatic extension at the ridge axis. This paper will show that, although accretion near the eastern ridge–Vema transform intersection (RTI) has been nearly symmetrical for most of the 26 Ma history recorded along

the VLS, it became quasi-amagmatic and possibly asymmetric during a ~1.4 Ma time interval.

## 2. Ultramafic Mylonites at the Vema Lithospheric Section

[5] The mantle-ultramafic basal unit exposed for ~300 km along the VSL is made of variably deformed granular to porphyroclastic peridotites that have been sampled at 48 closely spaced sites (horizontal spacing average of ~8 km) during a number of cruises. Petrological and geochemical studies of these peridotites demonstrated a steady increase in the degree of melting of the subridge mantle from ~18.5 to 2 Ma, preceded by an interval from 26 to 18.5 Ma of decreasing extent of melting [Bonatti et al., 2003; Brunelli et al., 2006; Cipriani et al., 2009].

[6] In contrast, strongly deformed ultramafic mylonites are the exclusive type of ultramafic sampled at five adjacent sites (Figure 1), representing a time interval of about 1.4 Ma (from 16.8 to 18.2 Ma). They are also present at nine other sites, between dredge sites S1901 and S1920, together with nondeformed ultramafics, for a total length of ~80 km. Ultramafic mylonites were dredged at a total of 14 sites along the VLS (Table 1 and Figure 1). Other lithologies sampled at these sites are basalts, dolerites, gabbros and limestones from the overlying crustal layers. Dunites were sampled at few sites, overall representing a rare lithology (<1%).

[7] Two types of ultramafic mylonites are exposed along the VLS: (1) “Dry” mylonites, with ol +

**Table 1.** Starting and Ending Latitude and Longitude, Bathymetric Depth, and Rock Recovery for the Dredge Sites Used in This Study

Dredge	Recovered Rocks		Start Latitude	End Latitude	Start Longitude	End Longitude	Depth Interval (m)
S1901	mylonite peridotite 98%, dolerite 2%	<i>R/V A.N. Strakhov, Cruise S19</i>	10°42'.20	10°40'.68	42°51'.80W	42°51'.30W	4700–3950
S1902	myl/porph peridotite 80%, dunite 1%, gabbro 18%, dolerite 1%		10°42'.30	10°40'.30	42°55'.10W	42°55'.10W	4800–3700
S1903	myl/porph peridotite 90%, dunite 1%, gabbro 10%, breccia 9%		10°42'.40	10°41'.30	42°57'.50W	42°57'.20W	4950–4260
S1904	myl/porph peridotite 34%, dunite 1%, gabbro 60% breccia 5%		10°42'.60	10°41'.50	43°02'.00W	43°01'.70W	4900–4500
S1905	gabbro 50%, myl/porph peridotite 45% basalt/dolerite 5%		10°43'.10	10°42'.64	43°04'.80W	43°04'.70W	5050–4750
S1907	mylonite peridotite 60%, gabbro 30%, breccia and limestone 10%		10°43'.40	10°41'.83	43°09'.10W	43°08'.69W	5100–4280
S1908	mylonite peridotite 90%, dolerite 10%		10°43'.40	10°42'.50	43°12'.00W	43°11'.70W	5100–4650
S1909	mylonite peridotite 100%		10°43'.30	10°41'.80	43°15'.50W	43°15'.60W	4900–4200
S1910	mylonite peridotite 85%, chromite 5%, breccia 10%		10°43'.90	10°42'.20	43°18'.30W	43°18'.20W	5000–4500
S1911	mylonite peridotite 100%		10°42'.40	10°42'.00	43°21'.10W	43°21'.40W	4470–3700
S1913	myl/porph peridotite 80% and limestone 20%		10°42'.50	10°42'.30	43°26'.50W	43°27'.30W	4370–4100
S1915	myl/porph peridotite 90%, breccia and limestone 10%		10°43'.10	10°42'.80	43°30'.60W	43°30'.60W	4470–4200
S1920	dDolerite and basalt 80%, breccia 13%, mylonite peridotite 5%, gabbro 2%		10°45'.40	10°44'.70	43°34'.60W	43°35'.10W	5000–4550
L2621	myl/porph peridotite 15%, gabbro 70%, dolerite 15%	<i>R/V Logachev, Cruise L26</i>	10°45',05	10°44',30	43°32',60W	43°33',20W	5112–4515
S2201	porphyroclastic peridotite 50%, basalt/dolerite 32%, gabbro 6%, breccia 6%, sedimentary rock 6%	<i>R/V A.N. Strakhov, Cruise S22</i>	10°43,50	10°43,10	41°03,20W	41°04,40W	4700–4300

opx + cpx + sp. ( $\pm$ plg) as the main constituents (Figure 2a), and (2) “Wet” mylonites, where amphibole is an important constituent (Figure 2b), implying that deformation and dynamic recrystallization occurred in the presence of circulating fluids.

[8] Amph-mylonites are the only type of ultramafics recovered at site S1901 in 14.9 Ma old crust and from sites S1907 to S1911 (a  $\sim$ 22 km long stretch, corresponding to 1.4 Ma time interval). Four contiguous dredge sites released amph-free ultramafic proto-mylonites, with the exception of site S1915, where a few samples of amph-bearing ultramafic mylonites were collected together with prevailing dry mylonites. This last stretch, 15 km long, extends from 18.7 to 19.6 Ma, corresponding to a time interval of  $<1$  Ma.

[9] Peridotite sample S2201-01 from dredge S2201 located in 1.31 Ma old crust along the VLS [Cipriani et al., 2009] was also selected for this study because of the presence of a late stage crosscutting amphibole vein. We compare the Sr, Nd and Oxygen isotopic composition of the amphibole vein with the amphiboles in the wet mylonites. We note that the major element chemistry of the residual mineral phases of sample S2201-01 is reported by Cipriani et al. [2009].

### 3. Methods

[10] About 60 ultramafic mylonite samples were selected for this study. Standard petrographic observations on rock thin sections, including textural analysis, were carried out by optical micro-

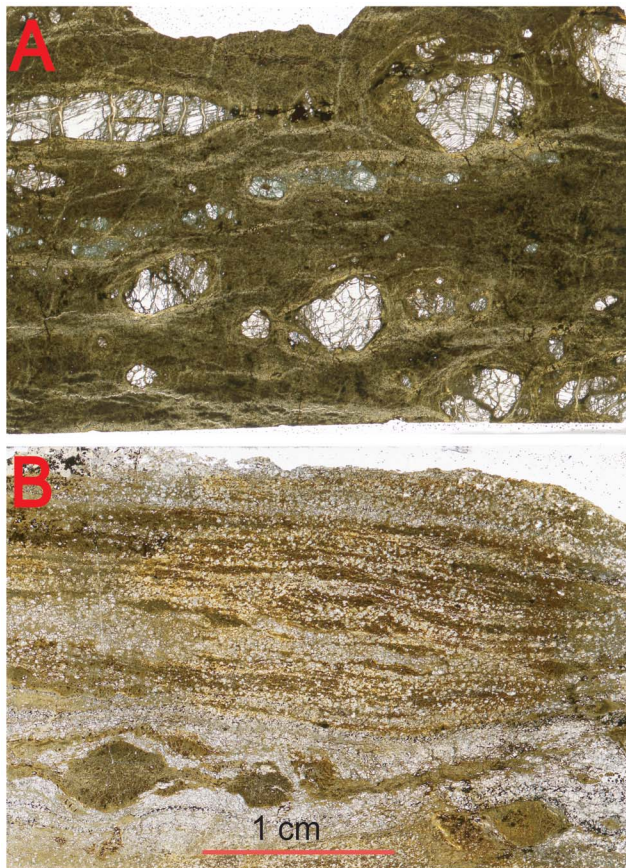


**Figure 2.** Thin section scans of VLS ultramafic mylonites. (a) “Dry” serpentinized mylonitic peridotite (A1 type L2621-02) showing pyroxenes and Cr-Al spinel porphyroclasts in a matrix of recrystallized olivine and pyroxenes. (b) “Wet” serpentinized mylonitic peridotite (S1907-03): A5 type mylonitic amphibole ultramafics. A previous amphibole ultramafic (A4) assemblage is preserved as brownish amphibole porphyroclasts and polycrystalline lenses of serpentinized olivine and pyroxenes; recrystallized matrix contains colorless actinolite and chlorite in addition to serpentinized olivine.

copy complemented by scanning electron microscopy done at the University of Lille (France).

[11] The major element composition of the mineral phases was determined with a Cameca SX-100 electron probe at the American Museum of Natural History, New York; with a Jeol JXA 8600 at CNR-Istituto di Goscienze e Georisorse (IGG), Firenze; and with a Cameca-Camebax at the CAMPARIS micro analyses center (Paris, Campus Jussieu), using 15 kV acceleration voltage, 10 nA and focused beam. Matrix correction was carried out according to *Bence and Albee* [1968]. To reduce interlaboratory analytical variations we adopted, for each probe session, a linearization procedure described by *Brunelli et al.* [2006].

[12] Trace elements in amphiboles were analyzed by secondary ion mass spectrometry (SIMS) with a Cameca IMS 3f ion microprobe, located at WHOI and a Cameca IMS 4f ion microprobe, located at CNR-IGG, Pavia (Italy). Rare earth elements

(REEs) and other trace elements (Ti, V, Cr, Sr, Y, Zr) were measured separately with the WHOI ion probe, applying different high-energy offsets of  $-60$  V and  $-100$  V, respectively. The detailed analytical conditions for these measurements have been reported by *Shimizu et al.* [1978] and *Johnson et al.* [1990]. Polished, Au-coated thin sections analyzed for trace elements at the CNR-IGG ion probe, were bombarded with a  $^{16}\text{O}^-$  primary beam of 9.6 nA current intensity that was focused onto a microspot area of  $\sim 15\ \mu\text{m}$  in diameter, following analytical procedures fully described by *Scribano et al.* [2009]. For REE analysis we used a deconvolution procedure [*Bottazzi et al.*, 1994] to (1) remove BaO interferences from Eu isotopes, (2) discriminate the Gd (and Dy) signal from CeO and NdO interferences, and (3) correct the  $^{151}\text{Eu}^{16}\text{O}$  contribution on the mass 167 and GdO interference at mass 174. With reference to the other trace elements, the following isotopes  $^{39}\text{K}$ ,  $^{45}\text{Sc}$ ,  $^{47}\text{Ti}$ ,  $^{51}\text{V}$ ,  $^{52}\text{Cr}$ ,  $^{88}\text{Sr}$ ,  $^{89}\text{Y}$ ,  $^{90}\text{Zr}$ ,  $^{93}\text{Nb}$ ,  $^{133}\text{Cs}$  and  $^{138}\text{Ba}$

were measured along with the REE ion signals in the same analytical run.  $^{30}\text{Si}^+$  was selected as the isotope of the reference element (Si) for these matrixes. Conversion of ion intensities into concentrations was empirically accomplished by measuring the ion yield relative to Si of each element in reference samples, represented by the international reference material, i.e., NIST SRM 610 and a CNR-IGG inner standard, i.e., kaersutite Soda Springs (KSS).

[13] For isotopic determinations, 30 to 50 mg of amphibole grains were separated by grinding, sieving (60–150  $\mu\text{m}$ ), heavy liquid separation, magnetic separation and hand-picking under a binocular microscope. Amphiboles were leached for Nd and Sr isotopic determination following a procedure by *Snow et al.* [1993]. Dissolution and separation were performed using standard techniques. The Sr and Nd isotopic compositions were measured in dynamic mode using a VG Sector 54 mass spectrometer housed at LDEO. The mass fractionation corrections were based on  $^{86}\text{Sr}/^{88}\text{Sr} = 0.1194$  and  $^{146}\text{Nd}/^{144}\text{Nd} = 0.7219$ . Over the period of analytical work, repeated analyses yielded a  $^{87}\text{Sr}/^{86}\text{Sr}$  ratio of  $0.710255 \pm 0.000021$  for the NBS-987 Sr standard ( $2\sigma$  mean of 23 analyses) and a  $^{143}\text{Nd}/^{144}\text{Nd}$  ratio of  $0.511852 \pm 0.000024$  for the La Jolla Standard ( $2\sigma$  mean of 15 analyses). Total blanks for Sr and Nd did not exceed 80 pg.

[14] Oxygen isotope compositions of amphibole were performed at the CNR-IGG, Pisa, by conventional laser fluorination [Sharp, 1990], reacting the samples under an  $\text{F}_2$  gas atmosphere. Purified oxygen gas was directly transferred into a Finnigan Delta XP Mass Spectrometer via a 13A zeolite molecular sieve for isotopic ratio determinations [Sharp, 1995]. All the data are given following the standard  $\delta$  notation versus SMOW (Standard Mean Oceanic Water). During the course of analysis, an in-house laboratory QMS quartz standard was used ( $\delta^{18}\text{O}_{\text{SMOW}} = \pm 14.05\text{\textperthousand}$ ) yielding an average  $\delta^{18}\text{O}$  value =  $+14.08\text{\textperthousand}$ ,  $1\sigma = 0.14$ . NBS28 standard ( $\delta^{18}\text{O} = +9.58\text{\textperthousand}$ ) gave an average value of  $\delta^{18}\text{O} = 9.52\text{\textperthousand}$  ( $1\sigma = 0.16$ ).

[15] Amphiboles for  $^{40}\text{Ar}/^{39}\text{Ar}$  age determinations were separated from three mylonite samples. The samples were crushed, sieved to 60–150  $\mu\text{m}$ , and washed in distilled water. Amphiboles were separated from the rock powders using heavy liquids and a Franz Iso-dynamic magnetic separator. The final preparation step included hand-picking under a binocular microscope. Samples were loaded into Al irradiation disks with a monitor mineral stan-

dard (Fish Canyon (27.84 Ma)) and encapsulated in a quartz tube for neutron irradiation. The samples were irradiated for 10 h in the Cadmium-Lined, In-Core Irradiation Tube (CLICIT) facility at the Oregon State University TRIGA Research Reactor. The  $^{40}\text{Ar}/^{39}\text{Ar}$  step-heating measurements were done using a double-vacuum furnace at the LDEO  $^{40}\text{Ar}/^{39}\text{Ar}$  laboratory.

#### 4. Texture and Petrography

[16] The VLS ultramafic mylonites display well-defined mineral layering and foliation. Although extensively serpentinized, original metamorphic textures have been preserved, as silicate minerals were replaced by serpentine pseudomorphs. Mineral grain size (<0.5 mm) is significantly smaller than in coarse-grained and porphyroclastic peridotite samples prevalent along the VLS. Olivine and pyroxenes neoblasts are replaced in part or totally by a serpentine (lizardite) mesh with magnetite (from olivine) or by bastite (from pyroxenes) pseudomorphs, although the distinction between the two serpentine types is blurred out in most samples. Calcic amphibole is less affected by serpentinization, with ~30% alteration along rims and cleavages. Spinel and chlorite also underwent limited alteration, whereas plagioclase is frequently replaced by a chlorite-smectite mesh. Because of its very low content (<5%) and fine grain size, altered plagioclase might have been missed in some samples.

[17] Finely recrystallized textures and extensive serpentinization make it often difficult to identify primary silicate phases, and we were not able to obtain accurate prealteration modal compositions, except for the amphibole content. Nevertheless, mafic minerals form  $\geq 95\%$  of the metamorphic assemblages. Olivine (including its alteration products) is the major mineral phase in all the mylonites but one (sample S1907-32, consisting of  $\sim 95\%$  calcic amphibole and  $\sim 5\%$  magnetite). Unambiguous olivine grains form at least 60% of the metamorphic assemblages, up to 90% in some samples, whereas olivine + pyroxenes pseudomorphs make up 80–95% of the rocks, except in a few amphibole-rich layers. Cr-Al spinel or chromite is present in all the assemblages and may coexist with plagioclase or chlorite.

[18] On the basis of mineral associations and compositions, we identified five major mineral assemblages (Table 2), that can be interpreted in terms of progressively increasing mylonitization and hydration, and decreasing temperature.

**Table 2.** Mineral Assemblages in Vema Lithospheric Section Mylonites Based on Mineral Associations and Mineral Compositions<sup>a</sup>

	Sample	Si in Amph (Si Mini)	Amph	Cpx	Opx	Pl	Chl	Description
<i>A1 Protomylonites<sup>b</sup></i>								
High-T	S1902-11pp	-	no	x	x	no	no	porph/mylon
High-T	S1902-23	-	no	x	x	no	no	porph/mylon
High-T	S1902-32	-	no	x	x	no	no	porph/mylon
High-T	S1907-06	-	no	x	x	no	no	porph/mylon
High-T	S1911-53	-	no	x	x	no	no	porph/mylon
High-T	S1913-36pp	-	no	x	x	no	no	porph/mylon
High-T	S1915-06pp	-	no	x	x	no	no	porph/mylon
High-T	S1915-15pp	-	no	x	x	no	no	porph/mylon
High-T	S1915-36	-	no	x	x	no	no	porph/mylon
High-T	S1915-40pp	-	no	x	x	no	no	porph/mylon
High-T	S1920-84pp	-	no	x	x	no	no	porph/mylon
High-T	S1920-85pp	-	no	x	x	no	no	porph/mylon
High-T	S1920-87pp	-	no	x	x	no	no	porph/mylon
High-T	S1920-88pp	-	no	x	x	no	no	porph/mylon
High-T	L2621-02	-	no	x	x	no	no	porph/mylon
<i>A2 Mylonites<sup>c</sup></i>								
High-T	S1915-37 (cores)	5.90–6.46	x	x	x	x	no	px-am-sp-pl granoblastic
High-T	S1915-44	6.26–6.38	x	x	x	?	no	granoblastic - rare amphiboles
High-T	S1911-58pp	6.28–7.09 <sup>d</sup>	x	?	x	x	no	granoblastic - Opx Sp relicts
High-T	S1909-01 pp	6.30–6.64 <sup>d</sup>	x	?	x	?	no	banded-granoblastic- large range of amphibole compositions
High-T	S1911-05	6.32–6.39	x	x	x	x	no	banded-granoblastic- rare amph-Opx relicts; EDS analyses of ol, opx, cpx, pl, sp,amph
High-T	S1911-47	6.36–6.43	x	x	x	x	no	banded-granoblastic - rare amphiboles
High-T	S1911-04 pp	6.43	x	?	x	?	no	granoblastic - Sp relicts
<i>A3 Mylonites<sup>e</sup></i>								
High-T	S1903-09	6.46–6.72	20–25	x	x	?	no	banded-granoblastic layers/lenses of px + am + sp
High-T	S1911-38	6.46–6.79	x	?	x	x	no	granoblastic
High-T	S1904-61	6.48–6.74	10	x	x	?	no	banded-granoblastic
<i>A4 Mylonites<sup>f</sup></i>								
High/Medium-T	S1905-95	6.51–7.02	x	no	x	no	no	CaO in opx = 0.3% (EDS); banded-granoblastic, very rich in am + sp: former pyroxenite?
High/Medium-T	S1910-02pp	6.60–7.69	x	no	?	no	no	granoblastic
High/Medium-T	S1911-03	6.62–7.01	x	no	x	no	no	granoblastic
Medium-T	S1911-04 pp	6.63–7.24	x	no	?	no	no	granoblastic
Medium-T	S1911-02	6.70–7.03	x	no	x	no	no	granoblastic
Medium-T	S1907-03	6.71–7.10	x	no	?	no	no	granoblastic
Medium-T	S1915-40pp	6.71–7.65 <sup>g</sup>	1–3	no	x	no	no	amph in matrix on opx
Medium-T	S1905-87	6.72–6.97	x	no	?	no	no	banded-granoblastic
Medium-T	S1901-03	6.73–7.11	36	no	?	no	no	a thick am-sp granoblastic layer (former pyroxenite?)
Medium-T	S1901-04	6.74–7.05	34	no	x	no	no	granoblastic lenses - opx relicts
Medium-T	S1902-09	6.74–7.40	x	no	x	no	no	banded - granoblastic; CaO in opx = 0.2% (EDS)
Medium-T	S1909-01 pp	6.74–7.00	35–40	no	?	no	no	banded-granoblastic- large range of amphibole compositions
Medium-T	S1907-25	6.76–7.01	34	no	?	no	no	granoblastic- a section rich in am (former pyroxenite?)
Medium-T	S1908-02	6.77–7.43	x	no	?	no	no	granoblastic
Medium-T	S1902-11pp	na	x	no	?	no	no	ol + am + sp granoblastic layers
Medium-T	S1902-14	na	x	no	?	no	no	banded - granoblastic
Medium-T	S1902-16	na	x	no	?	no	no	banded - granoblastic
Medium-T	S1903-25	na	9 <sup>h</sup>	no	?	no	no	granoblastic

**Table 2.** (continued)

	Sample	Si in Amph (Si Mini)	Amph	Cpx	Opx	Pl	Chl	Description
Medium-T	S1903-34	na	x	no	?	no	no	granoblastic
Medium-T	S1907-07pp	na	x	no	?	no	no	amphibole as porphyroclasts
Medium-T	S1908-04	na	x	no	x	no	no	granoblastic
Medium-T	S1911-12A	na	x	no	x	no	no	granoblastic- Sp relics
Medium-T	S1915-20pp	na	x	no	?	no	no	amphibole as porphyroclasts
Medium-T	S1901-02pp	6.80–6.98	44	no	?	no	x	banded-granoblastic - Sp relics
Medium-T	S1904-62	6.80–7.17	x	x	?	no	no	banded-granoblastic
Medium-T	S1911-64	6.82–7.07	x	no	?	no	no	banded-granoblastic
Medium-T	S1911-63pp	6.83–7.16	x	no	?	no	no	amphibole as porphyroclasts
Medium-T	S1907-23pp	6.89–7.44	12–13 <sup>h</sup>	no	?	no	x	amph as porphyroclasts (Amph Fe-rich)
Medium-T	S1910-01	6.95–7.09	x	no	?	no	no	granoblastic - thin layer with amph + sp + phlogo? + ap?
Medium-T	S1905-85	6.97–7.17	x	no	?	no	no	banded-granoblastic
Medium-T	S1902-20	7.00–7.07	x	no	?	no	no	granoblastic
Medium-T	S1908-03	7.03–7.43	x	no	?	no	no	granoblastic
Medium-T	S1905-83	7.16–7.28	1.2	no	x	no	no	granoblastic
Medium-T	S1910-02pp	7.16–7.60	x	no	?	no	x	secondary mineral assemblage-very small crystals
Medium-T	S1911-13pp	7.23–7.37	x	no	x	no	no	amph as porphyroclasts
Medium-T	S1910-04	7.27–7.57	x	no	?	no	no	granoblastic-very poor in amph
Medium-T	S1904-38	7.36–7.54	0.3	no	?	no	no	porphyroclastic
Medium/Low-T	S1910-03	7.44–7.55	x	no	?	no	x	very small amph - sp relics
Medium-T	S1904-62pp	7.47	x	no	?	no	no	secondary amphibole
Medium/Low-T	S1915-37 (rims)	7.00–7.74 <sup>g</sup>	x	no	?	no	no	rims of amphibole crystals
Medium/Low-T	S1915-20pp	7.06–7.74 <sup>g</sup>	x	no	x	no	no	amph porphyroclasts
<i>A5 Mylonites<sup>i</sup></i>								
Low-T tremolite + chlorite <sup>j</sup>								
Low-T	S1911-04 pp	7.60–7.67	x	no	no	no	x	secondary mineral assemblage
Low-T	S1902-34	7.63–7.83	x	no	no	no	x	
Low-T	S1901-02pp	na	x	no	no	no	x	secondary mineral assemblage
Ultramytonites								
Low-T	S1910-02pp	7.69	x	no	no	no	x	2 amphibole generations
Low-T	S1907-07pp	na	x	no	no	no	x	microfolds - 2 mylonitizations -medium-T assemblage replaced
Low-T	S1907-23pp	na	x	no	no	no	x	microfolds- 2 mylonitizations
Low-T	S1902-11pp	na	x	no	no	no	x	in microfractures-chlorite surrounding sp
Low-T	S1911-63pp	na	x	no	no	no	?	2 amphibole generations
Low-T	S1911-13pp	na	x	no	no	no	x	2 mylonitizations- Tremolite
Low-T	S1915-17A	na	12 <sup>h</sup>	no	no	no	x	cataclastic - 2 mylonitizations
Low-T	S1915-20pp	na	x	no	no	no	x	2 mylonitizations- Tremolite + chlorite
Protomytonites <sup>k</sup>								
Low-T	S1911-58pp	-	no	no	no	no	x	chlorite at spinel rims
Low-T	S1913-36pp	na	x	no	no	no	no	porphyroclastic - amph on opx relics
Low-T	S1915-06pp	na	x	no	no	no	no	porphyroclastic - amph on opx relics
Low-T	S1915-15pp	na	x	no	no	no	no	porphyroclastic - amph on opx relics
Low-T	S1920-84pp	na	x	no	no	no	no	porphyroclastic - amph on opx relics
Low-T	S1920-85pp	na	x	no	no	no	no	porphyroclastic - amph on opx relics
Low-T	S1920-87pp	na	x	no	no	no	no	porphyroclastic - amph on opx relics
Low-T	S1920-88pp	na	x	no	no	no	no	porphyroclastic - amph on opx relics
Ol + talc + tremolite + chlorite <sup>l</sup>								
Low-T	S1907-12	7.91–8.00	x	no	no	no	x	cataclastic - 2 mylonitizations- former amph reequilibrated at low T (Fe-rich)
Special sample	S1907-32	7.31–7.86	x	no	no	no	no	amphibole + magnetite (Fe rich)

[19] 1. A1 assemblages (~16% of the samples) are ductily deformed spinel harzburgites/herzolites, dynamically recrystallized into the same primary minerals. Elongate porphyroclasts of olivine, opx, cpx and spinel define a stretching lineation. Cm-size orthopyroxenes and mm-size clinopyroxenes are commonly kinked and fractured, and partially recrystallized into small (0.05–0.1 mm in size) polygonal neoblasts, whereas primary olivine, 1–5 mm in size, has recrystallized into ~0.5 mm-size neoblasts. Spinel occurs as fine intergrowths with relict opx and as coarse, stretched and often fragmented grains. Thin, anastomosing neoblasts layers define a foliation. Rare, scattered grains of a colorless amphibole have grown replacing pyroxenes porphyroclasts, while chlorite locally mantles spinel coarse grains.

[20] 2. A2 assemblages (~9% of the samples) are characterized by a higher percentage of fine-grained matrix composed of the same minerals as the original peridotite, plus plagioclase and rare yellow-pale brownish pargasitic amphibole. A mineralogical banding is parallel to the mylonitic foliation; the composition of the bands depends on the porphyroblast phases they contain. Mm- to cm-wide pyroxene-rich bands are equigranular assemblages, made of 0.02–0.1 mm-sized polygonal neoblasts of (by decreasing amounts) opx, cpx, olivine, spinel, plagioclase and amphibole. Similar mineral assemblages fill irregular grain boundary embayments of mm-size, elongate, relicts of opx and cpx (opx porphyroclasts are mm- to cm-sized; rare cpx porphyroclasts are mm-sized). The five silicate phases display straight and sharp grain boundaries, with frequent triple junctions, indicating textural equilibrium. Cr-spinel is present in all the meta-

morphic silicate phases as minute inclusions or as small interstitial grains. Cm-wide olivine-rich bands are made of slightly flattened to polygonal, 0.2–0.5 mm, olivine neoblasts and rare subhedral amphiboles (0.1 mm in average). Pyroxenes neoblasts were not identified with certainty but were probably present before serpentinization. Olivine-rich bands also contain occasional, fine-grained, Cr-spinel-plagioclase aggregates deriving from coarse (up to 2 mm in size) primary spinel crystals. Plagioclase and Cr-spinel neoblasts show textural equilibrium; both minerals contain minute inclusions of each other. One sample contains zoned amphiboles, with yellow-pale cores and green rims, indicating re-equilibration at lower temperature (sample S1915-37). In summary, A2 mylonites are on average more finely recrystallized than A1 mylonites.

[21] 3. A3 assemblages (~4% of the samples) show an abundance of amphibole higher than A2 assemblages. Amphibole grains, oriented parallel to compositional banding and foliation, are relatively coarse (up to 0.5 mm), yellow-pale to colorless, euhedral crystals, that grew replacing primary and neoblastic pyroxenes, but also plagioclase (0.01–0.03 mm). Metamorphic cpx is not abundant. Mineralogical banding, strengthened by segregation of thin amphibole layers (1–2 mm wide), is well defined, while relicts of premylonitic minerals are represented only by small, elongate crystals of opx (up to 0.5 mm, smaller than in A2 mylonites) and spinel (up to 1 mm). Spinel fragments are commonly recrystallized into small porphyroblasts characterized by poikilitic rims that enclose olivine, opx and amphibole grains. Minute spinel inclusions are present in these metamorphic

#### Notes to Table 2:

<sup>a</sup>Samples are listed by decreasing metamorphic grade, based on increasing Si contents in their amphiboles. Metamorphic grade is according to Evans [1982] and Spear [1993], based on correlations between amphibole Si contents and mineral assemblages. Notes: pp (pro parte) means that a second paragenesis is superimposed (the assemblage described is the one in equilibrium); x, mineral is present (if a number is reported, it is modal abundance in percent); no, mineral not observed in that metamorphic mineral assemblage; na, not analyzed; question mark ("?") means that the mineral should be present (given the composition of the amphiboles) but has not been observed (likely because of serpentinization); EDS, energy dispersive analysis.

<sup>b</sup>OI + Opx + Cpx + Sp assemblages belong to granulite facies. Even if late stage amph is present, amph is nevertheless considered as not observed in the high-T assemblage.

<sup>c</sup>Intermediate-P. granulite facies: OI + Opx + Cpx + Sp ± Pl ± Amph with Si = 5.9–6.6 apf. For consistency, all these samples should contain cpx and plag, but they were not observed because of serpentinization.

<sup>d</sup>Some amph have Si > 6.6, but most have Si < 6.6; thus, cpx and pl may have been replaced by Si-richer amphibole during progressive metamorphism.

<sup>e</sup>Amphibolite facies (olivine + opx + amph + spinel) starts with amph Si = 6.5. These three samples are just at the limit. Sample 1911-38, which contains pl, must also contain cpx, but it was not observed because of serpentinization.

<sup>f</sup>Typical upper amphibolite facies: OI + Opx + Amph + Cr – Sp, with amph Si = 6.5–7.6.

<sup>g</sup>Amph with Si > 7.6; all of the A4 mylonites samples, however, start to crystallize at upper amphibolite facies conditions.

<sup>h</sup>Calculated amphibole: based on whole rock CaO content, i.e., equivalent amphibole, not necessarily real amphibole.

<sup>i</sup>Lower amphibolite facies: OI + Opx + tremolite + Chlorite + chromite assemblages, with amph Si = 7.5–7.9. Tremolites are colorless and fibrous, so even with no analyses they can be distinguished from hornblendes.

<sup>j</sup>These three samples have low-T tremolite + chlorite (in addition to higher-T hornblendes) but do not show two mylonitizations.

<sup>k</sup>These 10 samples below are protomylonites with static tremolite and chlorite after px and sp.

<sup>l</sup>The amph has Si = 7.9–8.0; this is the only sample with tremolite end-member.

silicates. This cpx-poor, plagioclase-bearing metamorphic paragenesis may be considered as transitional between the A2 and A4 ultramafic mylonites.

[22] 4. A4 assemblages (~49% of the samples) represent the prominent mylonite type. They are typically made (before serpentinization) of 85–95% olivine + pyroxenes, 5–15% colorless amphibole and ~1% Cr-spinel. Amphibole (0.25–0.7 mm in length by 0.1–0.3 mm wide) is concentrated in up to 2 mm wide layers parallel to the mylonitic foliation, alternating with 1 to a few cm-wide, olivine-rich bands. Olivine forms small neoblasts (0.2–0.5 mm) with grains flattened parallel to mylonitic foliation. Opx is the major pyroxene phase, occurring mainly as neoblasts (0.02–0.1 mm) in the amphibole-rich bands. A few small elongated opx porphyroclasts are still present. Cpx neoblasts have been recognized with certainty in a single sample (S1904-62). Amphiboles are subhedral, occurring as unzoned, lozenge-shaped crystals with rounded corners, also oriented parallel to mylonitic foliation. They commonly show poikilitic grain boundaries enclosing olivine and opx grains. Spinel neoblasts occur as euhedral to subhedral grains in the serpentine matrix and as minute inclusions within opx and amphibole. Up to 1 mm, anhedral spinel grains are present locally, probably inherited from the primary peridotite. Although unzoned, they are overgrown by neoblastic rims that poikilitically include grains of olivine, opx and amphibole. Small, elongated, symplectite-textured domains made of serpentinized opx (bastite), or of serpentine-chlorite mesh, associated with spinel rods, appear as relicts within some amphiboles; these symplectites may represent former opx-spinel ± plagioclase aggregates.

[23] A number of A3 and A4 samples contain thick (cm to a few cm in width) amphibole layers, poor in opx but relatively rich in spinel. These samples may contain up to 45% amphibole in a thin section. Conversely, other A4 samples, extremely poor in amphibole (1–5% in a thin section), are characterized by mostly serpentinized olivine, mixed with some serpentinized opx.

[24] 5. A5 assemblages (~23% of the samples) are extremely fine-grained ultramylonites that overprint a higher temperature mineral assemblage. In most cases, A4 mineral assemblages are locally preserved as amphibole porphyroclasts and as elongate, polycrystalline aggregates of serpentinized olivine/oxp. Matrix is very fine-grained (~2  $\mu\text{m}$ ), made of serpentinized olivine, chlorite and tremolite (up to 0.1 mm in length), occasion-

ally showing tight microfolds. Tremolite forms thin, colorless prisms, whose orientation defines a second mylonitic lineation and foliation that cross-cuts the previous foliation and mineralogical banding at low angle; in microfolded samples, tremolite is oriented parallel to fold axes. Very thin lamellae of hornblende and ilmenite have been observed in the cleavages of some chlorite grains. Lens-shaped, coarse chlorite lenses contain former Cr-spinels re-equilibrated to Ti-rich, Cr-rich ferromagnetite (probably a mixture of oxide phases). Chromite and magnetite are common accessory phases. Their shapes vary from equidimensional to tabular, the latter being oriented along the foliation. In some A4 ultramafics (e.g., S1901-02), the A5 low temperature assemblage consists of tremolite that occurs as few scattered prisms, while chlorite and magnetite formed after earlier spinels; however, magnetite occurs as plate-shaped grains oriented parallel to the foliation. Tremolite and chlorite also crystallized in the A1–A2 anhydrous assemblages, where tremolite is scattered, replacing pyroxenes, while chlorite occurs only as breakdown product of spinel.

[25] 6. In addition to these five major groups, we observed also a few unique specimens. Sample S1907-32 is represented by a single olivine and Cr-spinel-free rock made of ~95% calcic amphibole and ~5% magnetite, with a strong mineral layering achieved by alternation of magnetite-rich and magnetite-poor layers. Amphibole is colorless, commonly including minute inclusions of magnetite. SEM observation shows that magnetite composition is highly variable from Cr-rich to Cr-poor. Most Cr-rich magnetite grains have morphology (anhedral with poikilitic rims) suggesting late stage replacement of Cr-spinel. Cr-poor magnetite may also have replaced olivine grains. Ni-Fe sulfide grains are very abundant throughout this sample.

[26] A single sample (S1907-12) contains talc. Like A5 ultramafic mylonites, this sample has been affected by secondary mylonitization, with elongate porphyroclasts of hornblende showing Ti-Fe oxide exsolution phases and polycrystalline lenses of serpentinized olivine ± opx + tiny euhedral Cr-spinels. The very fine-grained matrix consists of serpentine + chlorite + tremolite + talc intergrowths, with accessory magnetite.

## 5. Mineral Chemistry

[27] Mineral chemistry results are reported in Tables 3a to 3e.

**Table 3a.** Average Major Element Oxide Composition of Orthopyroxenes From VLS Ultramafic Mylonites

Sample	Min.	Ass. <sup>a</sup>	N.	An.	Spot	SiO <sub>2</sub>	1σ	TiO <sub>2</sub>	1σ	Al <sub>2</sub> O <sub>3</sub>	1σ	Cr <sub>2</sub> O <sub>3</sub>	1σ	FeO	1σ	MnO	1σ	MgO	1σ	CaO	1σ	Na <sub>2</sub> O	1σ	NiO	1σ	Total	Mg #	1σ	C#	1σ
S1902-23	A1	5	core	54.49	0.33	0.04	0.02	5.07	0.39	0.89	0.11	6.13	0.14	0.12	0.02	32.46	0.70	0.53	0.10	0.03	0.03	0.10	0.04	99.84	91.12	0.65	10.50	0.95		
S1913-36	A1	9	core	54.51	0.39	0.08	0.04	5.17	0.47	0.88	0.11	5.80	0.14	0.12	0.02	32.00	0.62	1.57	0.56	0.06	0.04	0.02	0.07	0.04	100.19	90.77	0.12	10.21		
S1915-15	A1	4	core	54.33	0.59	0.09	0.06	4.64	1.37	0.76	0.15	6.47	0.29	0.13	0.02	32.89	0.64	0.52	0.11	0.01	0.01	0.07	0.01	99.82	91.41	1.09	10.20	2.34		
S1915-35	A1	1	core	54.14	0.10	0.83	0.77	6.23	0.12	32.14	0.66	0.10	0.10	0.09	0.04	0.04	0.04	0.04	0.04	0.04	0.04	0.04	0.04	0.04	100.09	90.40	8.14			
S1915-36	A1	4	core	55.14	0.60	0.08	0.02	4.95	0.51	0.71	0.07	6.05	0.21	0.11	0.06	32.85	0.50	0.99	0.36	0.09	0.04	0.04	0.04	0.04	100.96	91.45	0.66	8.82	0.48	
S1915-40	A1	8	core	54.98	0.41	0.09	0.03	4.22	0.46	0.57	0.11	6.16	0.23	0.13	0.03	33.22	0.53	0.91	0.38	0.02	0.03	0.09	0.04	0.04	100.39	92.11	1.10	8.22	0.92	
S1915-40	A1	3	rim	54.93	0.39	0.12	0.01	3.81	0.59	0.48	0.05	6.34	0.28	0.16	0.03	33.53	0.23	0.82	0.37	0.04	0.03	0.10	0.03	0.03	100.33	92.85	0.44	7.90	0.85	
S1915-40	A1	2	opxII <sup>b</sup>	55.51	0.48	0.13	0.03	3.34	0.51	0.44	0.13	6.47	0.10	0.10	0.02	34.20	0.00	0.63	0.06	0.01	0.01	0.10	0.05	0.05	100.91	90.40	0.13	8.27	3.29	
S1920-84	A1	4	core	54.76	0.65	0.06	0.03	5.44	0.36	0.66	0.08	6.35	0.24	0.13	0.03	32.42	0.57	1.13	0.17	0.06	0.04	0.04	0.04	0.04	101.91	90.10	0.40	7.54	0.32	
S1920-84	A1	5	core	54.90	0.33	0.09	0.03	5.31	0.28	0.60	0.09	6.41	0.24	0.12	0.08	31.87	0.54	1.45	0.65	0.07	0.03	0.03	0.03	0.03	100.82	89.86	0.24	6.99	0.87	
S1920-88	A1	4	core	54.82	0.48	0.05	0.03	5.19	0.39	0.62	0.03	6.30	0.08	0.15	0.05	32.27	0.28	1.19	0.18	0.02	0.03	0.03	0.03	0.03	100.61	90.12	0.10	7.38	0.43	
S1921-02	A1	3	core	54.91	0.56	0.07	0.03	4.82	0.21	1.07	0.03	6.11	0.01	0.13	0.02	32.13	0.19	1.58	0.09	0.04	0.00	0.00	0.00	0.00	0.00	100.86	90.36	1.11	13.02	0.16
S1911-04	A2	7	core	54.65	0.69	0.10	0.01	5.28	0.61	0.72	0.04	6.31	0.18	0.13	0.03	32.27	0.67	1.10	0.52	0.03	0.04	0.02	0.02	0.02	100.62	90.76	1.04	8.52	1.12	
S1911-04	A2	6	rim	55.29	0.91	0.14	0.02	4.15	0.93	0.72	0.08	6.32	0.19	0.13	0.02	32.99	0.60	0.80	0.31	0.01	0.01	0.09	0.03	0.03	100.64	90.43	0.49	10.46	2.01	
S1911-05	A2	10	core	57.82	0.44	0.08	0.06	1.69	0.17	0.31	0.06	6.63	0.17	0.14	0.03	34.95	0.30	0.58	0.05	0.02	0.02	0.05	0.04	0.04	102.27	91.35	0.63	11.03	1.40	
S1911-58	A2	1	core	55.29	0.07	4.38	0.64	6.18	0.16	32.66	0.65	0.00	0.00	0.00	0.00	0.00	0.00	0.00	0.00	0.00	0.00	0.00	0.00	0.00	100.03	90.40	8.93			
S1915-44	A2	1	core	56.44	0.07	2.95	0.54	6.92	0.12	34.21	0.65	0.00	0.00	0.00	0.00	0.00	0.00	0.00	0.00	0.00	0.00	0.00	0.00	0.00	101.90	91.60	10.93			
S1903-09	A3	13	core	57.44	0.65	0.03	0.02	1.60	0.36	0.23	0.08	6.52	0.18	0.15	0.03	35.39	0.46	0.44	0.08	0.00	0.01	0.06	0.03	0.03	101.86	92.89	1.22	8.74	1.80	
S1904-61	A3	3	opxII <sup>b</sup>	56.78	1.27	0.02	0.02	1.37	0.05	0.23	0.01	6.40	0.09	0.14	0.04	34.97	0.36	0.48	0.06	0.00	0.00	0.09	0.04	0.04	100.47	92.85	1.27	10.00	0.74	
S1901-04	A4	7	core	55.16	0.81	0.12	0.04	3.98	1.21	0.70	0.20	7.02	0.24	0.15	0.05	32.99	0.54	0.63	0.43	0.01	0.02	0.09	0.01	0.01	100.84	90.51	1.09	9.95	1.69	
S1901-04	A4	5	rim	56.26	0.73	0.09	0.03	2.73	0.52	0.54	0.18	6.90	0.13	0.15	0.01	33.85	0.42	0.44	0.12	0.01	0.02	0.07	0.04	0.04	101.05	90.68	0.61	11.60	2.81	
S1905-83	A4	9	core	54.85	0.42	0.09	0.01	4.69	0.30	0.69	0.19	6.11	0.20	0.13	0.01	32.69	0.35	1.05	0.07	0.03	0.00	0.07	0.01	0.01	0.01	100.41	91.25	0.04	8.99	1.81
S1905-83	A4	5	rim	54.64	0.78	0.10	0.02	4.70	0.11	0.69	0.06	6.13	0.06	0.11	0.04	32.97	0.30	1.28	0.46	0.02	0.02	0.07	0.01	0.01	100.71	92.46	1.55	8.91	0.94	
S1911-02	A4	2	core	53.98	0.49	0.16	0.10	4.99	1.23	0.72	0.13	6.60	0.24	0.16	0.01	32.35	0.05	1.39	0.81	0.08	0.01	0.01	0.01	0.01	0.01	100.41	92.46	0.49	9.19	3.48
S1911-13	A4	3	core	54.50	2.03	0.08	0.06	5.08	2.31	0.78	0.42	6.38	0.29	0.15	0.01	32.24	1.43	0.96	0.66	0.04	0.06	0.09	0.01	0.01	100.30	90.58	0.67	9.18	0.86	
S1915-20	A4	1	core	54.69	0.14	5.72	0.71	6.31	0.15	32.99	0.57	0.00	0.00	0.00	0.00	0.00	0.00	0.00	0.00	0.00	0.00	0.00	0.00	0.00	101.28	91.01	7.69			

<sup>a</sup> Mineral assemblage.<sup>b</sup> Opx neoblasts.

**Table 3b.** Average Major Element Oxide Composition of Clinopyroxenes From VLS Ultramafic Mylonites

Min.	Ass. N.	An.	Spot	SiO <sub>2</sub>	1σ	TiO <sub>2</sub>	1σ	Al <sub>2</sub> O <sub>3</sub>	1σ	Cr <sub>2</sub> O <sub>3</sub>	1σ	FeOt	tot	1σ	MnO	1σ	MgO	1σ	CaO	1σ	Na <sub>2</sub> O	1σ	NiO	1σ	Total	Mg#	1σ	C#	1σ	T <sup>a</sup> (°C)
S1915-40	A1	8	core	51.27	0.49	0.27	0.11	5.43	1.12	0.16	2.58	0.24	0.09	0.03	15.76	1.00	23.18	0.83	0.76	0.21	0.04	0.04	100.49	91.57	0.62	12.29	0.93	735		
S1915-40	A1	3	core of cpxII <sup>b</sup>	52.22	0.15	0.49	0.10	3.90	0.39	0.92	0.09	2.34	0.06	0.07	0.05	16.48	0.16	24.07	0.18	0.49	0.01	0.03	0.05	101.00	92.61	0.22	13.70	2.00	663	
S1915-40	A1	5	rim	51.83	1.25	0.39	0.10	4.64	1.26	0.92	0.25	2.54	0.20	0.04	0.06	16.55	0.87	22.86	0.95	0.66	0.19	0.03	0.03	100.46	92.06	0.54	11.84	1.41	830	
S1915-40	A1	2	cpxII <sup>b</sup> - small xx	53.43	0.14	0.37	0.08	2.18	0.23	0.75	0.10	2.32	0.34	0.03	0.04	17.37	0.21	23.96	0.58	0.43	0.06	0.06	0.02	100.91	93.04	0.87	18.82	0.42	724	
S1902-23	A1	4	core	50.94	0.23	0.15	0.01	6.10	0.45	1.22	0.13	2.23	0.17	0.09	0.05	15.23	0.19	23.76	0.19	0.24	0.02	0.04	0.02	100.00	92.41	0.59	11.80	0.85	775	
S1913-36	A1	3	core	52.61	0.41	0.25	0.04	5.17	1.34	1.15	0.35	2.28	0.09	0.06	0.03	16.08	0.78	22.32	0.05	1.00	0.21	0.05	0.01	100.97	92.64	0.17	12.90	1.22	843	
S1920-84	A1	5	core	51.10	0.66	0.26	0.03	6.69	0.76	0.98	0.17	2.72	0.34	0.10	0.03	15.61	0.30	22.38	0.95	0.72	0.07	0.00	0.00	100.56	91.10	0.08	8.90	0.61	889	
S1920-85	A1	6	core	50.92	0.46	0.31	0.07	6.93	0.16	1.04	0.07	2.98	0.28	0.11	0.03	15.25	0.64	22.08	0.83	0.69	0.08	0.04	0.01	100.35	90.13	0.49	9.14	0.47	916	
S1920-88	A1	4	core	50.98	0.46	0.23	0.05	6.91	0.13	1.08	0.11	2.94	0.08	0.10	0.04	15.31	0.23	21.45	0.53	0.74	0.07	0.07	0.04	99.81	90.28	0.32	9.43	0.81	972	
L26621-02	A1	8	core	51.26	0.02	0.20	0.06	5.79	0.06	1.60	0.02	2.73	0.19	0.09	0.01	16.07	0.44	21.69	0.62	0.64	0.02	0.04	0.01	100.10	91.30	0.33	15.62	0.10	980	
S1911-05	A2	4	cpxII <sup>b</sup> - small xx	54.45	0.30	0.21	0.04	2.31	0.36	0.55	0.11	2.45	0.03	0.06	0.01	17.69	0.15	23.65	0.28	0.31	0.03	0.04	0.00	101.73	92.79	0.12	13.81	1.30	873	
S1915-37	A2	3	rim small xx	54.10	0.81	0.17	0.07	1.54	0.37	0.50	0.17	2.61	0.14	0.07	0.03	17.56	0.18	24.43	0.24	0.34	0.08	0.03	0.03	101.35	92.31	0.32	17.51	1.48	680	
S1915-37	A2	1	core small xx	53.85	0.21	1.89	0.61	2.91	0.14	17.43	0.27	0.32	0.14	101.78	91.43	0.14	17.87	0.43	744											
S1915-37	A2	2	cpxII <sup>b</sup> - small xx	53.57	0.03	0.17	0.03	2.13	0.47	0.28	0.01	2.72	0.30	0.04	0.01	17.51	0.14	24.24	0.11	0.31	0.04	0.09	0.09	101.07	91.98	0.76	8.42	1.94	728	
S1903-09	A3	7	cpxII <sup>b</sup> - small xx	54.47	0.30	0.14	0.04	1.69	0.35	0.43	0.10	2.12	0.21	0.08	0.03	18.16	0.17	24.27	0.37	0.13	0.02	0.05	0.03	101.55	93.84	0.57	14.61	1.47	827	
S1904-61	A3	4	cpxII <sup>b</sup> - small xx	53.35	1.22	0.10	0.02	1.34	0.06	0.32	0.02	2.17	0.20	0.03	0.03	17.68	0.35	24.86	0.16	0.09	0.02	0.02	0.02	99.96	93.57	0.47	13.72	0.28	604	
S1904-62	A4	1	rim cpxII <sup>b</sup>	54.85	0.05	1.10	0.14	2.19	0.06	17.83	0.04	0.03	0.03	101.02	93.55	0.02	9.96	7.96	738											
S1904-62	A4	1	cpxII <sup>b</sup> - small xx	54.79	0.06	1.02	0.25	1.96	0.08	17.79	0.02	0.02	0.02	100.72	94.18	0.02	14.31	7.34	734											
S1904-62	A4	2	cpxII <sup>b</sup> - small xx	54.14	0.61	0.07	0.02	1.32	0.13	0.23	0.03	2.10	0.03	0.05	0.01	17.74	0.18	24.65	0.06	0.03	0.01	0.06	0.01	100.39	93.77	0.03	10.44	0.12	725	

<sup>a</sup>T calculated with the thermometer of *Nimis and Taylor [2000]*. P = 0.5 Gpa.

<sup>b</sup>Cpx neoblasts.

**Table 3c.** Average Major Element Oxide Composition of Spinsels From VLS Ultramafic Mylonites

Sample	Min.	Ass.	N.	An.	Spot	SiO <sub>2</sub>	1σ	TiO <sub>2</sub>	1σ	Al <sub>2</sub> O <sub>3</sub>	1σ	Cr <sub>2</sub> O <sub>3</sub>	1σ	FeOt <sub>ot</sub>	1σ	MnO	1σ	MgO	1σ	NiO	1σ	Total	Mg#	1σ	Cr#	1σ
S1902-23	A1	5	core	0.02	0.03	0.06	0.04	48.56	0.36	20.74	0.38	12.51	0.30	0.14	0.05	18.25	0.35	0.24	0.05	100.51	73.57	1.20	22.27	0.23		
S1913-36	A1	15	core	0.03	0.02	0.07	0.04	49.01	0.74	19.48	0.93	12.13	0.30	0.12	0.04	18.61	0.21	0.29	0.02	99.74	73.24	0.54	21.05	1.04		
S1915-15	A1	1	core	0.00	0.19	51.13	16.47	14.17	0.00	18.65	0.37	100.98	73.87	17.77												
S1915-20	A1	1	core	0.00	0.17	53.03	15.82	13.12	0.08	19.10	1.01	101.32	74.39	16.67												
S1915-35	A1	1	core	0.00	0.10	52.11	15.64	12.26	0.00	19.41	0.30	99.82	76.96	16.76												
S1915-36	A1	4	core	0.00	0.17	0.04	52.03	0.97	15.68	0.87	13.30	0.62	0.02	0.03	19.10	0.53	0.31	1.00	60	75.14	1.56	16.81	1.03			
S1915-40	A1	6	core	0.03	0.02	0.19	0.06	48.95	3.35	16.17	2.68	13.87	1.20	0.01	0.02	18.38	0.97	0.27	0.10	97.87	74.89	2.65	18.22	3.57		
S1920-84	A1	4	core	0.00	0.00	0.05	0.01	55.70	0.44	12.43	0.25	11.73	0.19	0.08	0.04	19.60	0.24	0.35	0.05	99.94	74.86	0.22	13.02	0.27		
S1920-85	A1	5	core	0.00	0.00	0.07	0.02	53.91	0.65	13.43	0.58	12.43	0.18	0.11	0.04	19.01	0.06	0.32	0.03	99.28	73.17	0.31	14.32	0.62		
S1920-88	A1	4	core	0.01	0.02	0.09	0.02	53.24	0.15	14.21	0.49	12.15	0.35	0.06	0.04	19.59	0.26	0.33	0.03	99.68	74.19	0.79	15.18	0.42		
L2621-02	A1	9	core	0.01	0.11	0.03	44.18	1.39	25.00	0.88	14.02	0.30	0.34	0.05	17.28	0.28	0.22	0.01	101.16	71.10	0.38	27.48	1.38			
S1909-01	A2	7	core	0.01	0.02	0.07	0.02	50.41	2.26	19.21	2.07	17.28	0.81	0.10	0.05	15.89	0.78	1.02	0.97	62.99	2.91	20.37	2.34			
S1911-04	A2	2	core	0.01	0.11	0.00	41.89	0.52	26.02	0.71	16.82	0.28	0.17	0.02	14.57	0.21	0.16	0.04	99.74	61.72	1.54	29.41	0.30			
S1911-04	A2	8	spnII <sup>a</sup>	0.07	0.07	0.14	0.04	33.47	1.41	32.70	1.44	20.24	0.85	0.08	0.11	11.48	0.56	0.10	0.02	98.28	51.48	2.18	39.60	1.96		
S1911-04	A2	2	spnII <sup>a</sup>	0.05	0.01	0.15	0.03	29.57	1.41	36.58	0.65	21.20	0.66	0.11	0.15	10.58	0.38	0.08	0.02	98.31	48.47	1.30	45.36	1.62		
S1911-05	A2	1	spnII <sup>a</sup>	0.00	0.11	32.59	34.08	20.37	0.26	13.07	0.13	100.59	57.56	41.22												
S1911-47	A2	2	spnII <sup>a</sup>	0.14	0.16	0.11	0.04	32.67	0.31	33.09	0.08	21.22	0.44	0.21	0.05	12.73	0.04	0.13	0.04	100.30	55.97	0.07	40.45	0.28		
S1911-58	A2	3	core	0.02	0.04	0.87	1.23	37.99	2.10	28.20	1.09	17.95	0.87	0.04	0.05	13.98	0.44	0.15	0.08	99.19	59.31	1.01	33.27	1.82		
S1911-58	A2	2	spnII <sup>a</sup>	0.00	0.00	0.37	0.08	30.84	0.10	36.51	0.26	21.86	0.28	0.05	0.01	10.99	0.06	0.06	0.01	100.60	48.69	0.42	44.26	0.26		
S1915-37	A2	4	spnII <sup>a</sup>	0.04	0.03	0.17	0.05	29.66	3.03	34.03	1.16	22.20	3.91	0.00	0.00	11.78	1.92	0.11	0.04	97.98	53.34	7.31	43.58	2.79		
S1915-44	A2	1	core	0.02	0.13	37.79	37.79	27.67	0.04	20.06	0.04	14.60	0.04	100.31	61.97	32.93										
S1903-09	A3	3	spnII <sup>a</sup>	0.00	0.00	0.11	0.04	35.05	1.33	30.22	0.97	19.97	0.64	0.00	0.00	13.81	0.35	0.14	0.02	99.31	60.21	1.04	36.65	1.62		
S1904-61	A3	5	spnII <sup>a</sup>	0.07	0.01	0.08	0.03	31.58	1.22	30.33	1.51	21.30	0.81	0.00	0.00	12.31	0.38	0.15	0.06	95.81	56.39	1.74	39.18	2.09		
S1911-38	A3	2	spnII <sup>a</sup>	0.02	0.00	0.12	0.01	34.81	0.55	30.85	0.06	21.77	0.39	0.26	0.02	12.51	0.03	0.08	0.01	100.42	54.74	0.07	37.29	0.42		
S1901-02	A4	9	core	0.07	0.02	0.08	0.04	42.47	1.54	23.99	1.61	15.91	0.54	0.04	0.07	15.69	0.43	0.18	0.05	98.43	66.26	1.37	27.49	2.04		
S1901-02	A4	10	small xx core	0.06	0.04	0.04	0.01	46.12	0.90	20.20	0.54	15.15	1.00	0.00	0.00	16.19	0.70	0.18	0.05	97.94	67.51	2.33	22.71	0.70		
S1901-02	A4	3	rim	0.04	0.01	0.17	0.13	36.23	0.95	30.10	0.82	17.38	0.55	0.12	0.10	14.49	0.51	0.11	0.10	98.64	62.93	1.72	35.79	1.22		
S1901-03	A4	3	core	0.05	0.04	0.03	0.04	43.53	5.02	23.98	4.68	16.34	0.29	0.17	0.09	15.80	0.35	0.15	0.05	100.04	65.88	0.24	27.08	6.12		
S1901-03	A4	1	spnII <sup>a</sup>	0.01	0.44	32.31	33.39	18.80	0.17	13.90	0.16	99.18	61.10	40.94												
S1901-04	A4	11	spnII <sup>a</sup>	0.03	0.02	0.17	0.14	32.48	1.69	33.59	1.81	19.41	0.67	0.00	0.00	13.14	0.50	0.11	0.05	98.94	58.14	1.78	40.97	2.41		
S1902-09	A4	4	core	0.02	0.03	0.09	0.04	41.50	3.89	27.39	3.41	16.91	1.03	0.10	0.11	14.95	1.16	0.14	0.02	101.09	62.47	3.62	30.77	4.54		
S1902-20	A4	1	core	0.11	0.06	45.09	22.58	16.87	0.21	14.98	0.21	99.90	62.32	25.14												
S1902-20	A4	1	spnII <sup>a</sup>	0.05	0.46	32.11	34.43	19.54	0.17	12.51	0.17	99.26	55.20	41.83												
S1904-62	A4	5	spnII <sup>a</sup>	0.05	0.04	0.09	0.01	31.97	1.03	32.91	1.05	19.90	1.71	0.00	0.00	12.76	0.86	0.15	0.03	97.83	57.28	3.65	40.85	1.51		
S1905-83	A4	9	core	0.02	0.02	0.10	0.04	46.51	1.13	20.78	0.99	13.60	0.26	0.07	0.08	17.57	0.14	0.20	0.06	98.85	72.28	0.91	23.06	1.11		
S1905-85	A4	2	core	0.06	0.00	0.04	0.03	45.33	0.05	22.61	1.23	14.68	0.34	0.21	0.03	15.66	0.72	98.59	65.48	3.19	25.06	1.04				
S1905-85	A4	4	spnII <sup>a</sup>	0.08	0.05	0.06	0.03	33.77	0.97	33.13	1.21	18.07	0.71	0.27	0.04	12.68	0.61	98.08	56.69	2.65	39.69	1.53				
S1905-87	A4	2	spnII <sup>a</sup>	0.00	0.12	0.04	32.09	0.48	34.43	0.69	19.07	0.11	0.00	0.00	13.08	0.35	0.10	0.07	98.89	58.10	1.34	41.85	0.85			
S1905-95	A4	5	spnII <sup>a</sup>	0.02	0.01	0.05	0.01	38.38	1.27	30.97	1.16	15.78	0.65	0.39	0.02	15.03	0.62	0.10	0.03	100.71	64.19	2.41	35.12	1.79		
S1907-03	A4	3	spnII <sup>a</sup>	0.04	0.02	0.09	0.03	39.11	1.94	24.79	2.01	21.39	0.06	0.00	0.12	11.0	0.57	0.14	0.05	97.66	53.17	2.06	29.85	2.72		

**Table 3c.** (continued)

Sample	Min.	Ass.	N.	An.	Spot	SiO <sub>2</sub>	1σ	TiO <sub>2</sub>	1σ	Al <sub>2</sub> O <sub>3</sub>	1σ	Cr <sub>2</sub> O <sub>3</sub>	1σ	FeOt <sub>tot</sub>	1σ	MnO	1σ	MgO	1σ	NiO	1σ	Total	Mg#	1σ	C#	1σ
S1907-03	A4	2			rim	0.03	0.00	0.23	0.08	29.33	1.14	35.43	0.44	23.86	0.75	0.00	0.03	0.44	0.09	0.06	98.99	45.70	1.70	44.77	1.27	
S1907-25	A4	2			core	0.04	0.02	0.04	0.00	48.18	0.01	18.34	0.07	15.94	0.10	0.00	0.00	16.59	0.02	0.17	0.00	99.30	67.85	0.05	20.33	0.06
S1907-25	A4	5			small xx core	0.03	0.01	0.05	0.03	42.97	1.52	23.49	1.32	16.89	1.06	0.00	0.00	15.49	0.56	0.12	0.06	99.03	65.05	1.93	26.84	1.74
S1907-25	A4	4			rim	0.03	0.03	0.13	0.08	36.44	1.94	30.03	1.74	18.95	0.84	0.00	0.00	13.98	0.70	0.13	0.05	99.68	60.25	2.29	35.62	2.53
S1908-02	A4	5			spnII <sup>a</sup>	0.01	0.02	0.10	0.03	33.21	1.53	33.11	1.64	20.54	0.55	0.05	0.10	12.56	0.65	0.09	0.07	99.67	55.42	2.40	40.09	2.24
S1908-03	A4	12			core	0.03	0.02	0.05	0.03	52.99	0.90	13.95	0.77	12.39	0.44	0.00	0.00	18.36	0.43	0.22	0.04	97.99	73.88	1.58	15.01	0.88
S1910-02	A4	3			spnII <sup>a</sup>	0.04	0.07	0.05	0.04	33.16	2.39	35.15	2.19	16.27	0.61	0.00	0.00	13.82	0.46	0.07	0.06	98.55	61.02	1.31	41.59	3.26
S1910-03	A4	2			spnII <sup>a</sup>	0.01	0.01	0.03	0.04	37.96	1.56	31.87	1.03	16.68	0.35	0.00	0.00	14.16	0.69	0.00	0.00	100.70	60.21	1.96	36.03	1.69
S1910-04	A4	5			spnII <sup>a</sup>	0.04	0.03	0.03	0.01	29.85	1.83	35.87	1.22	19.04	1.25	0.00	0.00	12.29	0.95	0.08	0.06	97.20	56.08	3.47	44.66	2.32
S1911-02	A4	3			spnII <sup>a</sup>	0.00	0.00	0.26	0.05	33.14	0.76	34.25	2.19	19.64	0.56	0.05	0.01	12.76	0.48	0.00	0.10	100.10	54.47	1.22	40.92	2.00
S1911-03	A4	1			core	0.00	0.14			44.65		20.47		15.77		0.00		16.88		0.33		98.24	70.52			
S1911-03	A4	1			spnII <sup>a</sup>	0.00	0.32			32.31		32.44		20.96		0.00		13.57		0.17		99.77	59.40			
S1911-13	A4	6			core	0.02	0.03	0.05	0.01	53.33	0.44	15.16	0.19	12.22	0.16	0.27	0.36	18.70	0.18	0.32	0.02	100.07	74.54	0.71	16.01	0.26
S1911-63	A4	3			core	0.06	0.03	0.05	0.02	48.22	1.64	19.59	1.45	14.34	0.82	0.15	0.03	16.31	0.58	0.00	0.00	98.71	67.07	1.54	21.42	1.76
S1911-64	A4	2			core	0.03	0.04	0.07	0.05	53.28	0.87	15.00	0.56	12.76	0.12	0.10	0.00	17.85	0.23	0.00	0.00	99.10	71.23	0.22	15.89	0.71
S1907-23	A5	1			spnII <sup>a</sup>	0.00	0.13			39.09		24.58		21.22		0.00		13.44		0.15		98.61	58.11			

<sup>a</sup> Spn neoblasts.**Table 3d.** Average Major Element Oxide Composition of Olivine From VLS Ultramafic Mylonites

Sample	Min.	Ass.	N.	An.	SiO <sub>2</sub>	1σ	FeOt <sub>tot</sub>	1σ	MnO	1σ	MgO	1σ	CaO	1σ	NiO	1σ	Total	Mg#	1σ
S1915-40	A1	2			41.14	0.23	9.47	0.12	0.13	0.00	50.12	0.02	0.00	0.02	0.36	0.05	101.22	90.41	0.11
S1915-44	A2	1			43.16		10.20		0.14		47.86		0.04		0.38		101.78	89.32	
S1904-61	A3	2			40.32	0.39	9.45	0.12	0.16	0.01	49.78	0.35	0.01	0.01	0.36	0.02	100.07	90.37	0.17

**Table 3e.** Average Major Element Oxide Composition, REE, Trace Element, and Isotopes of Selected Amphiboles From VLS Ultramafic Mylonites<sup>a</sup>

	Sample												
	S1901-02	S1901-04	S1902-09	S1904-61	S1904-62	S1905-85	S1905-95	S1907-03	S1909-01	S1910-03	S1911-63	S1915-44	S2201-01 (in Vein)
SiO <sub>2</sub>	49.34 (59)	49.44 (93)	49.63 (128)	46.06 (87)	50.32 (167)	50.27 (82)	49.49 (79)	49.49 (73)	46.56 (51)	54.53 (128)	50.09 (153)	44.68 (87)	48.49 (163)
TiO <sub>2</sub>	0.33 (9)	0.44 (6)	0.32 (8)	0.59 (4)	0.35 (11)	0.30 (6)	0.13 (7)	0.70 (19)	0.03 (1)	0.30 (6)	1.17 (8)	0.14 (3)	-
Al <sub>2</sub> O <sub>3</sub>	9.76 (75)	8.81 (67)	8.87 (138)	10.45 (70)	8.52 (142)	8.73 (48)	10.27 (39)	9.23 (68)	13.19 (63)	4.76 (3)	9.08 (122)	13.10 (55)	7.03 (86)
FeO	3.30 (13)	3.41 (11)	3.29 (40)	3.81 (13)	3.20 (26)	2.94 (11)	2.93 (17)	4.14 (13)	3.98 (17)	2.22 (18)	2.77 (9)	4.01 (3)	4.38 (24)
MnO	0.03 (3)	0.03 (4)	0.05 (3)	0.03 (2)	0.02 (3)	0.06 (5)	0.06 (3)	0.06 (3)	0.05 (3)	0.08 (0)	0.07 (4)	0.03 (4)	0.07 (4)
MgO	19.54 (46)	19.88 (43)	21.05 (124)	18.96 (49)	19.62 (63)	19.74 (41)	20.29 (48)	19.44 (47)	19.09 (34)	21.95 (6)	20.40 (52)	17.95 (49)	20.63 (50)
CaO	12.70 (17)	12.83 (29)	11.54 (96)	12.91 (30)	13.16 (17)	12.35 (17)	12.51 (38)	12.72 (29)	12.85 (10)	12.31 (19)	12.28 (14)	11.49 (9)	-
Na <sub>2</sub> O	1.33 (10)	1.28 (29)	1.16 (23)	1.83 (12)	0.91 (18)	0.92 (8)	1.25 (14)	1.28 (13)	2.01 (10)	0.69 (6)	2.93 (6)	1.48 (20)	1.99 (25)
K <sub>2</sub> O	0.03 (1)	0.02 (2)	0.02 (1)	0.02 (2)	0.02 (1)	0.02 (1)	0.08 (1)	0.08 (1)	0.05 (1)	0.03 (2)	0.05 (1)	0.04 (2)	0.04 (1)
<sup>143</sup> Nd/ <sup>144</sup> Nd	-	-	-	-	0.513400	0.513183	0.513235	0.513171	0.513114	-	0.513126	-	0.513182
±2σ	-	-	-	-	0.000011	0.000018	0.000018	0.000011	0.000009	-	0.000012	-	0.000103
<sup>87</sup> Sr/ <sup>86</sup> Sr	-	-	-	-	0.703139	0.703028	0.703044	0.703078	0.702818	-	0.703058	-	0.703655
±2σ	-	-	-	-	0.000011	0.000008	0.000008	0.000013	0.000010	-	0.000011	-	0.000013
Sr ID (ppm)	-	-	-	-	1.86	3.12	0.58	5.10	8.99	-	36.85	-	82.67
Sm ID (ppm)	-	-	-	-	0.528	0.519	0.321	0.569	0.796	-	1.16	-	9.05
Nd ID (ppm)	-	-	-	-	0.622	0.693	0.658	1.12	1.66	-	3.42	-	25.87
<sup>147</sup> Sm/ <sup>144</sup> Nd	-	-	-	-	0.513	0.453	0.295	0.306	0.290	-	0.204	-	0.211
δ <sup>18</sup> O	-	-	-	-	5.84	6.20	5.88	6.30	6.01	-	6.20	-	6.63
Ti	1729	2065	1857	1622	2704	1951	2151	7868	4594	223	2146	6447	-
Cr	5634	6300	2582	4122	9483	7345	10135	3573	6463	6871	2023	12945	-
Sr	7.04	3.37	6.46	4.95	5.66	11.87	7.24	21.78	39	6.32	15.51	12.92	-
Y	8.50	13.50	8.67	9.22	17.62	10.76	12.12	21.63	17.18	2.28	117.86	76	-
Zr	5.08	4.61	8.44	5.90	5.18	7.22	9.88	36.76	35.4	11.5	78.99	83	-
K	-	114	-	-	-	-	-	-	329	252	-	367	-
Sc	-	60	-	-	-	-	-	-	42	75	-	123	-
V	-	335	-	-	-	-	-	-	278	295	-	534	-
Nb	-	0.08	-	-	-	-	-	-	2.1	0.10	-	1.9	-
Cs	-	0.00	-	-	-	-	-	-	0.00	0.01	-	0.03	-
Ba	-	0.3	-	-	-	-	-	-	4.2	0.9	-	0.7	-
La	0.54	0.15	0.21	0.92	0.26	0.96	0.74	0.53	1.43	0.32	10.58	0.20	-
Ce	0.73	0.80	1.09	0.30	0.53	1.09	1.19	2.41	4.29	0.23	47.78	2.73	-
Nd	1.36	2.08	1.40	1.60	0.97	1.09	1.23	3.70	4.96	0.46	46.67	9.26	-
Sm	0.70	0.92	0.85	1.01	0.61	0.42	0.70	1.45	1.74	0.14	13.35	5.65	-
Eu	0.41	0.37	0.41	0.50	0.29	0.28	0.33	0.67	0.61	0.07	2.34	1.57	-
Gd	-	1.43	-	-	-	-	-	-	2.22	0.21	-	8.64	-
Dy	1.42	2.12	1.64	3.01	2.30	1.42	1.67	3.18	2.87	0.32	20.35	11.5	-
Er	1.01	1.44	1.15	1.98	1.50	1.12	1.09	2.12	1.96	0.30	13.64	7.56	-
Yb	1.14	1.68	1.30	2.38	1.75	0.98	1.10	2.06	1.81	0.55	14.48	7.69	-

<sup>a</sup>The 1σ standard deviation in parentheses refers to the last digit.

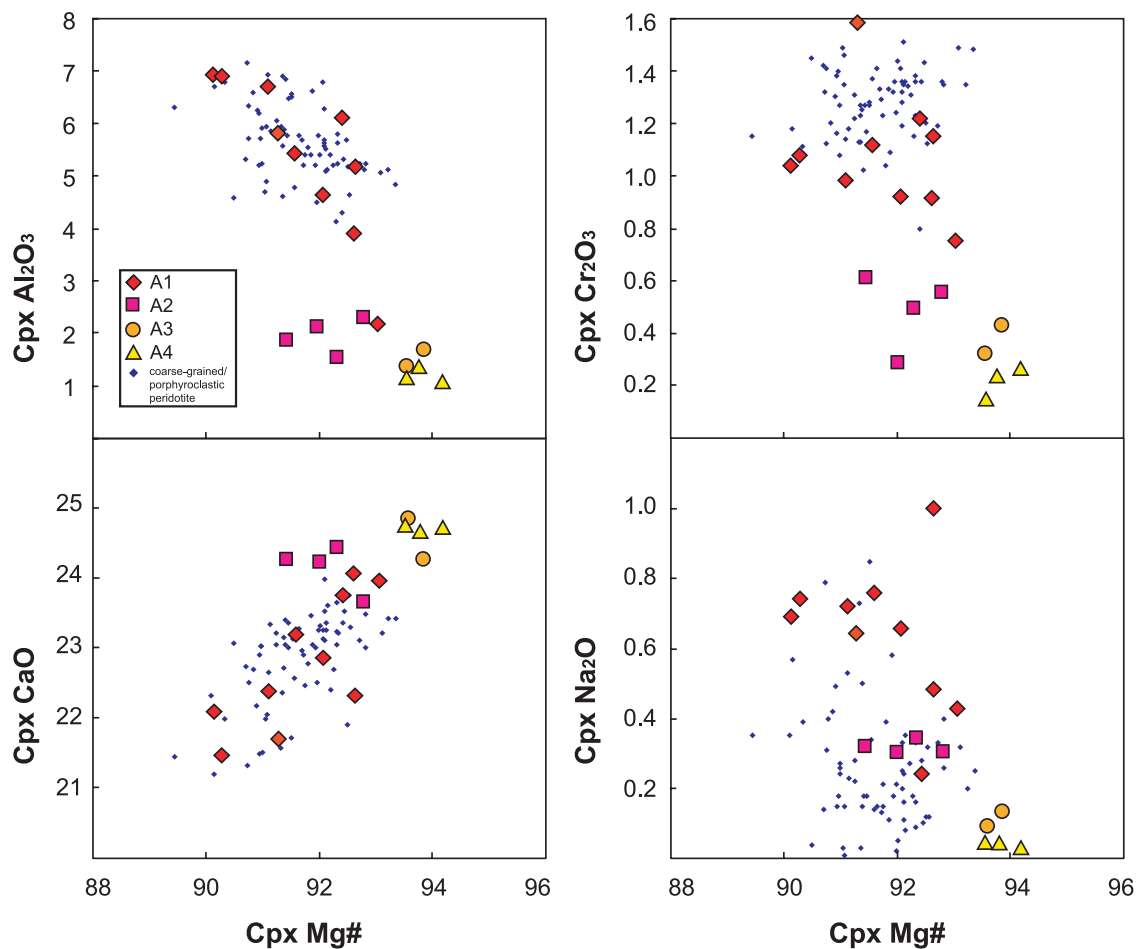


**Figure 3.**  $\text{Al}_2\text{O}_3$ ,  $\text{CaO}$ ,  $\text{Cr}_2\text{O}_3$ , and  $\text{Na}_2\text{O}$  (wt%) versus  $\text{Mg}\#$  [=100Mg/(Mg + Fe)] in clinopyroxenes from the VLS ultramafic mylonites and coarse-grained/poikiloblastic peridotites. A1 to A4 mineral assemblages are defined in the text.

### 5.1. Olivine and Pyroxene

[28]  $\text{Mg}\#$  [=Molar Mg/(Mg + Fe)] vary from 0.893 to 0.904 in olivine, from 0.899 to 0.929 in opx, and from 0.901 to 0.942 in cpx (Figure 3). The values of rims and small recrystallized pyroxenes are slightly higher than those of the coarse porphyroblast cores.  $\text{Al}_2\text{O}_3$  and  $\text{Cr}_2\text{O}_3$  in both pyroxenes,  $\text{CaO}$  in opx and  $\text{Na}_2\text{O}$  in cpx, show decreasing contents from porphyroblast cores to porphyroblast rims and to neoblasts. In all the mineral assemblages,  $\text{Al}_2\text{O}_3$  and  $\text{Cr}_2\text{O}_3$  contents range from 1.37 to 5.83 wt% and from 0.23 to 1.07 wt%, respectively, in opx, and from 1.02 to 6.93 wt% and from 0.14 to 0.92 wt%, respectively, in cpx.  $\text{CaO}$  contents in opx decrease from 0.52 to 1.58 wt% in A1 ultramafics, through 0.58–1.1 wt% in A2 ultramafics, to 0.44–0.48 wt% in A3 ultramafics.  $\text{CaO}$  content in opx from A4 ultramafics is very scattered (0.44–1.39 wt%) but consistent with the overall decreasing trend.  $\text{Na}_2\text{O}$  contents in cpx

neoblasts decrease from 0.43 to 0.49 wt% in A1 ultramafics, 0.31–0.34 wt% in A2 ultramafics, through 0.09–0.13 wt% in A3 ultramafics, to <0.04 wt% in A4 ultramafics. Cpx neoblasts in all the mineral assemblages have higher  $\text{CaO}$  contents (24–24.9 wt%) than cpx porphyroblasts (21.7–23.8 wt%). Thus,  $\text{CaO}$  in opx and  $\text{Na}_2\text{O}$  in cpx show overall trends consistent with decreasing metamorphic grade from A1 to A4 mineral assemblages.

### 5.2. Spinel

[29]  $\text{Cr}\#$  [=100 × Cr/(Cr + Al)] of coarse spinel relics ranges from 13 to 36 encompassing the  $\text{Cr}\#$  range of the VLS coarse-grained/poikiloblastic peridotites (Figure 4). Spinel relics, with  $\text{TiO}_2 < 0.1\%$ , have low  $\text{Cr}\#$  (~15–25) in line with the idea that the parent mantle rocks were residual peridotites that underwent a low degree of melting. Small grains and porphyroblast rims show higher  $\text{Cr}\#$

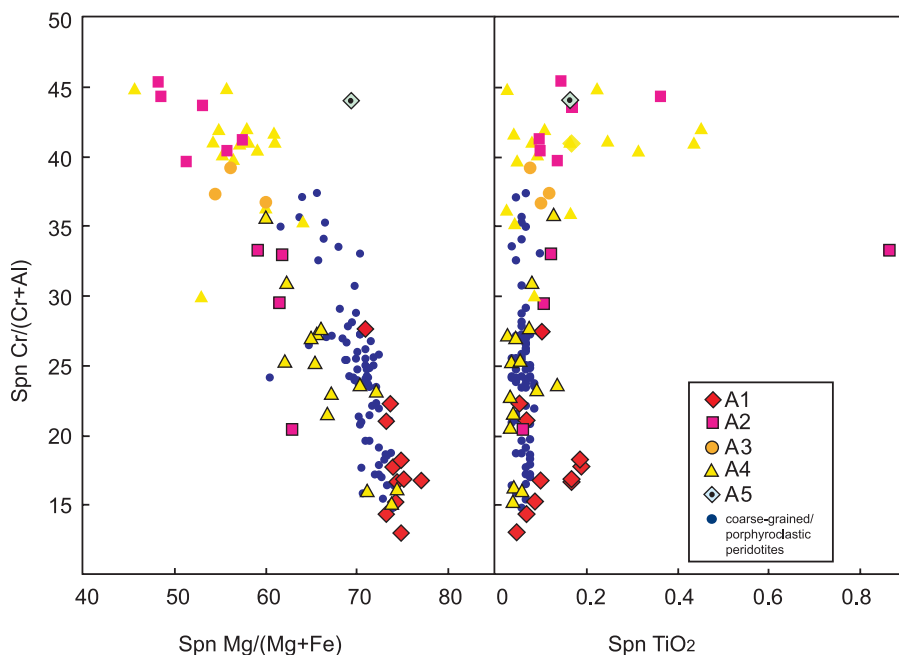


**Figure 4.** Cr# [=100Cr/(Al + Cr)] versus Mg# [=100Mg/(Mg + Fe)] and TiO<sub>2</sub> (wt.%) in spinel from the VLS ultramafic mylonites and coarse-grained/polyphroclastic peridotites. Symbols with black border represent spinel coarse grain cores. Symbols without black border represent coarse grain rims and neoblasts. A1 to A5 mineral assemblages are defined in the text.

(~35–45) and extend to higher TiO<sub>2</sub>. They probably represent grains recrystallized during metamorphism, a process known to increase the Cr# [Evans and Frost, 1975].

### 5.3. Amphiboles

[30] Their composition in representative samples (major elements, trace and REE elements as well as isotopic data) is shown in Table 3e. The complete data set of amphibole analyses by dredge site is presented in Tables A1a–A11. Analyses have been recalculated on an anhydrous basis of 23 oxygens and FeO = total iron, as suggested for low-iron amphiboles [Evans, 1982]. Amphiboles from the entire sample set, except four samples from Sites S1907 and S1910 enriched in Fe and Ti, define a single trend characterized by decrease in Al, Na, [Na + K]<sub>A</sub>, Ti and Fe/Mg as Si content increases (Figure 5). Their compositions, according to Leake *et al.*'s [1997] nomenclature, vary from pargasites in A2 ultramafics through magnesiohornblendes in A3 and A4 ultramafics to tremolites in A5 ultramafics. Amphibole grains are unzoned, except in sample S1915-37, where pargasitic cores are mantled by magnesiohornblende. Individual samples have more restricted ranges of composition, generally unimodal (Figure 6), but also bimodal, as in the polyphased A4–A5 ultramylonites.

[31] The majority of the amphiboles are REE-depleted relative to VLS basalts (A. Cipriani *et al.*, manuscript in preparation, 2009) but REE-enriched relative to the VLS cpxs in polyphroclastic peridotites [Brunelli *et al.*, 2006] (Figure 7). The amphiboles HREE patterns are somewhat flat and mimic those of the basaltic glasses, although they are more depleted. The LREEs of the amphiboles are more scattered and exhibit a wider range of depletion than the basalts. We found only one amphibole (S1911-63) more enriched than the basaltic glasses.

[32] The chlorine content of the amphiboles stays below 0.6 wt%, being mostly below 0.2%.

### 5.4. Plagioclase

[33] Plagioclase composition was obtained in sample S1911-05 using SEM-EDS. Grains are unzoned, but show large variations from one grain to another, varying from An<sub>42</sub> to An<sub>89</sub>. Chlorite compositions are close to the clinochlore end-member. Si/Al ratios in five samples average  $1.33 \pm 0.07$ .

### 5.5. Amphibole Isotopic Chemistry

#### 5.5.1. Sr-Nd Isotopes

[34] The Sr and Nd isotopic composition of seven different amphiboles (Table 3e and Figure 8) shows

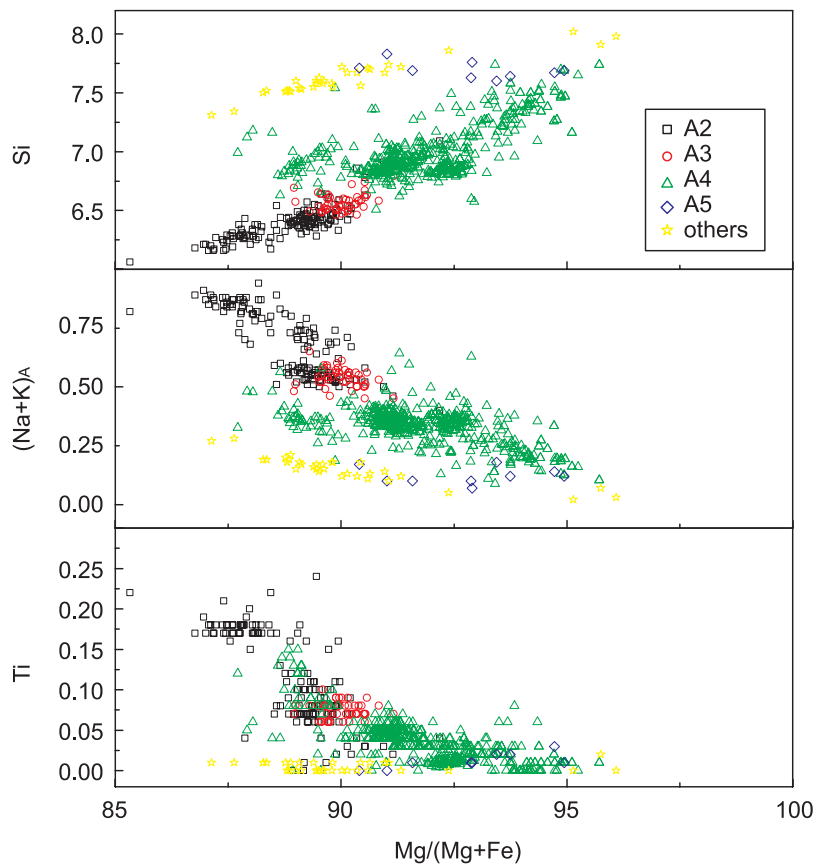


**Figure 5.** Si,  $\text{Na}^+\text{K}$ , and Ti (at. pfu) versus Mg# [=100Mg/(Mg + Fe)] in amphiboles from VLS ultramafic mylonites (individual spot analyses are plotted). A2 to A5 mineral assemblages are defined in the text. “Others” are special samples S1907-12 and S1907-32.

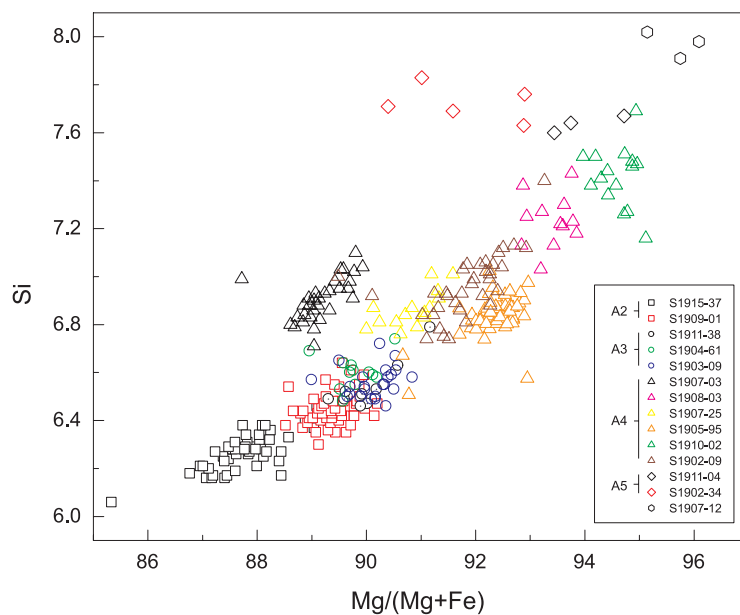


**Figure 6.** Si (at. pfu) versus Mg# [=100Mg/(Mg + Fe)] of amphiboles in selected samples from VLS ultramafic mylonites (individual spot analyses are plotted). Samples were chosen to encompass the whole range of compositions. Note that S1907-12 is the only sample with talc.

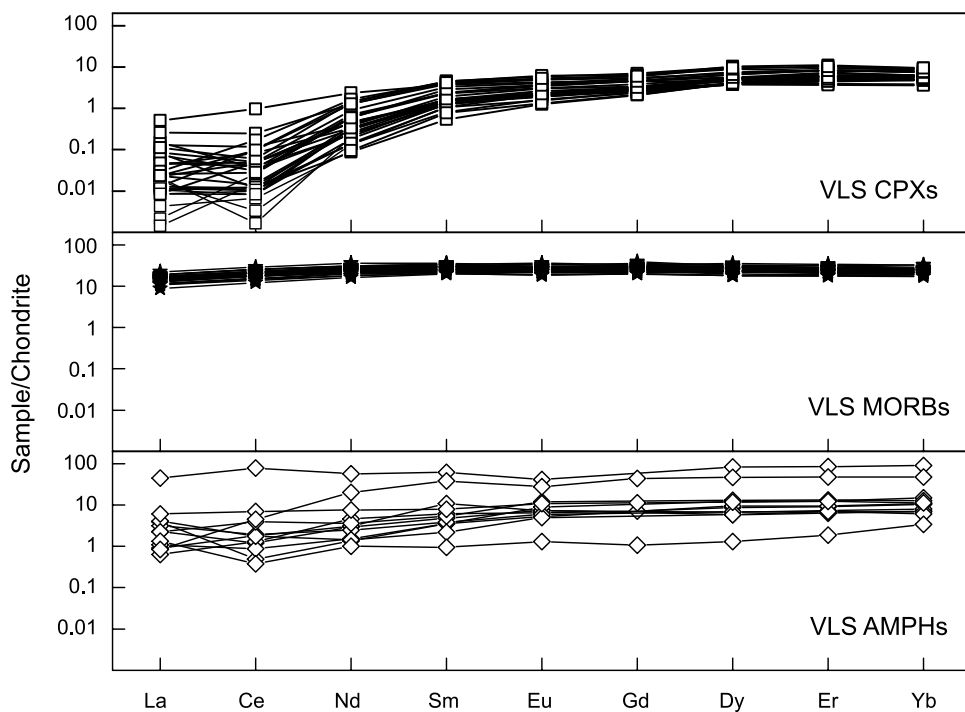


**Figure 7.** Chondrite-normalized REE distributions in VLS formations. (top) Clinopyroxenes from porphyroclastic peridotites [Brunelli et al., 2006], (middle) basaltic glasses (A. Cipriani et al., manuscript in preparation, 2009), and (bottom) amphiboles from ultramafic mylonites (this study). Normalizing values are from Anders and Grevesse [1989].

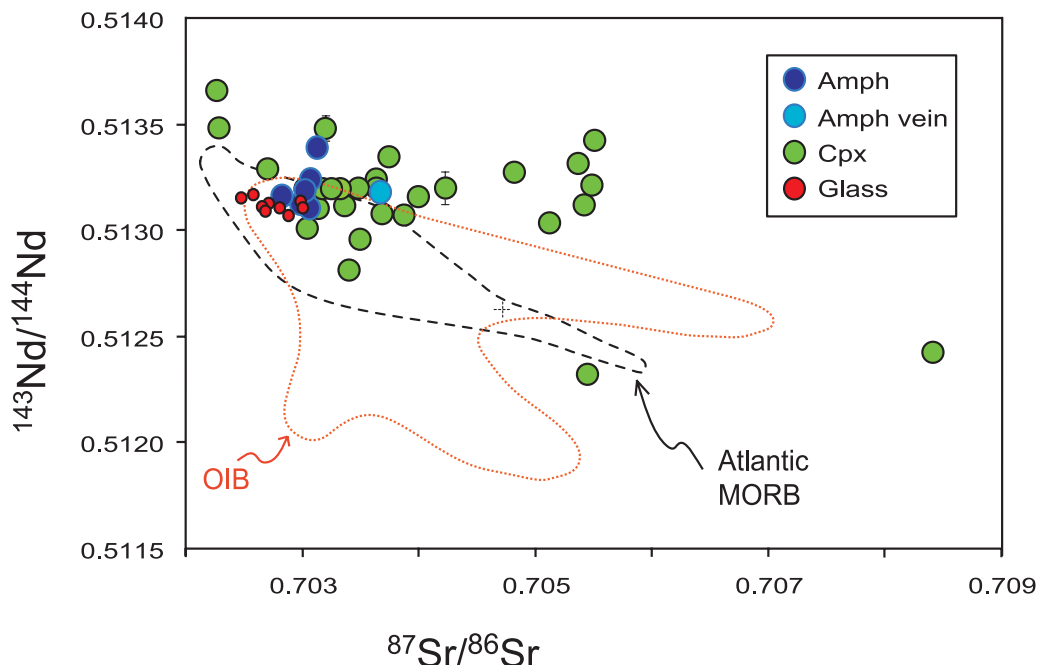


**Figure 8.** Nd versus Sr isotopic compositions of VLS amphiboles from ultramafic mylonites and clinopyroxenes from porphyroclastic peridotites and associated basaltic glasses (cpx and glass data from Cipriani et al. [2004] and unpublished data). The fields of Atlantic MORB glass and OIB glass are reported for comparison (<http://www.petdb.org>).

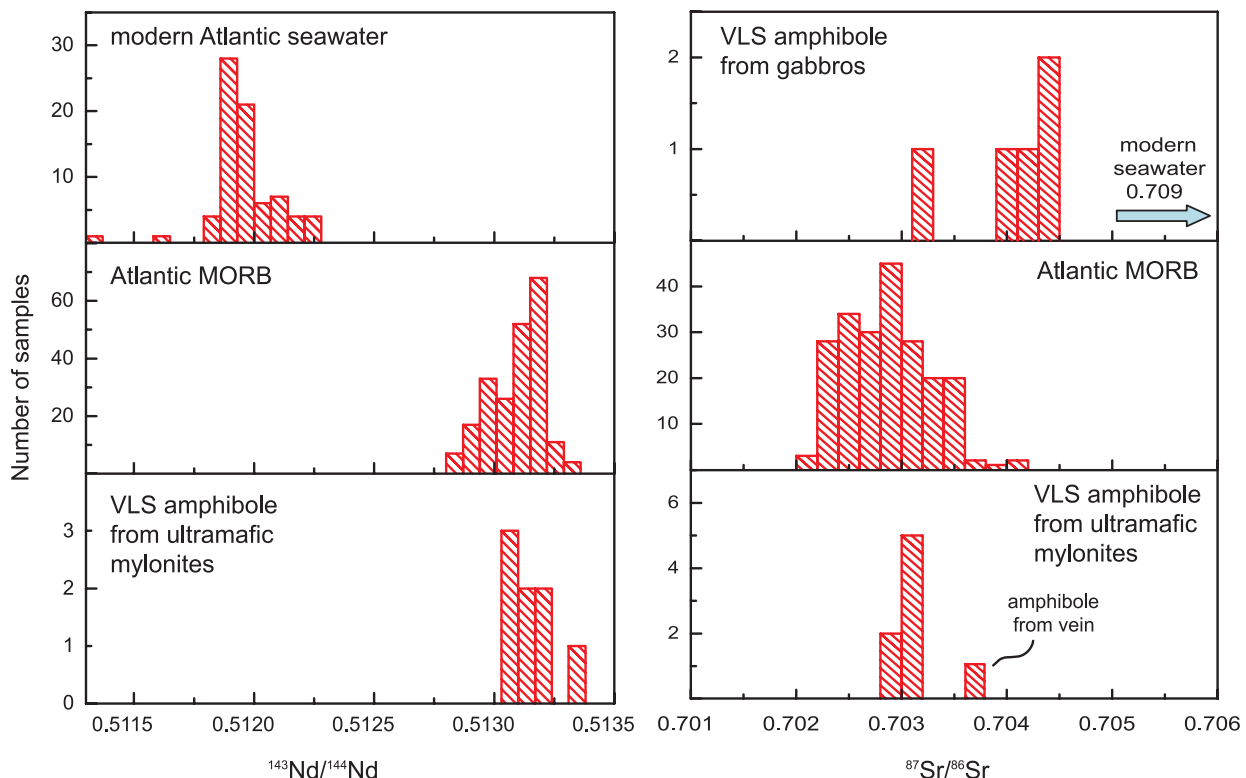


**Figure 9.** Histograms of Nd and Sr isotopic compositions for amphiboles from VLS ultramafic mylonites, Atlantic MORB, and Atlantic seawater and amphiboles from VLS gabbros (<http://www.petdb.org>) [Talbi et al., 1999; Lacan and Jeandel, 2004, and references therein].

depleted, MORB-type ratios ( $^{143}\text{Nd}/^{144}\text{Nd} = 0.513114 \pm 12$  and  $0.513400 \pm 11$ ;  $^{87}\text{Sr}/^{86}\text{Sr} = 0.702818 \pm 10$  and  $0.703139 \pm 11$ , respectively). The amphibole  $^{87}\text{Sr}/^{86}\text{Sr}$  ratios do not show the seawater signature detected in some clinopyroxenes from abyssal peridotites [Snow et al., 1994; Salters and Dick, 2002; Cipriani et al., 2004], suggesting either little or no involvement of seawater or isotopic re-equilibration during fluid circulation in the upper mantle. The amphibole isotopic data generally overlap with those of the VLS basaltic glasses [Cipriani et al., 2004] with three amphiboles showing a Sr isotopic composition slightly higher than that of the VLS basalts. One amphibole has also higher Nd isotopic composition, just outside the Atlantic MORB field. Amphibole separated from a vein crosscutting a porphyroclastic peridotite (vein from sample S2201-01) has a  $^{143}\text{Nd}/^{144}\text{Nd}$  ratio of 0.513182 ( $\pm 13$ ), in the range of other VLS amphiboles. However, its  $^{87}\text{Sr}/^{86}\text{Sr}$  is much higher ( $0.703655 \pm 13$ ) just outside the Atlantic MORB field.

[35] A histogram of the Nd and Sr isotopic composition of the VLS peridotitic amphiboles compared to Atlantic MORB and Atlantic seawater

values is presented in Figure 9, including also the  $^{87}\text{Sr}/^{86}\text{Sr}$  composition of five amphiboles from two VLS gabbros [Talbi et al., 1999]. The VLS gabbro amphiboles have on average higher  $^{87}\text{Sr}/^{86}\text{Sr}$  than the VLS peridotitic amphiboles and Atlantic MORB. The VLS gabbro amphibole  $d^{18}\text{O}$  values (5.1 to 2.8) indicate interaction with seawater between 300° and 600°C [Talbi et al., 1999], whereas our Sr data show no evidence for this interaction. The Sr isotopic composition of the amphibole vein is more radiogenic and closer to that of the gabbroic amphiboles.

### 5.5.2. Oxygen Isotopes

[36] The  $\delta^{18}\text{O}$  values of the VLS peridotitic amphiboles fall within the MORB field ranging from +5.8‰ to +6.6‰ (Table 3e) with an average of  $+6.1 \pm 0.3\text{‰}$  (Figure 10), although their average is 0.4‰ higher than the MORB average ( $+5.7 \pm 0.2\text{‰}$  [Harmon and Hoefs, 1995]). The  $\delta^{18}\text{O}$  values of the VLS peridotitic amphiboles are also comparable to the higher end of the  $\delta^{18}\text{O}$  distribution in amphiboles from oceanic and ophiolitic gabbros (Figure 10), where low  $\delta^{18}\text{O}$  gabbros are usually altered by high temperature hydrothermal

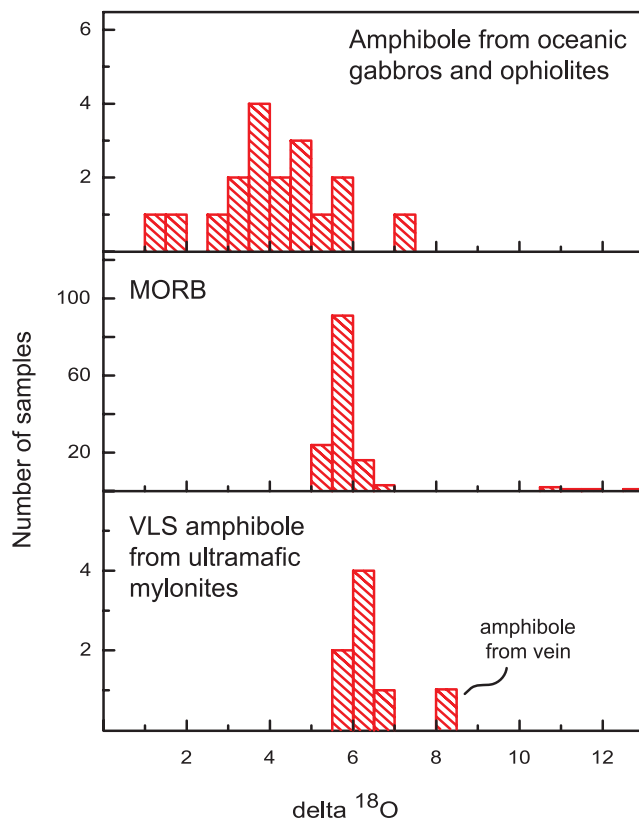


**Figure 10.** Oxygen isotope compositions of amphiboles from VLS ultramafic mylonites and normal MORB and amphiboles from oceanic and ophiolitic gabbros (<http://www.petdb.org>) [Talbi et al., 1999; Tribuzio et al., 1999].

fluids [Gregory and Taylor, 1981; Eiler, 2001]. Amphibole separated from the vein crosscutting peridotite S2201-01 has a  $\delta^{18}\text{O}$  value of  $+8.08 \pm 0.2\text{\textperthousand}$ , clearly due to low temperature alteration.

[37] The bulk oxygen isotope fractionation between peridotite and melts is on the order of  $+0.2\text{\textperthousand}$  for high degrees of partial melting at  $1400^\circ\text{C}$  (mantle =  $+5.5 \pm 0.7\text{\textperthousand}$  [Mattey et al., 1994]). At a lower peridotite solidus temperature the mineral-melt fractionation will be larger but the highest  $\delta^{18}\text{O}$  values of basaltic liquids in equilibrium with the peridotitic mantle should not be higher than  $+6\text{\textperthousand}$  to  $+6.5\text{\textperthousand}$  [Mattey et al., 1994]. Indeed, the  $\delta^{18}\text{O}$  average of the VLS peridotitic amphiboles is close to these values (being  $+6.1 \pm 0.3\text{\textperthousand}$ ); if mantle-like fluids/melts have contributed to the formation of the VLS peridotitic amphiboles, then, slightly higher than mantle  $\delta^{18}\text{O}$  values might indicate lower mantle temperatures during their formation.

## 6. Amphibole Ar/Ar Ages

[38] Four  ${}^{40}\text{Ar}/{}^{39}\text{Ar}$  ages were obtained from three mylonites. All four samples yielded plateau ages

(Tables 4a and 4b and Figure 11). The analytical precision of the data, however, are limited because of the small sample size and low K content of the amphiboles. Evaluation of the results follows the protocol of Turrin et al. [1998, 2007], which in turn is based on Fleck et al. [1977] and Dalrymple and Lanphere [1969, 1974]. The most precise age ( $14.2 \pm 0.8$  Ma) is the plateau age obtained on sample S1905-95. The seven-step plateau comprises 100% of the total  ${}^{39}\text{Ar}_\text{K}$  and has a corresponding integrated total fusion age of  $14.2 \pm 1.4$  Ma. When the plateau data are cast on an isotope correlation diagram, the isotopic data produce a well-defined mixing line with a MSWD of 1.1, suggesting that the dispersion of the data about the regression line is due to measurement errors. The mixing line that corresponds to an age  $14.6 \pm 1.2$  Ma and an initial  ${}^{40}\text{Ar}/{}^{36}\text{Ar}$  ratio of  $293.2 \pm 5.8$ , that is analytically indistinguishable from atmospheric Ar at the  $\alpha$ -95% confidence level.

[39] A six-step plateau age of  $16 \pm 4$  Ma was obtained on sample S1905-85. The plateau is defined by 99% the total  ${}^{39}\text{Ar}_\text{K}$  and is concordant with the integrated age of  $18 \pm 6$  Ma. The plateau

**Table 4a.** Ar/Ar Data From Three Selected Amphiboles From VLS Ultramafic Mylonites

Run ID	Temp. (°C)	Ca/K	Cl/K	$^{36}\text{Ar}/^{39}\text{Ar}$	% $^{36}\text{Ar}_{\text{Ca}}$	$^{40}\text{Ar}^*/^{39}\text{Ar}$	%Step	Cum%	% $^{40}\text{Ar}^*$	Age (Ma)	$\pm 1\sigma$
<i>S1905-95(c5), Run ID 1029-01<sup>a</sup></i>											
1029-01A <sup>b</sup>	546	24.09	0.687	0.241	1.3	2.88	4.2	4.2	3.9	12.4	9.2
1029-01B <sup>b</sup>	651	45.45	0.611	0.842	0.7	2.24	1.1	5.3	0.9	9.7	34.5
1029-01C <sup>b</sup>	748	118.85	0.233	0.157	10	6.09	1.6	6.9	12.1	26.2	25.2
1029-01D <sup>b</sup>	855	177.13	0.259	0.094	25	3.27	20.3	27.2	12.7	14.1	2.3
1029-01E <sup>b</sup>	953	175.30	0.260	0.044	52.3	3.31	64.2	91.4	32.8	14.3	0.9
1029-01F <sup>b</sup>	1003	178.61	0.257	0.080	29.6	3.86	5.3	96.7	17.6	16.6	7.3
1029-01G <sup>b</sup>	1100	179.26	0.208	0.121	19.6	1.99	3.3	100	6	8.6	9.5
<i>S1905-85(c4), Run ID 1028-01<sup>c</sup></i>											
1028-01A <sup>d</sup>	550	16.46	0.408	0.128	1.7	5.98	14	14	13.8	25.7	8.7
1028-01B <sup>d</sup>	651	24.08	0.200	0.419	0.8	12.59	4.7	18.7	9.2	53.7	28.5
1028-01D <sup>d</sup>	847	538.43	0.679	0.192	37	2.59	36.6	55.3	5.2	11.2	7.4
1028-01E <sup>d</sup>	953	481.28	0.695	0.141	45.2	3.23	37.1	92.4	9.9	13.9	5.4
1028-01F <sup>d</sup>	997	402.18	0.520	0.396	13.4	4.50	3.9	96.3	3.5	19.4	59.6
1028-01G <sup>d</sup>	1057	505.80	0.550	0.523	12.8	6.77	2.6	99	3.7	29.1	71.3
1028-01H	1100	634.64	-0.019	1.090	7.7	17.61	1	100	4	74.7	235.7
<i>S1909-01(c1a), Run ID 1030-01<sup>e</sup></i>											
1030-01A <sup>f</sup>	546	35.73	0.281	0.125	3.8	2.63	52.3	52.3	6.8	11.4	8.5
1030-01D <sup>f</sup>	847	192.45	0.291	0.225	11.3	13.57	10.1	62.4	17.3	57.8	57.7
1030-01E <sup>f</sup>	902	207.54	0.452	0.127	21.6	1.25	28.5	91	3.7	5.4	18.2
1030-01F <sup>f</sup>	954	185.42	0.697	0.597	4.1	-37.03	4.4	95.3	-25	-167.9	131.1
1030-01G	1003	214.39	-0.663	0.432	6.6	127.62	2.3	97.6	49.1	482.0	156.7
1030-01H	1102	144.64	0.118	1.069	1.8	3.65	3.3	100.9	1.1	15.7	108.6
1030-01I	1302	-4.69	-2.557	-11.719	0	-51.06	-0.9	100	1.5	-235.8	803.5
<i>S1909-01(c1), Run ID 1027-01<sup>g</sup></i>											
1027-01A	560	10.04	0.203	0.125	1.1	12.13	9	9	24.8	51.8	11.9
1027-01K <sup>h</sup>	851	213.35	0.358	0.151	18.7	2.02	12.4	21.4	4.8	8.7	23.2
1027-01L <sup>h</sup>	879	215.25	0.435	0.063	45.1	5.44	52.7	74	32.4	23.4	4.9
1027-01M <sup>h</sup>	902	212.70	0.396	0.050	56.3	3.70	24	98.1	34.1	16.0	10.1
1027-01Q	1004	226.51	0.197	0.137	21.9	39.39	1.9	100	52.7	163.0	111.0

<sup>a</sup>J = 0.0024 ± 6.568000e-6. Integrated age is 14.2 ± 1.4 Ma.<sup>b</sup>Plateau age is %<sup>39</sup>Ar<sub>K</sub> = 100: 14.2 ± 0.8 Ma.<sup>c</sup>J = 0.0024 ± 6.568000e-6. Integrated age is 18 ± 6 Ma.<sup>d</sup>Plateau age is %<sup>39</sup>Ar<sub>K</sub> = 99: 16 ± 4 Ma.<sup>e</sup>J = 0.0024 ± 6.568000e-6. Integrated age is 21 ± 8 Ma.<sup>f</sup>Plateau age is %<sup>39</sup>Ar<sub>K</sub> = 95.3: 11 ± 8 Ma.<sup>g</sup>J = 0.0024 ± 6.568000e-6. Integrated age is 25 ± 4 Ma.<sup>h</sup>Plateau age is %<sup>39</sup>Ar<sub>K</sub> = 89.1: 22 ± 4 Ma.**Table 4b.** Isochron Ages and Initial  $^{40}\text{Ar}/^{36}\text{Ar}$  for Three Selected Amphiboles From VLS Ultramafic Mylonites

Sample	Run ID	Age (Ma)	$\pm 1\sigma$	$^{40}\text{Ar}/^{36}\text{Ar}_{\text{init}}$	$\pm 1\sigma$	MSWD
Isochron plateau data						
S1905-95(c5)	1029	14.6	1.2	293.2	5.8	1.1
S1905-85(c4)	1028	6.8	3.9	312.5	16.8	0.6
S1909-01(c1a)	1030	27.5	14.0	263.3	51.3	1.2
S1909-01(c1)	1027	23.6	8.6	283.3	50.9	0.7
Isochron all data						
S1905-95(c5)	1029	14.6	1.2	293.2	5.8	1.1
S1905-85(c4)	1028	7.2	4.0	311.8	15.7	0.5
S1909-01(c1a)	1030	5.6	2.4	306.4	19.8	2.7
S1909-01(c1)	1027	11.5	5.0	360.7	35.9	1.0
Isochron plateau data						
S1909-01	1027 and 1030	26.0	5.2	267.4	18.3	0.7
Isochron all data						
S1909-01	1027 and 1030	18.9	4.4	307.1	15.9	2.3

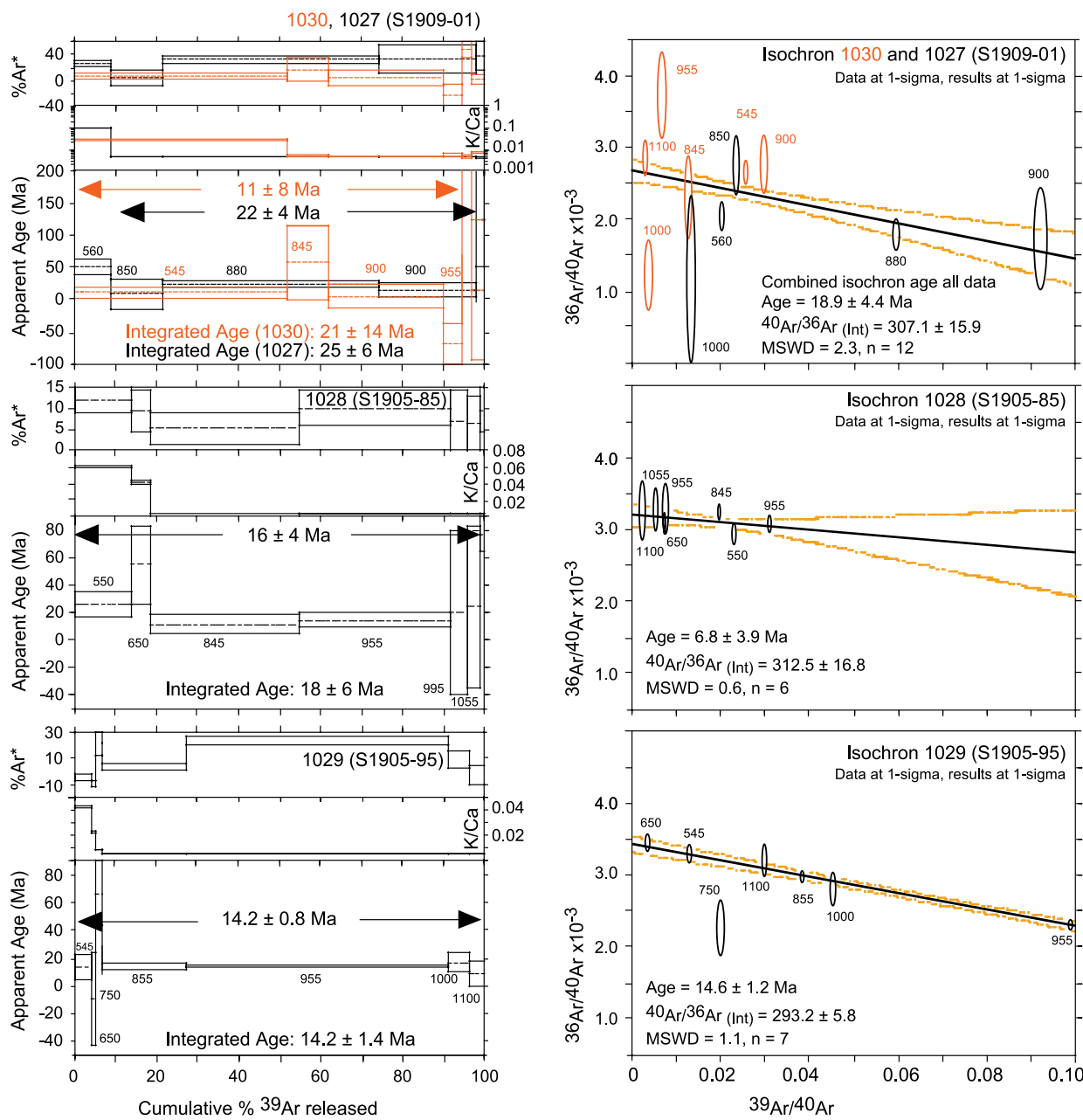


**Figure 11.** Step-heating and isotope correlation diagrams for samples S1909-01, S1905-85, and S1905-95.

isotopic data yield an isochron age of  $6.8 \pm 3.9$  Ma. The intercept on the isotope correlation diagram indicates an initial  $^{40}\text{Ar}/^{36}\text{Ar}$  ratio of  $312.5 \pm 16.8$  and a MSWD of 0.6. These results are concordant at the  $\alpha$ -95% confidence level with the plateau age and the atmospheric Ar ratio, respectively. When all the isotopic data for sample S1905-85 are used for the isochron calculation similar results are obtained. The isochron age for all the isotopic data

is  $7.2 \pm 4$  Ma and an initial  $^{40}\text{Ar}/^{36}\text{Ar}$  ratio of  $311.8 \pm 15.7$  is indicated. Similarly, the MSWD value of 0.5 for all the data suggests that the dispersion of the data about the regression line is due to measurement errors.

[40] Samples S1905-85 and S1905-95 belong to the same dredged site. Their plateau ages,  $16 \pm 4$  Ma and  $14.2 \pm 0.8$  Ma, respectively, are concordant at the  $\alpha$ -95% confidence level. Moreover, the

ages of these two samples are in good agreement with the model crustal age of 16.4 Ma, obtained from spreading rates and tectonic plate reconstructions [Cande *et al.*, 1988].

[41] Sample S1909-01 was run in duplicate. Plateau ages were obtained for both splits (Figure 11). A combination of all the isotopic data for sample S1909-01 will take advantage of the heterogeneity of sample S1909-01, effectively producing a mineral isochron. Combining all the plateau isotopic data for sample S1909-01 on to a single isotope correlation diagram produces an isochron age of  $18.9 \pm 4.4$  Ma with a MSWD of 2.3. The y intercept indicates an initial  $^{40}\text{Ar}/^{36}\text{Ar}$  ratio of  $307 \pm 16$ . This is the best age estimate for sample S1909-01 because the fewest assumptions are made about the initial  $^{40}\text{Ar}/^{36}\text{Ar}$  ratio. This age ( $18.9 \pm 4$  Ma) is consistent with the model crustal age of 17.5 Ma.

[42] Given the analytical errors, the apparent, integrated and isochron Ar/Ar ages of the amphiboles do not give us a precise age for their formation. However, they are consistent with the estimated ages of the overlying crust, suggesting that the amphibole-bearing mylonites were generated in the vicinity of the ridge axis and not later during the flexure and uplift of the Vema Lithospheric Section due to transform tectonics, an event that took place between 10 and 12 Ma [Bonatti *et al.*, 2005].

## 7. Discussion

### 7.1. VLS Mantle Deformation: Where and When?

[43] Deformation zones of limited extent (meter length/cm width) and intensity are commonly observed in mantle-derived peridotites from ophiolites or from the ocean floor. One such occurrence has been reported from the VLS by Cannat and Seyler [1995]. The ultramafic mylonites under study represent something different. Sampling by dredging does not provide precise information on field relationships and deformation features. However, that several contiguous sites along the VLS for distances of tens of km released exclusively highly deformed ultramafic mylonites suggests a major, km-length, hundreds of meter width mega- or multi-shear zone.

[44] The deformation event or events that caused this shear zone could be related either to the emplacement of lithosphere at ridge axis near its

intersection with the transform, or to transform-related vertical tectonic motions due to lithosphere flexure and uplift of the VLS.

[45] We tend to exclude the latter process because if the mylonites were due to deformation during lithospheric uplift in the transform domain, they would be distributed all along the  $\sim 300$  km long VLS and not be limited to a stretch of  $\sim 80$  km. Moreover, flexure/uplift of the entire VLS took place probably within a relatively short time span, i.e., 10–12 Ma [Bonatti *et al.*, 2005]. The zone where mylonites were recovered is restricted to an area located instead in a stretch of the VLS with crustal ages ranging between 16.8 and 18.2 Ma. Finally, Ar/Ar ages of mylonitic amphiboles are close to crustal ages. We conclude that the VLS mylonites formed close to ridge axis between 16.8 and 18.2 Ma.

### 7.2. Physical Conditions of Mylonitization

[46] Equilibrium P, T,  $\text{P}_{\text{H}_2\text{O}}$  in metamorphic assemblages can be estimated from mineral parageneses, amphibole composition, and, for anhydrous or near anhydrous assemblages, from style of deformation (rheology). Ultramafic mineral assemblages that developed isochemically, or largely isochemically from recrystallization of lherzolites/harzburgites, are multiphase, low-variance rocks, where abundance and chemical compositions of the calcic amphiboles are determined by metamorphic grade [Evans, 1982]. Phase relations in the system  $\text{MgO}-\text{CaO}-\text{SiO}_2-\text{H}_2\text{O}$  suggest that calcic amphibole forms at  $700-800^\circ\text{C}$  over a large pressure range by the reaction enstatite + diopside +  $\text{H}_2\text{O} =$  forsterite + tremolite. The presence of  $\text{Al}_2\text{O}_3$  expands the stability field of amphibole relative to the simple system. In addition, Fe and some amounts of Na, Cr, Ti, and K also enter calcic amphibole in proportions that increase with temperature [Ernst and Liu, 1998]. At upper mantle pressure, amphibole compositional variations are controlled by the pargasite substitution, which increases as P-T increase. The presence of Al-Cr spinel and/or chlorite + chromite in the VLS mylonites indicates that the amphiboles are saturated in Al and Cr, whereas Na (and perhaps, K) can be drawn by intake from the fluid. If the compositional conditions for the pargasite substitution are satisfied, amphibole Si or Al contents, as the most sensitive compositional parameters for metamorphic grade in ultramafic rocks [Evans, 1982], can be used jointly with the mineral

assemblages to estimate temperatures of formation of our mylonites.

[47] Because of uncertainties in the mineral assemblages composition, resulting from fine-grained textures and extensive serpentinization, our interpretation of mineral parageneses and metamorphic grade must rely mostly on correlations between metamorphic facies, ultramafic mineral assemblage, aluminous phases and amphibole composition in natural metaperidotites [Evans, 1982; Spear, 1993]. Following these criteria, we attempted to reconstruct the conditions that led to the different assemblages we identified in the VLS ultramafic mylonites.

[48] A1 and A2 mineral assemblages formed during the earlier stages of ductile deformation, characterized by tectonic transposition and recrystallization of pyroxene-rich domains, from Al-rich opx + Al-rich cpx + Al-rich spinel  $\pm$  olivine, into Al-poor opx + Al-poor-cpx + Cr-spinel  $\pm$  plagioclase  $\pm$  olivine neoblastic bands [Cannat and Seyler, 1995]. High variability in composition of neoblasts of the same mineral phases within the same rock samples suggests that continuous net transfer and exchange reactions occurred over a range of P-T, after initiation of the reaction  $\text{opx} + \text{cpx} + \text{spinel} = \text{olivine} + \text{plagioclase}$  [Newman et al., 1999; Spear, 1993]. Continuous, syntectonic, reequilibration from high-P spinel lherzolite stability field to intermediate-P plagioclase + spinel lherzolite stability field under granulite facies conditions ( $T > 950^\circ\text{C}$ , based on two-pyroxene geothermometry), results in progressive decrease of spinel and pyroxenes  $\text{Al}_2\text{O}_3$ , opx CaO and cpx Na<sub>2</sub>O contents and increase of plagioclase anorthite content, accommodated by nucleation of new grains. The transition from A1 to A2 mineral assemblages went together with an increase of deformation, as fabrics grade from protomylonitic to well-foliated mylonitic. Amphibole in A1 mineral assemblages is tremolite, clearly in chemical disequilibrium with the other mineral phases [Evans, 1982; Ernst and Liu, 1998]. We interpret its crystallization after relic and metamorphic pyroxenes and coeval development of chlorite at spinel grain boundaries as an effect of posttectonic, low-temperature alteration. On the other hand, the very low abundance in A2 mylonites of low-Si ( $6.0 \leq 6.5$  at.) amphibole neoblasts, in textural equilibrium with pyroxenes, plagioclase and spinel, is consistent with the occurrence of pargasitic hornblende in the granulite facies. In a few samples, amphibole Si contents

extend to higher values (up to 7.1 at.), indicating that metamorphic recrystallization continued under decreasing temperatures.

[49] A3 mineral assemblages, richer in amphibole and poorer in cpx and plagioclase neoblasts, contain amphiboles transitional between pargasitic and magnesio-hornblendes (Si = 6.5–6.8 at.). This suggests crystallization under lower temperatures, close to the granulite-amphibolite facies transition [Evans, 1982].

[50] A4 ultramafic mylonites assemblages (ol + opx + Mg-hornblende + spinel) are characterized by disappearance of plagioclase and near disappearance of cpx, as well as by higher contents of amphibole with higher Si content (6.6–7.6 at.). The major amphibole-forming reaction is  $5 \text{ enstatite} + 2 \text{ diopside} + \text{H}_2\text{O} = \text{tremolite} + \text{forsterite}$  [Spear, 1993]. Whereas first-order variations in amphibole abundance are mainly controlled by bulk CaO content, second-order variations are likely to be controlled by continuous net transfer reactions producing nucleation of new amphibole grains as CaO decreases in opx. Modal data are lacking to support this proposition, but the low and variable CaO content measured in the few opx that escaped serpentinization, and the large amphibole compositional range, both suggest crystallization over a range of temperature. Similarly, spinel composition varies from grain to grain in the same sample. Furthermore, spinel poikilitic grain boundaries enclosing adjacent silicate neoblasts, and lack of zoning, both also suggest continuous crystallization and reequilibration in the upper amphibolite facies ( $T = 650\text{--}800^\circ\text{C}$  [Spear, 1993]).

[51] Alternatively, the A4 mylonite compositional variations may be explained by variations in the degree of hydration that controlled heat transfer and kinetics of the exchange and amphibole-forming reactions. Individual samples contain relatively restricted amphibole compositional ranges (Figure 6), suggesting small scale variations within shear zones, consistently with this second possibility. In addition, near lack of higher-temperature minerals (derived from protoliths or A1 and A2 mineral assemblages) and well-defined compositional layering and foliation both suggest that A4 ultramafics result from syntectonic recrystallization and not from oriented, static amphibole growths after pyroxenes  $\pm$  plagioclase following postmylonitic introduction of a metasomatic fluid, as was suggested by Cannat and Seyler [1995].

[52] A5 mineral assemblages correspond to the appearance of chlorite associated with Si-rich (7.5–7.9 at.) amphibole, close to the tremolite end-member. We make a distinction between A5 mineral assemblages in ultramylonitized samples (S1902-11, S1907-07, S1907-23, S1910-02, S1911-13, S1911-63, S1915-17, S1915-20), and static replacement of pyroxenes and spinel by amphibole and chlorite in A1–A2 mineral assemblages. The former results from continuous deformation of A4 mineral assemblages at lower temperature, as indicated by grain size decrease, relicts of earlier neoblastic bands crosscut at low angle by a second mylonitic foliation, and elongate porphyroclasts of higher temperature amphibole. The latter formed during fluid percolation into previously deformed material located between shear planes active during this new deformation stage. In both cases, chlorite formed by the reaction forsterite + enstatite + Al-spinel + 4 H<sub>2</sub>O = clinochlore [Mg<sub>5</sub>Al<sub>2</sub>Si<sub>3</sub>O<sub>10</sub>(OH)<sub>8</sub>] + chromite, in agreement with the very low modal content of chlorite and with its composition. A5 mineral assemblages are still equilibrated in the amphibolite facies, since opx is still stable in presence of water, corresponding to a temperature of 600–650°C [Evans, 1982; Spear, 1993].

[53] The only sample with abundant talc (S1907-12) is also the only sample containing tremolite with Si > 7.9 at. Serpentine pseudomorphs after opx neoblasts are still present. Our observations do not permit to identify the talc-forming reaction. Direct opx hydration occurs at P > ~0.65 GPa in the MgO-CaO-SiO<sub>2</sub>-H<sub>2</sub>O system by the reaction enstatite + H<sub>2</sub>O = talc + forsterite [Spear, 1993]. At lower pressure, opx disappears through two successive reactions enstatite + H<sub>2</sub>O = forsterite + Mg-cummingtonite, then, Mg-cummingtonite + H<sub>2</sub>O = talc + forsterite [Spear, 1993]. These reactions occur in the lower amphibolite facies (500–650°C [Evans, 1982; Spear, 1993]). We never observed Mg-amphibole in any of the VLS ultramylonites. However, the stability field of Mg-amphibole (anthophyllite or Mg-cummingtonite) is extremely narrow in ultramafic rocks [Gilbert et al., 1982], and given the scarcity of tremolite + chlorite-bearing mylonites in our sample set, it is possible that this paragenesis exists but was not sampled. Alternatively, replacement of opx by talc + tremolite, without olivine involvement, may accompany serpentinization in abyssal peridotites at T < 500°C under greenschist facies conditions [Escartín et al., 2003; Bach et al., 2004]. In this

case, there will be a temperature gap between the A5 mylonites and the talc-bearing sample, and this mineral paragenesis would be unrelated to the mylonitization.

[54] Tremolite + chlorite-bearing ultramafics thus appear to be the lowest temperature mineral assemblages present in the VLS ultramafic mylonites. Since opx is still present in these assemblages, we conclude that mylonitization near the Vema transform occurred successively first in the granulite then in the amphibolite facies, at T > 600°C. Serpentinization, that overprints all the mineral assemblages, proceeded after mylonitization at T < 500°C by static replacement of preexisting relict and metamorphic phases.

### 7.3. Geothermometry

[55] Equilibration temperatures, which mark the closure of chemical exchanges between pyroxenes in the peridotite system during cooling, were calculated in the VLS peridotites by Cipriani et al. [2009] on the basis of two pyroxenes [Taylor, 1998; Wells, 1977] and single clinopyroxene [Nimis and Taylor, 2000] equilibria. We chose to plot equilibration temperatures calculated at a pressure of 1.0 Gpa, with the cpx-thermometer of Nimis and Taylor [2000] so as to include a few samples without opx.

[56] A comparison of the closure temperatures of the two main populations of the VLS peridotites shows that the ultramafic mylonites have lower closure temperatures than the coarse-grained/porphyroclastic peridotites and overlap with their lower temperature values (Figure 12).

[57] Temporal variations of equilibration temperatures show a decreasing trend from 26 to ~18.5 Ma, followed by an increasing trend from 16.4 to 4 Ma [Cipriani et al., 2009, Figure 15C]. The mylonitic stretch lies between the two trends. Variations of the degree of melting, as indicated by primary spinel Cr number, follow similar trends with a minimum in degree of melting clearly corresponding to the mylonitic stretch (Figure 13).

[58] Unfortunately, most of the ultramafic mylonites, especially those that were collected in the mylonitic stretch, do not preserve fresh pyroxenes to allow geothermometric calculations. Within the limits of the number of samples for which equilibration temperatures were calculated, we recognize that cpx cores in A1 mylonites have higher equilibration temperatures (average = 873°C, N = 7)

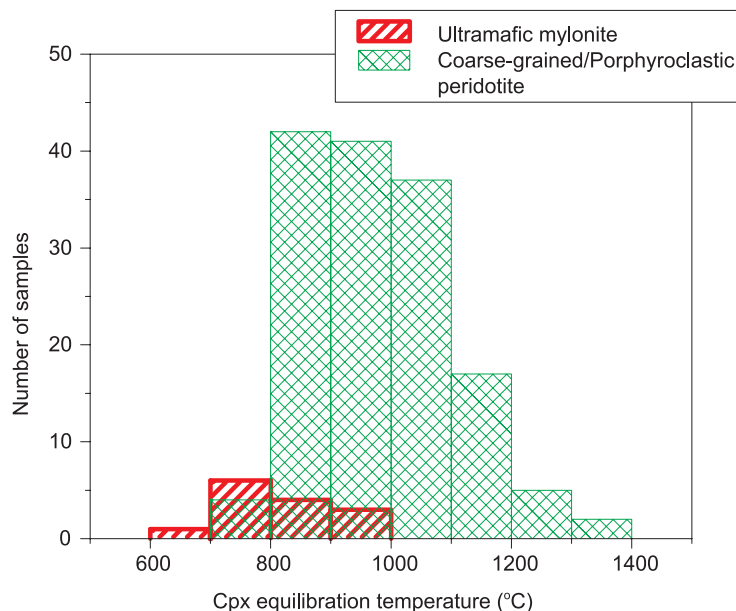


**Figure 12.** Single-clinopyroxene equilibration temperatures [Nimis and Taylor, 2000] calculated from the VLS ultramafic mylonites (red thick bars) and the VLS porphyroclastic peridotites (green bars). The width of each bin is approximately the same as the  $2\sigma$  uncertainty of the within-dredge average. Temperatures were calculated with the single-cpx geothermometer so as to include a few peridotites that only had cpx relics.

than neoblasts in A3 and A4 mylonites (average = 730°C, N = 4).

[59] These values are consistent with the temperature estimates for the granulite and upper amphibolite metamorphic facies based on metamorphic mineral assemblages discussed in the previous paragraph.

#### 7.4. Isochemical Versus Metasomatic Metamorphism of the VLS Peridotites

[60] Whereas olivine + opx + cpx + plagioclase (<5%) + spinel mineral assemblages have been shown to form by isochemical recrystallization of lherzolite [Cannat and Seyler, 1995; Newman et al., 1999], hydrous recrystallization is commonly associated with metasomatism. Comparison between a porphyroclastic spinel lherzolite, a plagioclase-bearing ultramafic mylonite and two amphibole ultramafic mylonites led Cannat and Seyler [1995] to conclude that syntectonic hydration of the VLS peridotites was accompanied by the introduction of Ca, Na and Ti. Our larger sample set allows us to reevaluate this conclusion. Modal compositions of coarse-grained to porphyroclastic VLS peridotites show a large variation in the olivine/opx/cpx contents, at all scales (from sample to interdredge), which is only broadly correlated with mineral compositions [Brunelli et

al., 2006]. The protoliths of the five samples studied by Cannat and Seyler [1995] may have thus contained different amounts of cpx, which would invalidate their conclusion.

[61] Simple hydration of spinel peridotites at  $T > 650^\circ\text{C}$  triggers the reaction  $5 \text{ enstatite} + 2 \text{ diopside} + \text{H}_2\text{O} = \text{tremolite} + \text{forsterite}$  [Spear, 1993]. The maximum amphibole content forms when all the cpx contained in the peridotite and cpx component in the primary opx, react out. We have compared the amphibole mode observed in A4 ultramafic mylonites with the proportion of amphibole that can theoretically form upon hydration of “typical” VLS protogranular peridotites. Primary bulk compositions were reconstructed, using coarse-grained peridotite modal proportions and mineral core analyses [Brunelli et al. 2006; M. Seyler, unpublished data, 2009]; they are assumed to be similar in composition to those of the protoliths of the A4 amphibole mylonites. Most VLS protogranular lherzolites/harzburgites contain 66–78% olivine, 20–25% opx (1–1.5 wt% CaO), 2–6% cpx (21–23 wt% CaO), and 0.5–3 wt% spinel. Calculations in the  $\text{MgO}-\text{FeO}-\text{CaO}-\text{Al}_2\text{O}_3-\text{SiO}_2-\text{H}_2\text{O}$  system show that complete recrystallization of cpx leads to mineral assemblages containing 6–17 vol% aluminous tremolite ( $\text{Al} \leq 2 \text{ at.}$ ) in addition to olivine (71–84%) and opx (9–14%); excess  $\text{Al}_2\text{O}_3$  will allow crystallization of accessory

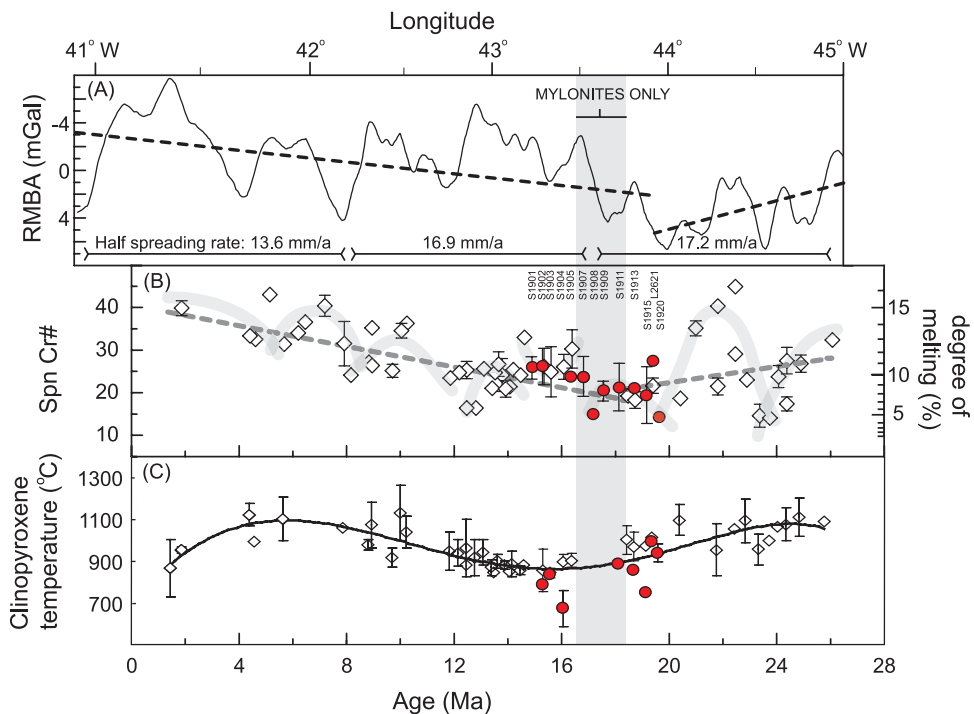


**Figure 13.** Temporal variations in (a) Residual Mantle Bouguer Anomaly (RMBA), (b) mantle degree of melting as inferred from spinel Cr number ( $=[100\text{Cr}/(\text{Al} + \text{Cr})]$ ; porphyroclasts core average per site  $\pm 1\sigma$ ), and (c) calculated single clinopyroxene equilibration temperature [Nimis and Taylor, 2000]. Red circles are ultramafic mylonites. Open diamonds are peridotites from Bonatti et al. [2003], Brunelli et al. [2006], and Cipriani et al. [2009]. The temporal variation curve of RMBA is shifted by  $\sim 34$  km ( $\sim 2.2$  Ma) with respect to the mantle degree of melting curve (for details, see Cipriani et al. [2009]). Mantle degree of melting is calculated from the Cr number of spinel according to Hellebrand et al. [2001]. The vertical gray bar indicates the  $\sim 1.4$  Ma stretch where ultramafic mylonites were the exclusive ultramafic rock type recovered. Dashed regression lines show decreasing RMBA and degree of melting from 26 to 18.5 Ma and increasing RMBA and degree of melting from 18.5 to 2 Ma. The black continuous line in Figure 13c is a polynomial regression that suggests a decreasing trend from 26 to 18.5 Ma and an increasing trend from 16.5 to 2 Ma. Gray bands in Figure 13b show a possible interpretation of the small 3–4 Ma oscillations in the mantle degree of melting curve [from Cipriani et al., 2009]. Note that half spreading rate, indicated at the bottom of Figure 13a, decreases toward younger ages.

spinel (or chlorite at lower temperature). The volume of amphibole estimated in thin sections varies from 5 to 15% in most A4 ultramafics, thus in good agreement with isochemical (for CaO) recrystallization of average VLS peridotites. Samples with very small amounts of amphibole (<5%) scattered in the serpentinite matrix may have recrystallized from opx-poor harzburgites or dunites. On the other hand, coarse-grained peridotites highly enriched in cpx (up to 13%) and cm-wide, coarse-grained, websterite layers are not uncommon along the VLS; they are similar to samples described in MARK Iherzolites [Cannat et al., 1990]. A websterite layer composed of 40% olivine, 30% opx, 25% cpx and 5% spinel, could form upon hydration and recrystallization of a thick ultramafic band containing up to 50% calcic

amphibole. Calculated bulk Na<sub>2</sub>O contents in VLS protogranular peridotites range from <0.002 to 0.073 wt%, whereas amphibole Na<sub>2</sub>O contents in A4 ultramafics range from 0.5 to 2.4 wt%, corresponding to 0.025–0.36 wt% bulk Na<sub>2</sub>O in the hydrous mylonites. On average, bulk Na<sub>2</sub>O in the hydrous mylonites is thus much higher than calculated primary bulk Na<sub>2</sub>O, supporting metasomatism by Na-rich fluids.

[62] Concerning Ti, our data are not precise enough for accurate mass balance calculations. TiO<sub>2</sub> contents in A4 hornblendes range from 0.01 to 0.06 wt% and trace amounts of TiO<sub>2</sub> are also present in spinel and opx neoblasts. Nevertheless, first order calculations suggest that, in the whole, the hydrous mylonites are not enriched in TiO<sub>2</sub> relative to the

protogranular peridotites. Four samples (S1907-03, S1907-23, S1907-32, S1910-01) contain amphiboles enriched in Fe and Ti ( $\text{TiO}_2 = 0.5\text{--}1.5 \text{ wt } \%$ ). Sample S1907-32, in particular, is made of  $\sim 95\%$  tremolite and  $\sim 5\%$  magnetite, and may derive from clinopyroxenite veins that crystallized in the protoliths, prior to mylonitization.

[63] In conclusion, expected compositions of isochemically recrystallized hydrous peridotites and compositions observed in A4 ultramafics (the prominent mylonite type at the VLS) suggest that the hydrous fluids were enriched in Na, but not in Ca and Ti. Concerning the origin of the metasomatic fluids, the MORB-like Sr and Nd isotopic composition of the amphiboles suggests that, if hydrothermal circulation with a seawater component was involved, the seawater signature must have been lost, possibly by reactions of the fluids with gabbroic-basaltic crustal rocks prior to interacting with mantle peridotites.

## 7.5. Depth of Metamorphism

[64] There are almost no constraints on pressure that we can derive from the mineral assemblages, thus few constraints on the depth of the deformation events. The  $500^\circ\text{C}$  isotherm, close to the limit of the greenschist facies, is located between  $\sim 7.5$  and  $3.5 \text{ km}$  beneath ridge axis [Shaw and Lin, 1996], suggesting that VLS mylonitization occurred at  $P > 0.3 \text{ GPa}$ . The maximum pressure recorded by our assemblages corresponds to the intermediate-P granulite facies,  $P = 0.6\text{--}0.85 \text{ GPa}$  ( $20\text{--}25 \text{ km}$  depth) at  $T \sim 950^\circ\text{C}$ . Coarse-grained residual peridotites cooled beneath ridge axis probably within the plagioclase lherzolite stability field; however, no plagioclase generally forms, because no dynamic recrystallization occurs (just exsolutions and melt-assisted exchange reactions), with aluminous spinel and pyroxenes being metastable. Subsolidus deformation-recrystallization leading to porphyroclastites, then to protomylonites and finally to mylonites started probably in this depth range. Deviatoric stress allowed recrystallization into mineral assemblages more consistent with this depth, where aluminous phases are not stable anymore. It follows that the transition from spinel to plagioclase peridotite stability fields may have occurred nearly isobarically, reflecting increasing deformation and reequilibration through continuous mineral reactions. At this stage, fluid influx allowed amphibole formation, with mineral and mineral/fluid reactions continuously modifying the mineral compositions. Temperature decrease

and variable water influx also caused changes in the amphibole composition. Thus, the entire mylonitization event could have occurred within a relatively limited pressure range.

## 7.6. Fabric Analysis

[65] Fabric analysis of VLS ultramafic mylonites sampled *in situ* by submersible [Auzende et al., 1989] at crustal age  $\sim 14 \text{ Ma}$ , and representing local, small, meter length shear zones has been performed by Cannat and Seyler [1995]. They described an association of amphibole bearing ultramafic mylonites, plag-bearing mylonites and porphyroclastic peridotites, and argued that these rocks derived from one another through multistage, plastic deformation that took place at depth near the ridge-transform intersection. The plag-bearing ultramafics mylonites formed from dynamic recrystallization of aluminous (i.e., moderately depleted) spinel lherzolite in the plag-peridotite stability field, while the amph-bearing mylonites derived from metasomatic replacement of the previous mylonitic ultramafic assemblage following the introduction of hydrous fluids.

[66] This study shows that deformation events under granulite and amphibolite facies conditions have approximately the same geometry (parallel attitude of foliations and lineations and mineral banding) and occurred at high-T ( $> 950^\circ\text{C}$ , probably starting at subsolidus  $T \sim 1200\text{--}1250^\circ\text{C}$ ), and under low-deviatoric stress conditions. This suggests progressive deformation rather than geometrically distinct deformation events. The earlier stage of the ductile deformation was accompanied by tectonic transposition of primary, pyroxene-rich domains, where crystallization of plagioclase induced strain softening, facilitating strain localization and initiation of ductile shear zones. According to Cannat and Seyler [1995] and Newman et al. [1999], recrystallization of  $\text{Al}_2\text{O}_3$ -rich primary pyroxenes leads to plagioclase-induced strain softening, which in turn, allows continuous deformation in mylonitic shear zones.  $\text{H}_2\text{O}$ -rich fluid injections and high modal content of pyroxenes both also enhanced subsolidus recrystallization and strain softening, leading to the formation of amphibole ultramafics. Microstructures suggest that the deformation started in the deep lithosphere, near the eastern intersection of the Vema transform with the MAR, and continued along the transform zone.

[67] Cannat and Seyler [1995] observed elongate opx porphyroclasts, kinked, fractured and partially

recrystallized into polygonal neoblasts, with preferred crystal orientations, characterized by (100) crystal planes parallel to the major foliation and [100] axes close to the major stretch lineation. Opx neoblasts show no preferred crystallographic orientation, but straight to curvilinear grain boundaries with common triple junctions. These features indicate that the main mechanism of deformation in our A1 and A2 mineral assemblages was intracrystalline dislocation slip. Olivine neoblasts have a weak shape fabric (being slightly elongated), but both olivine porphyroclasts and neoblasts show preferred crystal orientations, also consistent with dislocation slip along [100] axes and on (001) and (010) planes. Similar patterns of dislocation are reproduced experimentally at T at or close to solidus T and low deviatoric stresses [Durham *et al.*, 1977; Kohlstedt *et al.*, 1995; Cordier, 2002]. Although considered as postdating foliation and mineralogical banding, amphibole crystal orientations are consistent with crystallographic growth in a deviatoric stress field, or with dislocation grid along the [001] axes and on (100) planes subparallel to the opx foliation and lineation.

[68] High-T (>600°C, granulite to upper amphibolite facies) ductile deformation prevails in VLS ultramafics. In contrast, at 15°45'N, deformation is restricted to low-T (<500°C, greenschist facies); high-T (~720–750°C) deformation-recrystallization has been observed at two sites only in mafic rocks; in addition, low-T microstructures have not been observed to overprint high-T deformation [Escartín *et al.*, 2003]. Instead, the widespread presence of talc-rich tremolite-chlorite schists (greenschist facies) results from large volume fluid flux leading to Si metasomatism [Escartín *et al.*, 2003; Früh-Green *et al.*, 2003] during the late stage of high-T syntectonic alteration along detachment faults. Drilling at the Fifteen-Twenty fracture zone (ODP Leg 209) suggests that mylonitization starts at high T, ~20–25 km depth, but is concentrated in gabbroic intrusions, peridotite being almost undeformed [Kelemen *et al.*, 2004, 2007]. At the Kane fracture zone (ODP Leg 153) the deformation is concentrated in areas rich in gabbroic veins, and ultramafic mylonites are rare and occur in very thin layers [Ceuleneer and Cannat, 1997; Karson, 1999]. It appears therefore that in the oceanic regions where mylonitization is the result of detachment fault shearing, the picture is somewhat different to what is observed at the VLS which is dominated by thick and abundant ultramafic mylonites. However, high-T ductile deformation (as in the Vema RTI and other RTIs along the

Mid-Atlantic Ridge) inducing strain softening and localization may trigger the development of shear zones and detachment faults [Escartín *et al.*, 2003]. In addition, petrological and structural studies on ophiolites report amphibole-bearing mylonites similar to our VLS ultramafic mylonites and associate them with detachment faults [Vissers *et al.*, 1991; Hoogerduijn Strating *et al.*, 1993]. The scarcity of low-T mylonites at the VLS may result from limited uplift of the mantle rocks, with no upper mantle denudation but with crust overlying the mantle peridotites.

## 7.7. Geodynamic Implications

[69] Mineral assemblages and composition suggest that deformation and recrystallization of the VLS mantle rocks during the “mylonitic interval” initiated probably at around ~900°C and 0.6–0.8 GPa pressure, corresponding roughly to 20–25 km depth. Grain size diminution followed during cooling, with gradual development of zones of weakness in the subridge mantle, followed by strain localization according to processes inferred from observation of ophiolitic and massif peridotite bodies and from theory [Hobbs *et al.*, 1990] and experiments [Karato *et al.*, 1986; Drury *et al.*, 1991]. Similar processes have been inferred to operate at other slow spreading RTIs [Jaroslow *et al.*, 1996].

[70] The VLS mylonitic interval may represent a period of quasi-amagmatic, mostly tectonic emplacement of lithosphere at ridge axis. It is likely, although with the data at hand we cannot prove it, that the VLS mylonitic stretch was associated with the development of detachment faults of the type observed today at a number of RTI (Atlantis, Kane, 15°20') along the Mid-Atlantic Ridge. The ~1.4 Ma approximate duration of the VLS mylonitic stretch is similar to the estimated duration of detachment fault regimes close to the Atlantis and Kane Transforms in the Mid-Atlantic Ridge [Tucholke *et al.*, 1998; Ildefonse *et al.*, 2007]. The VLS mylonitic interval implies scarcity of magmatism and a thermal minimum at and below the ridge axis, in contrast to the thermal regime prevailing during “normal” stages of lithosphere formation at the EMAR segment, represented by the equigranular/porphyroclastic peridotites and with significant melting and magmatism. Indeed, the mylonitic stretch is located in between and partially overlaps two different peridotites suites, an “older suite” to the west and a “younger suite” to the east, both with prevalent porphyroclastic relatively undeformed peridotites

(Figure 13). These two suites are different in composition, melting trends and calculated equilibration temperatures. The older suite shows a decrease in the extent of melting and equilibration temperature from 26 to 18.5 Ma, while the younger suite displays a long trend of increasing extent of melting and equilibrium temperature from 18.5 to 2 Ma. The dry mylonites are prevalently positioned at the end of the older suite decreasing trend of mantle temperature and degree of melting, while the amphibole mylonites are located at the beginning of the younger suite trend. The parent mantle rocks of both dry and wet mylonites underwent a low degree of melting and are relatively fertile. We speculate that the dry mylonites represent the last portion of an upwelling mantle mass or soliton which lost most of its heat and therefore underwent low degrees of partial melting. The amphibole mylonites could represent the initial emplacement of a new rising mantle soliton fertile but still not very hot at the top; therefore it also underwent a low extent of melting. The fluids involved in the formation of the amphiboles could derive from an enriched portion of the inner part of the soliton, much hotter than the periphery. These fluids/melts, owing to their buoyancy, would rise faster through the porosity of the peridotite and metasomatize the in fieri mylonite, forming the amphiboles. Another possibility is that seawater fluids, chemically re-equilibrated with the surrounding lithospheric rocks, infiltrated into the upper mantle during a quasi-amagmatic event, contributing to the upwelling soliton the necessary budget to crystallize amphiboles.

[71] The lithologic sequence of the VLS peridotites may reflect a long-term ( $\sim$ 10–20 Ma) cyclicity of mantle upwelling below a ridge axis [Cipriani et al., 2009]. The mylonitic stretch could be related to a thermal minimum in the subridge upwelling mantle, with nearly amagmatic emplacement of the lithosphere resulting in strong deformation of the mantle rocks. When upwelling of hot and/or fertile mantle resumes a new cycle starts with injection of magmas and generation of igneous crust.

## 8. Conclusions

[72] 1. The VLS ultramafic mylonites might represent a  $\sim$ 4.7 Ma long interval when emplacement of lithosphere at ridge axis occurred through quasi-amagmatic, prevalently tectonic mechanisms, involving possibly low-angle detachment faults. This interval of strongly deformed mantle rocks (if related to detachment fault shearing) contrasts with

the present-day nearly symmetric and “magmatic” emplacement of lithosphere at the Vema RTI, a mode that appears to have prevailed for most of the 26 Ma history recorded along the VLS.

[73] 2. Deformation of the mantle rocks probably started at around 900°C about  $\sim$ 20 km below ridge axis, with decrease of mineral grain size, recrystallization and reorientation of the primary phases, weakening and strain localization all occurring during cooling.

[74] 3. Ultramafic mylonites recovered at the VLS are more fertile than porphyroclastic ultramafics recovered all along the 300 km long stretch of oceanic lithosphere created at the EMAR segment, supporting the idea that deformation and metamorphism of the mantle rocks went together with a low-melt regime.

[75] 4. Amphiboles were formed close to ridge axis, most likely by the action of water rich fluids with a depleted N-MORB signature. The fluids appear not to be derived from seawater (low Cl, low  $^{87}\text{Sr}/^{86}\text{Sr}$ , mantle like  $\delta^{18}\text{O}$ ), but are probably of mantle derivation.

[76] 5. Ar/Ar ages of the amphiboles, although affected by large uncertainties, are in agreement with modeled crustal ages, supporting the hypothesis that the mylonites formed close to ridge axis and not due to transform-related vertical tectonics.

[77] 6. Peridotite mantle degree of melting and calculated equilibration temperature show a decreasing trend from 26 Ma to 18.5 Ma ago, followed by a steady increase from 16 Ma to 2 Ma ago. The ultramafic mylonites stretch lies between the two opposite trends, as if marking a change in mantle thermal regime. It may reflect a thermal minimum in the subridge upwelling mantle, with nearly amagmatic emplacement of the lithosphere resulting in strong deformation of the mantle rocks. These results hint at the existence of  $\sim$ 10–20 Ma cycles in the activity of the northern Mid-Atlantic Ridge [Cipriani et al., 2009].

## Appendix A

[78] Tables A1a–A11 report the major element compositions (in wt %) of all amphiboles from VLS ultramafic mylonites analyzed by electron microprobe. Samples are grouped by dredge site (each of Tables A1a–A11 is a single dredge site). Within each of Tables A1a–A11, analyses are ordered by increasing sample number and Si content.

**Table A1a.** Major Element Compositions of Amphiboles From VLS Ultramafic Mylonites Analyzed by Electron Microprobe: Site S1901<sup>a</sup>

Sample	Min.	Ass.	SiO <sub>2</sub>	TiO <sub>2</sub>	Al <sub>2</sub> O <sub>3</sub>	Cr <sub>2</sub> O <sub>3</sub>	FeO	MnO	NiO	MgO	CaO	Na <sub>2</sub> O	K <sub>2</sub> O	Total	F.S./23 O	Si	Ti	Al	Cr	Fe <sup>2+</sup>	Mn	Ni	Mg	Ca	Na	K	Total	Mg%/ <sup>o</sup> Mg + Fe	Fe%/ <sup>o</sup> Fe + Mg
S1901-02	A4	48.67	0.36	10.99	1.00	3.28	0.03	0.07	19.05	12.57	1.47	0.03	97.53	6.80	0.04	1.81	0.11	0.38	0.00	0.01	3.97	1.88	0.40	0.01	15.40	91.10	8.81		
S1901-02	A4	48.82	0.15	10.77	0.87	3.60	0.00	0.13	19.12	12.39	1.40	0.00	97.25	6.84	0.02	1.78	0.10	0.42	0.00	0.02	3.99	1.86	0.38	0.00	15.40	90.44	9.56		
S1901-02	A4	48.74	0.43	9.87	1.15	3.21	0.07	0.10	19.20	12.60	1.33	0.02	96.71	6.87	0.05	1.64	0.13	0.38	0.01	0.01	4.03	1.90	0.36	0.00	15.38	91.24	8.57		
S1901-02	A4	49.52	0.40	10.16	1.16	3.20	0.05	0.12	19.44	12.64	1.38	0.04	98.10	6.87	0.04	1.66	0.13	0.37	0.01	0.01	4.02	1.88	0.37	0.01	15.38	91.42	8.44		
S1901-02	A4	49.09	0.31	9.82	1.16	3.31	0.03	0.09	19.46	12.63	1.37	0.05	97.32	6.88	0.03	1.62	0.13	0.39	0.00	0.01	4.06	1.90	0.37	0.01	15.40	91.21	8.71		
S1901-02	A4	49.01	0.44	9.39	1.28	3.23	0.03	0.00	19.27	12.84	1.36	0.03	96.89	6.90	0.05	1.56	0.14	0.38	0.00	0.00	4.04	1.94	0.37	0.01	15.39	91.33	8.58		
S1901-02	A4	49.27	0.27	9.87	0.72	3.34	0.00	0.04	19.34	12.72	1.34	0.03	96.93	6.92	0.03	1.63	0.08	0.39	0.00	0.00	4.05	1.91	0.36	0.00	15.38	91.17	8.83		
S1901-02	A4	50.00	0.28	8.93	0.93	3.19	0.04	0.05	20.18	13.00	1.25	0.03	97.88	6.96	0.03	1.46	0.10	0.37	0.00	0.01	4.18	1.94	0.34	0.01	15.40	91.75	8.14		
S1901-02	A4	49.91	0.32	8.80	0.59	3.44	0.06	0.14	20.33	12.74	1.15	0.01	97.48	6.97	0.03	1.45	0.07	0.40	0.01	0.02	4.23	1.91	0.31	0.00	15.39	91.19	8.66		
S1901-02	A4	50.40	0.37	9.02	1.09	3.18	0.00	0.11	20.03	12.84	1.22	0.01	98.28	6.98	0.04	1.47	0.12	0.37	0.00	0.01	4.13	1.90	0.33	0.00	15.35	91.82	8.18		
S1901-03	A4	46.98	0.44	10.68	0.97	3.95	0.07	0.09	19.19	11.67	1.30	0.05	95.39	6.73	0.05	1.80	0.11	0.47	0.01	0.01	4.10	1.79	0.36	0.01	15.45	89.49	10.33		
S1901-03	A4	49.23	0.32	10.84	1.06	3.37	0.09	0.09	20.04	12.27	1.45	0.05	98.79	6.79	0.03	1.76	0.12	0.39	0.01	0.01	4.12	1.81	0.39	0.01	15.44	91.17	8.61		
S1901-03	A4	49.47	0.43	10.55	1.08	3.45	0.08	0.12	20.03	12.43	1.43	0.02	99.08	6.81	0.04	1.71	0.12	0.40	0.01	0.01	4.11	1.83	0.38	0.00	15.43	91.01	8.79		
S1901-03	A4	48.96	0.47	10.10	0.96	3.36	0.03	0.06	20.56	12.02	1.31	0.03	97.87	6.81	0.05	1.66	0.11	0.39	0.00	0.01	4.26	1.79	0.35	0.01	15.44	91.52	8.39		
S1901-03	A4	49.05	0.38	10.64	0.85	3.58	0.06	0.05	19.65	12.38	1.44	0.06	98.14	6.81	0.04	1.74	0.09	0.42	0.01	0.01	4.07	1.84	0.39	0.01	15.43	90.58	9.25		
S1901-03	A4	49.22	0.35	10.35	0.97	3.59	0.06	0.11	20.10	12.29	1.43	0.04	98.52	6.82	0.04	1.69	0.11	0.42	0.01	0.01	4.15	1.82	0.38	0.01	15.45	90.74	9.10		
S1901-03	A4	48.86	0.42	10.57	1.10	3.50	0.05	0.12	19.61	11.94	1.45	0.05	97.66	6.82	0.04	1.74	0.12	0.41	0.01	0.01	4.08	1.78	0.39	0.01	15.41	90.79	9.09		
S1901-03	A4	49.03	0.40	10.34	1.00	3.57	0.02	0.07	19.80	12.37	1.47	0.07	98.14	6.82	0.04	1.69	0.11	0.42	0.00	0.01	4.10	1.84	0.40	0.01	15.44	90.76	9.19		
S1901-03	A4	49.30	0.44	10.43	1.11	3.38	0.08	0.06	19.79	12.46	1.47	0.02	98.56	6.82	0.05	1.70	0.12	0.39	0.01	0.01	4.08	1.85	0.39	0.00	15.42	91.05	8.74		
S1901-03	A4	48.59	0.48	10.52	1.11	3.39	0.06	0.12	19.07	12.27	1.47	0.03	97.10	6.82	0.05	1.74	0.12	0.40	0.00	0.01	3.99	1.85	0.40	0.00	15.40	90.76	9.07		
S1901-03	A4	49.12	0.42	10.34	0.88	3.53	0.05	0.12	19.89	12.31	1.41	0.03	98.09	6.83	0.04	1.69	0.10	0.41	0.01	0.01	4.12	1.83	0.38	0.01	15.43	90.83	9.04		
S1901-03	A4	48.58	0.39	10.00	0.97	4.02	0.08	0.06	19.68	12.10	1.30	0.03	97.20	6.83	0.04	1.66	0.11	0.47	0.01	0.01	4.12	1.82	0.36	0.01	15.43	89.55	10.25		
S1901-03	A4	49.49	0.41	10.92	0.36	3.40	0.01	0.09	19.90	12.31	1.48	0.03	98.40	6.83	0.04	1.78	0.04	0.39	0.00	0.01	4.10	1.82	0.39	0.01	15.42	91.21	8.75		
S1901-03	A4	49.29	0.43	10.55	0.84	3.46	0.03	0.12	19.70	12.30	1.46	0.04	98.22	6.83	0.04	1.72	0.09	0.40	0.00	0.01	4.07	1.83	0.39	0.01	15.41	90.96	8.96		
S1901-03	A4	49.02	0.34	10.30	0.84	3.58	0.07	0.07	19.81	12.30	1.41	0.05	97.78	6.84	0.04	1.69	0.09	0.42	0.01	0.01	4.12	1.84	0.38	0.01	15.43	90.62	9.19		
S1901-03	A4	49.64	0.37	10.47	0.64	3.68	0.09	0.12	20.00	12.42	1.47	0.04	98.94	6.84	0.04	1.70	0.07	0.42	0.01	0.01	4.11	1.83	0.39	0.01	15.44	90.43	9.34		
S1901-03	A4	49.51	0.36	10.35	0.96	3.48	0.10	0.10	19.93	12.41	1.39	0.03	98.64	6.84	0.04	1.69	0.10	0.40	0.01	0.01	4.10	1.84	0.37	0.01	15.41	90.85	8.90		
S1901-03	A4	48.96	0.35	10.26	0.47	3.48	0.10	0.08	20.17	12.05	1.41	0.06	97.40	6.84	0.04	1.69	0.05	0.41	0.01	0.01	4.20	1.80	0.38	0.01	15.45	90.92	8.81		
S1901-03	A4	49.38	0.47	10.23	1.06	3.52	0.01	0.10	19.82	12.26	1.44	0.02	98.30	6.85	0.05	1.67	0.12	0.41	0.00	0.01	4.09	1.82	0.39	0.00	15.41	90.92	9.07		
S1901-03	A4	49.43	0.42	10.34	0.71	3.56	0.07	0.14	19.87	12.31	1.40	0.04	98.28	6.85	0.04	1.69	0.08	0.41	0.01	0.02	4.11	1.83	0.38	0.01	15.41	90.72	9.11		
S1901-03	A4	49.51	0.44	10.19	0.81	3.47	0.08	0.10	20.23	12.15	1.34	0.04	98.35	6.85	0.05	1.66	0.09	0.40	0.01	0.01	4.17	1.80	0.36	0.01	15.41	91.04	8.76		
S1901-03	A4	49.31	0.38	10.38	0.81	3.48	0.08	0.08	19.74	12.28	1.37	0.04	97.94	6.85	0.04	1.70	0.09	0.40	0.01	0.01	4.09	1.83	0.37	0.01	15.40	90.81	8.98		
S1901-03	A4	49.48	0.40	10.09	1.04	3.63	0.01	0.10	19.76	12.27	1.34	0.06	98.18	6.87	0.04	1.65	0.11	0.42	0.00	0.01	4.20	1.82	0.36	0.01	15.39	90.62	9.35		
S1901-03	A4	49.64	0.47	10.08	1.19	3.30	0.04	0.10	19.86	12.27	1.39	0.04	98.38	6.87	0.05	1.64	0.13	0.38	0.00	0.01	4.10	1.82	0.37	0.01	15.39	91.39	8.51		
S1901-03	A4	49.81	0.41	10.12	0.58	3.49	0.07	0.08	20.19	12.39	1.34	0.03	98.50	6.88	0.04	1.65	0.06	0.40	0.01	0.01	4.16	1.83	0.36	0.00	15.41	90.99	8.82		
S1901-03	A4	49.99	0.37	10.17	0.72	3.50	0.07	0.15	20.11	12.34	1.33	0.05	98.80	6.88	0.04	1.65	0.08	0.40	0.01	0.02	4.13	1.82	0.36	0.01	15.39	90.94	8.87		
S1901-03	A4	50.00	0.46	9.81	1.05	3.38	0.04	0.11	20.24	12.38	1.28	0.03	98.78	6.89	0.05	1.59	0.11	0.39	0.00	0.01	4.16	1.83	0.34	0.00	15.38	91.33	8.57		
S1901-03	A4	50.04	0.41	9.76	0.93	3.47	0.06	0.09	20.35	12.45	1.34	0.03	98.92	6.89	0.04	1.58	0.10	0.40	0.01	0.01	4.17	1.84	0.36	0.00	15.41	91.13	8.72		
S1901-03	A4	50.01	0.42	9.74	1.16	3.25	0.05	0.14	20.18	12.41	1.26	0.02	98.63	6.90	0.04	1.58	0.13	0.38	0.01	0.02	4.15	1.83	0.34	0.00	15.37	91.58	8.29		
S1901-03	A4	49.75	0.39	9.86	0.67	3.41	0.09	0.09	20.35	12.10	1.24	0.02	97.97	6.90	0.04	1.61	0.07												

**Table A1a.** (continued)

Sample	Min. Ass.	SiO <sub>2</sub>	TiO <sub>2</sub>	Al <sub>2</sub> O <sub>3</sub>	Cr <sub>2</sub> O <sub>3</sub>	FeO	MnO	NiO	MgO	CaO	Na <sub>2</sub> O	K <sub>2</sub> O	Total F.S./23 O	Si	Ti	Al	Cr	Fe <sup>2+</sup>	Mn	Ni	Mg	Ca	Na	K	Total Mg%/ $Mg + Fe + Na + K$		
S1901-03	A4	49.99	0.44	9.61	0.96	3.19	0.08	0.09	20.33	12.56	1.21	0.02	98.47	6.91	0.05	1.56	0.10	0.37	0.01	0.01	4.19	1.86	0.32	0.00	15.38	91.72	8.07
S1901-03	A4	49.63	0.36	9.52	1.10	3.27	0.06	0.05	20.19	12.30	1.27	0.02	97.77	6.91	0.04	1.56	0.12	0.38	0.01	0.01	4.19	1.83	0.34	0.00	15.39	91.52	8.32
S1901-03	A4	49.74	0.44	9.78	0.78	3.37	0.08	0.07	19.98	12.33	1.31	0.04	97.91	6.91	0.05	1.60	0.09	0.39	0.01	0.01	4.14	1.84	0.35	0.01	15.38	91.18	8.63
S1901-03	A4	50.14	0.44	9.74	1.04	3.44	0.09	0.10	20.08	12.37	1.30	0.02	98.75	6.91	0.05	1.58	0.11	0.40	0.01	0.01	4.12	1.83	0.35	0.00	15.37	91.03	8.74
S1901-03	A4	50.10	0.32	9.92	0.32	3.28	0.01	0.08	20.39	12.49	1.30	0.02	98.22	6.92	0.03	1.61	0.04	0.38	0.00	0.01	4.20	1.85	0.35	0.00	15.39	91.71	8.27
S1901-03	A4	48.73	0.30	8.75	0.61	3.29	0.04	0.09	21.31	11.23	1.14	0.03	95.52	6.92	0.03	1.47	0.07	0.39	0.01	0.01	4.51	1.71	0.31	0.00	15.44	91.94	7.95
S1901-03	A4	49.44	0.44	9.49	0.62	3.35	0.03	0.12	19.54	12.43	1.31	0.03	96.79	6.95	0.05	1.57	0.07	0.39	0.00	0.01	4.09	1.87	0.36	0.00	15.37	91.16	8.76
S1901-03	A4	50.02	0.27	9.62	0.27	3.36	0.00	0.13	20.55	12.11	1.28	0.05	97.66	6.95	0.03	1.58	0.03	0.39	0.00	0.01	4.25	1.80	0.34	0.01	15.40	91.59	8.41
S1901-03	A4	50.54	0.37	9.55	0.64	3.23	0.09	0.07	20.44	12.45	1.29	0.03	98.70	6.95	0.04	1.55	0.07	0.37	0.01	0.01	4.19	1.83	0.34	0.00	15.37	91.64	8.12
S1901-03	A4	50.21	0.37	9.31	0.87	3.34	0.05	0.03	20.23	12.25	1.26	0.03	97.94	6.96	0.04	1.52	0.10	0.39	0.01	0.00	4.18	1.82	0.34	0.01	15.36	91.41	8.46
S1901-03	A4	50.31	0.29	9.37	0.76	3.34	0.07	0.12	20.17	12.42	1.27	0.05	98.17	6.97	0.03	1.53	0.08	0.39	0.01	0.01	4.16	1.84	0.34	0.01	15.37	91.34	8.50
S1901-03	A4	51.01	0.26	9.31	0.52	3.40	0.08	0.08	20.35	12.29	1.26	0.02	98.56	7.02	0.03	1.51	0.06	0.39	0.01	0.01	4.17	1.81	0.33	0.00	15.34	91.25	8.56
S1901-03	A4	51.63	0.25	8.72	0.27	3.26	0.08	0.11	20.78	12.40	1.14	0.03	98.66	7.08	0.03	1.41	0.03	0.37	0.01	0.01	4.25	1.82	0.30	0.01	15.32	91.74	8.07
S1901-03	A4	51.94	0.31	8.45	0.49	3.04	0.05	0.14	20.83	12.50	1.13	0.03	98.90	7.11	0.03	1.36	0.05	0.35	0.01	0.02	4.25	1.83	0.30	0.01	15.31	92.33	7.56
S1901-04	A4	46.87	0.50	9.25	1.62	3.41	0.00	0.11	19.37	12.97	1.47	0.05	95.65	6.74	0.05	1.57	0.18	0.41	0.00	0.01	4.15	2.00	0.41	0.01	15.54	91.00	9.00
S1901-04	A4	48.83	0.46	10.31	1.28	3.41	0.06	0.05	19.25	12.61	1.29	0.03	97.53	6.83	0.05	1.70	0.14	0.40	0.01	0.00	4.01	1.89	0.35	0.01	15.38	90.81	9.03
S1901-04	A4	48.51	0.46	8.85	1.65	3.52	0.00	0.05	19.97	12.97	1.39	0.01	97.37	6.83	0.05	1.47	0.18	0.41	0.00	0.01	4.19	1.96	0.38	0.00	15.48	91.00	9.00
S1901-04	A4	48.00	0.46	8.95	1.18	3.56	0.01	0.05	19.75	12.97	1.33	0.00	96.27	6.83	0.05	1.50	0.13	0.42	0.00	0.01	4.19	1.98	0.37	0.00	15.48	90.79	9.19
S1901-04	A4	48.92	0.49	9.17	1.19	3.28	0.02	0.00	19.94	13.02	1.38	0.03	97.44	6.86	0.05	1.52	0.13	0.39	0.00	0.00	4.17	1.96	0.38	0.01	15.45	91.49	8.45
S1901-04	A4	48.61	0.51	8.26	1.21	3.67	0.05	0.14	20.13	13.24	1.25	0.01	97.07	6.87	0.05	1.38	0.13	0.43	0.01	0.02	4.24	2.01	0.34	0.00	15.49	90.60	9.28
S1901-04	A4	49.08	0.52	9.12	1.36	3.33	0.00	0.08	19.13	13.02	1.28	0.01	96.93	6.92	0.05	1.52	0.15	0.39	0.00	0.01	4.02	1.97	0.35	0.00	15.37	91.11	8.89
S1901-04	A4	49.86	0.41	9.56	1.28	3.38	0.00	0.00	19.50	12.53	1.45	0.00	97.97	6.93	0.04	1.57	0.14	0.39	0.00	0.00	4.04	1.87	0.39	0.00	15.37	91.14	8.86
S1901-04	A4	49.77	0.39	8.90	0.87	3.57	0.06	0.00	20.23	12.66	1.42	0.03	97.90	6.94	0.04	1.46	0.10	0.42	0.01	0.00	4.20	1.89	0.38	0.01	15.44	90.85	9.00
S1901-04	A4	49.43	0.51	9.48	1.24	3.42	0.00	0.19	11.5	12.52	1.22	0.03	97.00	6.94	0.05	1.57	0.14	0.40	0.00	0.00	4.01	1.88	0.33	0.01	15.32	90.89	9.11
S1901-04	A4	49.79	0.35	9.77	1.17	3.44	0.07	0.04	19.36	12.25	1.35	0.02	97.57	6.94	0.04	1.61	0.13	0.40	0.01	0.00	4.02	1.83	0.36	0.00	15.34	90.76	9.05
S1901-04	A4	49.95	0.41	8.79	1.09	3.21	0.00	0.04	20.19	12.94	1.22	0.01	97.85	6.95	0.04	1.44	0.12	0.37	0.00	0.00	4.19	1.93	0.33	0.00	15.39	91.80	8.20
S1901-04	A4	48.99	0.42	7.87	0.95	3.36	0.00	0.07	20.24	12.99	1.16	0.00	96.05	6.97	0.05	1.32	0.11	0.40	0.00	0.01	4.29	1.98	0.32	0.00	15.43	91.47	8.53
S1901-04	A4	49.68	0.39	7.90	1.10	3.42	0.12	0.13	20.43	13.15	1.17	0.00	97.49	6.97	0.04	1.31	0.12	0.40	0.01	0.01	4.27	1.98	0.32	0.00	15.43	91.14	8.57
S1901-04	A4	50.28	0.48	8.56	1.09	3.19	0.02	0.11	20.13	13.16	1.26	0.03	98.32	6.97	0.05	1.40	0.12	0.37	0.00	0.01	4.16	1.96	0.34	0.01	15.39	91.79	8.16
S1901-04	A4	49.76	0.35	7.90	0.96	3.44	0.03	0.07	20.46	12.98	1.09	0.01	97.06	7.00	0.04	1.31	0.11	0.40	0.00	0.01	4.29	1.96	0.30	0.00	15.41	91.31	8.62
S1901-04	A4	50.07	0.42	8.85	0.95	3.43	0.05	0.00	19.89	12.30	1.19	0.04	97.19	7.00	0.04	1.46	0.11	0.40	0.01	0.00	4.15	1.84	0.32	0.01	15.34	91.06	8.81
S1901-04	A4	50.26	0.53	8.90	0.82	3.41	0.07	0.00	19.81	12.39	1.28	0.04	97.51	7.01	0.06	1.46	0.09	0.40	0.01	0.00	4.12	1.85	0.35	0.01	15.34	91.02	8.79
S1901-04	A4	50.52	0.42	8.72	0.74	3.48	0.00	0.08	19.93	12.83	1.32	0.00	98.02	7.01	0.04	1.43	0.08	0.40	0.00	0.01	4.12	1.91	0.35	0.00	15.37	91.08	8.92
S1901-04	A4	50.36	0.39	7.96	0.73	3.42	0.08	0.08	20.15	13.04	1.14	0.04	97.38	7.05	0.04	1.31	0.08	0.40	0.01	0.01	4.20	1.96	0.31	0.01	15.37	91.12	8.68
S1901-04	A4	50.67	0.31	7.98	0.93	3.32	0.08	0.05	20.36	12.84	1.24	0.00	97.79	7.05	0.03	1.31	0.10	0.39	0.01	0.01	4.22	1.91	0.34	0.00	15.38	91.42	8.36

<sup>a</sup>Major element compositions are in wt %. Analyses are ordered by increasing sample number and Si content. Min. Ass., mineral assemblage.

**Table Alb.** Major Element Compositions of Amphiboles From VLS Ultramafic Mylonites Analyzed by Electron Microprobe: Site S1902<sup>a</sup>

Sample	Min.	Ass.	SiO <sub>2</sub>	TiO <sub>2</sub>	Al <sub>2</sub> O <sub>3</sub>	Cr <sub>2</sub> O <sub>3</sub>	FeO	MnO	NiO	MgO	CaO	Na <sub>2</sub> O	K <sub>2</sub> O	Total	F,S,23	O	Si	Al	Cr	Fe <sup>2+</sup>	Mn	Ni	Mg	Ca	Na	K	Total	Mg% / Mg + Fe	Fe% / Fe + Mg
S1902-09	A4	47.30	0.41	9.75	0.56	3.55	0.08	0.06	21.98	10.46	1.33	0.03	95.51	6.74	0.04	1.64	0.06	0.42	0.01	0.01	4.67	1.60	0.37	0.00	15.56	91.51	8.30		
S1902-09	A4	48.39	0.46	11.23	0.71	3.41	0.02	0.09	19.68	12.31	1.58	0.03	97.90	6.74	0.05	1.84	0.08	0.40	0.00	0.01	4.08	1.84	0.43	0.00	15.47	91.10	8.85		
S1902-09	A4	49.06	0.34	11.51	0.54	3.29	0.06	0.06	20.02	12.37	1.55	0.02	98.82	6.75	0.04	1.87	0.06	0.38	0.01	0.01	4.11	1.82	0.41	0.00	15.46	91.42	8.42		
S1902-09	A4	47.34	0.28	9.91	0.71	3.44	0.10	0.08	20.92	10.74	1.37	0.04	94.93	6.78	0.03	1.67	0.08	0.41	0.01	0.01	4.47	1.65	0.38	0.01	15.50	91.35	8.42		
S1902-09	A4	48.58	0.35	10.79	0.73	3.06	0.03	0.11	19.49	12.23	1.57	0.02	96.96	6.81	0.04	1.78	0.08	0.36	0.00	0.01	4.07	1.84	0.43	0.00	15.43	91.83	8.09		
S1902-09	A4	49.59	0.43	10.48	0.71	3.37	0.10	0.12	20.27	12.23	1.34	0.03	98.67	6.84	0.04	1.70	0.08	0.39	0.01	0.01	4.17	1.81	0.36	0.00	15.41	91.23	8.52		
S1902-09	A4	48.57	0.43	11.03	0.87	3.23	0.09	0.14	18.95	11.67	1.38	0.02	96.39	6.84	0.05	1.83	0.10	0.38	0.01	0.02	3.98	1.76	0.38	0.00	15.34	91.03	8.72		
S1902-09	A4	48.90	0.26	9.76	0.72	3.36	0.02	0.07	20.98	11.34	1.26	0.03	96.70	6.86	0.03	1.62	0.08	0.39	0.00	0.01	4.39	1.71	0.34	0.01	15.44	91.71	8.24		
S1902-09	A4	49.60	0.32	9.80	0.71	3.47	0.08	0.13	20.99	11.67	1.28	0.04	98.10	6.87	0.03	1.60	0.08	0.40	0.01	0.01	4.33	1.73	0.34	0.01	15.43	91.31	8.48		
S1902-09	A4	49.69	0.30	10.02	0.83	3.05	0.03	0.12	20.66	11.96	1.27	0.02	97.95	6.88	0.03	1.64	0.09	0.35	0.00	0.01	4.26	1.78	0.34	0.00	15.40	92.27	7.65		
S1902-09	A4	50.12	0.40	9.80	1.00	3.31	0.04	0.11	20.54	12.30	1.31	0.02	98.95	6.89	0.04	1.59	0.11	0.38	0.00	0.01	4.21	1.81	0.35	0.00	15.40	91.63	8.27		
S1902-09	A4	47.92	0.31	7.02	0.52	3.97	0.03	0.06	24.13	9.17	0.88	0.01	94.03	6.92	0.03	1.19	0.06	0.48	0.00	0.01	5.19	1.42	0.25	0.00	15.55	91.48	8.45		
S1902-09	A4	48.17	0.37	7.76	0.72	4.33	0.05	0.08	22.36	9.96	0.99	0.03	94.83	6.92	0.04	1.31	0.08	0.52	0.01	0.01	4.79	1.54	0.28	0.01	15.49	90.10	9.78		
S1902-09	A4	49.96	0.32	9.81	0.72	3.09	0.01	0.16	20.39	12.28	1.28	0.03	98.05	6.92	0.03	1.60	0.08	0.36	0.00	0.02	4.21	1.82	0.34	0.00	15.38	92.13	7.84		
S1902-09	A4	48.47	0.34	7.96	0.60	3.73	0.05	0.04	22.74	9.87	1.07	0.02	94.88	6.93	0.04	1.34	0.07	0.45	0.01	0.01	4.84	1.51	0.30	0.00	15.48	91.46	8.41		
S1902-09	A4	48.86	0.32	8.18	1.01	3.38	0.09	0.09	21.66	11.21	1.12	0.01	95.93	6.93	0.03	1.37	0.11	0.49	0.01	0.01	4.58	1.70	0.31	0.00	15.45	91.75	8.04		
S1902-09	A4	49.09	0.39	8.62	0.84	3.56	0.06	0.08	21.12	11.12	1.12	0.01	95.93	6.93	0.04	1.43	0.09	0.42	0.01	0.01	4.45	1.72	0.32	0.00	15.42	91.24	8.62		
S1902-09	A4	50.40	0.35	9.30	1.02	2.99	0.05	0.07	20.78	12.45	1.20	0.02	98.62	6.94	0.04	1.51	0.11	0.34	0.01	0.01	4.26	1.84	0.32	0.00	15.38	92.40	7.47		
S1902-09	A4	49.54	0.29	8.14	1.01	3.31	0.05	0.08	21.46	11.55	1.20	0.02	96.64	6.97	0.03	1.35	0.11	0.39	0.01	0.01	4.50	1.74	0.33	0.00	15.44	91.93	7.96		
S1902-09	A4	48.85	0.29	7.57	0.56	3.52	0.00	0.15	22.58	10.13	1.03	0.02	94.71	6.99	0.03	1.28	0.06	0.42	0.00	0.02	4.81	1.55	0.29	0.00	15.46	91.96	8.04		
S1902-09	A4	50.38	0.40	9.45	0.53	2.99	0.02	0.10	20.13	12.34	1.17	0.02	97.52	6.99	0.04	1.55	0.06	0.35	0.00	0.01	4.16	1.84	0.31	0.00	15.32	92.26	7.69		
S1902-09	A4	49.30	0.19	7.41	0.48	4.59	0.09	0.11	22.38	10.44	0.93	0.03	95.94	7.00	0.02	1.24	0.05	0.55	0.01	0.01	4.73	1.59	0.26	0.00	15.46	89.49	10.30		
S1902-09	A4	50.61	0.28	8.96	0.63	3.04	0.04	0.02	20.62	12.42	1.14	0.02	97.76	7.01	0.03	1.46	0.07	0.35	0.00	0.00	4.26	1.84	0.31	0.00	15.35	92.26	7.63		
S1902-09	A4	50.26	0.35	8.92	0.93	2.96	0.07	0.12	20.04	12.30	1.19	0.03	97.17	7.02	0.04	1.47	0.10	0.35	0.01	0.01	4.17	1.84	0.32	0.01	15.33	92.19	7.63		
S1902-09	A4	48.79	0.42	9.04	0.78	2.96	0.11	0.07	19.25	11.29	1.18	0.03	93.92	7.03	0.05	1.53	0.09	0.36	0.01	0.01	4.13	1.74	0.33	0.00	15.28	91.77	7.93		
S1902-09	A4	51.11	0.31	8.53	0.82	3.00	0.02	0.01	20.86	12.58	1.16	0.02	98.42	7.04	0.03	1.39	0.09	0.35	0.00	0.00	4.28	1.86	0.31	0.00	15.35	92.48	7.46		
S1902-09	A4	50.46	0.36	8.20	0.61	3.24	0.06	0.07	20.88	12.13	1.08	0.02	97.11	7.05	0.04	1.35	0.07	0.38	0.01	0.01	4.35	1.82	0.29	0.00	15.35	91.84	8.00		
S1902-09	A4	51.35	0.22	8.87	0.69	3.14	0.04	0.06	20.76	12.34	1.21	0.03	98.70	7.05	0.02	1.44	0.07	0.36	0.00	0.01	4.25	1.81	0.32	0.01	15.34	92.09	7.82		
S1902-09	A4	50.40	0.31	8.67	0.61	2.89	0.10	0.11	20.17	12.37	1.21	0.02	96.86	7.05	0.03	1.43	0.07	0.34	0.01	0.01	4.21	1.85	0.33	0.00	15.33	92.32	7.42		
S1902-09	A4	49.24	0.24	9.40	0.43	4.92	0.05	0.03	19.53	11.10	0.98	0.04	93.95	7.06	0.03	1.59	0.05	0.35	0.01	0.00	4.17	1.71	0.27	0.01	15.24	92.18	7.68		
S1902-09	A4	49.75	0.27	6.42	0.39	3.35	0.08	0.11	23.46	9.96	0.79	0.02	94.59	7.10	0.03	1.08	0.04	0.40	0.01	0.01	4.99	1.52	0.22	0.00	15.42	92.42	7.40		
S1902-09	A4	50.60	0.18	6.57	0.67	3.17	0.00	0.05	23.35	10.52	0.91	0.02	96.03	7.12	0.02	1.00	0.07	0.37	0.00	0.01	4.89	1.59	0.25	0.00	15.41	92.92	7.08		
S1902-09	A4	51.29	0.27	7.98	0.85	2.90	0.05	0.08	20.46	12.58	1.16	0.02	97.66	7.12	0.03	1.31	0.09	0.34	0.01	0.01	4.23	1.87	0.31	0.00	15.31	92.50	7.36		
S1902-09	A4	51.92	0.26	7.93	0.73	2.87	0.08	0.06	21.05	12.62	1.03	0.02	98.57	7.13	0.03	1.28	0.08	0.33	0.01	0.01	4.31	1.86	0.27	0.00	15.30	92.70	7.10		
S1902-09	A4	53.27	0.13	5.76	0.22	2.79	0.06	0.08	22.19	11.53	0.40	0.01	96.46	7.40	0.01	0.94	0.02	0.32	0.01	0.01	4.60	1.72	0.11	0.00	15.15	93.26	6.59		
S1902-20	A4	49.90	0.36	9.01	0.54	3.36	0.07		19.97	12.30	1.15	0.02	96.67	7.00	0.04	1.49	0.06	0.39	0.01	0.00	4.18	1.85	0.31	0.00	15.34	91.21	8.62		
S1902-20	A4	51.20	0.37	9.04	0.45	3.30	0.06		20.05	12.31	1.10	0.04	97.93	7.07	0.04	1.47	0.05	0.38	0.01	0.00	4.13	1.82	0.30	0.01	15.28	91.41	8.43		
S1902-34	A5	55.17	0.08	2.36	0.09	3.10	0.12	0.03	23.62	12.31	0.36	0.01	97.26	7.63	0.01	1.39	0.01	0.36	0.01	0.00	4.87	1.82	0.10	0.00	15.21	92.88	6.84		
S1902-34	A5	55.24	0.11	1.94	0.04	3.62	0.17	0.03	23.15	12.23	0.34	0.02	96.89	7.69	0.01	1.32	0.00	0.42	0.02	0.00	4.80	1.82	0.09	0.00	15.19	91.58	8.03		
S1902-34	A5	55.18	0.04	2.09	0.05	4.09	0.07	0.05	21.96	12.74	0.62	0.02	96.91	7.71	0.00	1.34	0.00	0.48	0.01	0.01	4.57	1.91	0.17	0.00	15.				

**Table A1c.** Major Element Compositions of Amphiboles From VLS Ultramafic Mylonites Analyzed by Electron Microprobe: Site S1903<sup>a</sup>

Sample	Min. Ass.	SiO <sub>2</sub>	TiO <sub>2</sub>	Al <sub>2</sub> O <sub>3</sub>	Cr <sub>2</sub> O <sub>3</sub>	FeO	MnO	NiO	MgO	CaO	Na <sub>2</sub> O	K <sub>2</sub> O	Total F.S./23 O	Si	Ti	Al	Cr	Fe <sup>2+</sup>	Mn	Ni	Total Mg <sup>2+</sup> /Mg + Fe Fe <sup>2+</sup> /Fe + Mg						
S1903-09	A3	45.96	0.67	12.11	1.61	3.71	0.05	0.12	19.78	11.97	1.81	0.02	97.80	6.46	0.07	2.01	0.18	0.44	0.01	4.15	1.80	0.49	0.00	15.62	90.36	9.52	
S1903-09	A3	46.39	0.89	12.10	1.74	3.67	0.02	0.11	18.98	12.58	2.02	0.03	98.55	6.49	0.09	1.99	0.19	0.43	0.00	3.95	1.88	0.55	0.01	15.60	90.16	9.78	
S1903-09	A3	46.70	0.80	12.11	1.81	3.72	0.05	0.07	19.20	12.59	2.08	0.03	99.15	6.49	0.08	1.98	0.20	0.43	0.01	3.98	1.88	0.56	0.01	15.62	90.10	9.78	
S1903-09	A3	46.63	0.85	12.09	1.88	3.77	0.02	0.06	18.91	12.59	2.06	0.04	98.88	6.50	0.09	1.99	0.21	0.44	0.00	3.91	1.88	0.56	0.01	15.60	89.89	10.06	
S1903-09	A3	46.70	0.74	11.50	2.69	3.95	0.04	0.14	19.42	12.18	1.78	0.03	99.17	6.50	0.08	1.89	0.30	0.46	0.01	0.02	4.03	1.82	0.48	0.00	15.57	89.65	10.23
S1903-09	A3	46.83	0.76	12.07	1.85	3.69	0.01	0.10	19.06	12.73	2.07	0.02	99.20	6.50	0.08	1.98	0.20	0.43	0.00	0.01	3.95	1.89	0.56	0.00	15.61	90.17	9.79
S1903-09	A3	46.51	0.66	12.12	1.77	3.72	0.13	0.10	18.77	12.50	2.14	0.04	98.44	6.51	0.07	2.00	0.20	0.43	0.01	0.01	3.92	1.87	0.58	0.01	15.62	89.70	9.96
S1903-09	A3	46.69	0.69	12.07	1.65	3.52	0.06	0.07	19.14	12.59	1.84	0.03	98.35	6.53	0.07	1.99	0.18	0.41	0.01	0.01	3.99	1.89	0.50	0.00	15.57	90.51	9.34
S1903-09	A3	46.74	0.73	11.94	1.73	3.73	0.05	0.07	19.02	12.57	1.97	0.04	98.58	6.53	0.08	1.96	0.19	0.44	0.01	0.01	3.96	1.88	0.53	0.01	15.59	89.97	9.91
S1903-09	A3	46.78	0.79	11.88	1.92	3.81	0.02	0.03	18.69	12.55	2.10	0.04	98.60	6.54	0.08	1.96	0.21	0.44	0.00	0.00	3.89	1.88	0.57	0.01	15.58	89.70	10.25
S1903-09	A3	47.01	0.83	11.81	1.29	3.74	0.07	0.12	19.18	12.80	2.07	0.03	98.94	6.54	0.09	1.94	0.14	0.44	0.01	0.01	3.98	1.91	0.56	0.00	15.61	89.97	9.85
S1903-09	A3	47.18	0.77	11.61	1.59	3.67	0.05	0.09	19.47	12.72	1.95	0.03	99.14	6.55	0.08	1.90	0.17	0.43	0.01	0.01	4.03	1.89	0.52	0.01	15.60	90.31	9.56
S1903-09	A3	47.00	0.69	11.80	1.46	3.58	0.06	0.16	19.08	12.79	2.04	0.04	98.70	6.55	0.07	1.94	0.16	0.42	0.01	0.02	3.96	1.91	0.55	0.01	15.60	90.33	9.50
S1903-09	A3	47.19	0.76	11.51	1.14	4.28	0.03	0.07	19.54	12.41	1.87	0.03	98.83	6.57	0.08	1.89	0.12	0.50	0.00	0.01	4.06	1.85	0.50	0.01	15.60	89.00	10.94
S1903-09	A3	47.25	0.78	11.58	1.87	3.52	0.06	0.07	18.90	12.74	2.00	0.04	98.79	6.58	0.08	1.90	0.21	0.41	0.01	0.01	3.92	1.90	0.54	0.01	15.56	90.40	9.45
S1903-09	A3	46.77	0.78	11.79	1.82	3.64	0.00		18.26	12.55	2.12	0.00	97.73	6.58	0.08	1.96	0.20	0.43	0.00	0.00	3.83	1.89	0.58	0.00	15.55	89.94	10.06
S1903-09	A3	47.40	0.75	11.35	1.60	3.47	0.03	0.14	19.52	12.77	1.97	0.03	99.02	6.58	0.08	1.86	0.18	0.40	0.00	0.02	4.04	1.90	0.53	0.00	15.59	90.84	9.07
S1903-09	A3	46.98	0.73	11.22	1.59	3.61	0.00	0.08	19.20	12.67	1.94	0.03	98.03	6.59	0.08	1.86	0.18	0.42	0.00	0.01	4.01	1.90	0.53	0.00	15.58	90.46	9.54
S1903-09	A3	47.45	0.69	11.26	1.48	3.58	0.04	0.10	19.41	12.77	1.88	0.04	98.68	6.61	0.07	1.85	0.16	0.42	0.00	0.01	4.03	1.91	0.51	0.01	15.57	90.54	9.36
S1903-09	A3	47.70	0.71	11.12	1.46	3.70	0.02	0.16	19.59	12.83	1.83	0.05	99.18	6.61	0.07	1.82	0.16	0.43	0.00	0.02	4.05	1.91	0.49	0.01	15.57	90.36	9.59
S1903-09	A3	47.56	0.76	11.81	1.15	3.79	0.04	0.08	18.32	12.61	2.00	0.00	98.04	6.65	0.08	1.95	0.13	0.44	0.00	0.00	3.82	1.89	0.54	0.00	15.50	89.50	10.39
S1903-09	A3	48.11	0.70	10.92	1.34	3.57	0.07	0.09	19.56	12.78	1.85	0.02	99.00	6.67	0.07	1.78	0.15	0.41	0.01	0.01	4.04	1.90	0.50	0.00	15.54	90.53	9.29
S1903-09	A3	48.62	0.72	10.45	0.95	3.75	0.06	0.13	19.81	12.91	1.78	0.02	99.19	6.72	0.07	1.70	0.10	0.43	0.01	0.01	4.08	1.91	0.48	0.00	15.54	90.25	9.59

<sup>a</sup>Major element compositions are in wt %. Analyses are ordered by increasing sample number and Si content. Min. Ass., mineral assemblage.

**Table A1d.** Major Element Compositions of Amphiboles From VLS Ultramafic Mylonites Analyzed by Electron Microprobe: Site S1904<sup>a</sup>

Sample	Min. Ass.	SiO <sub>2</sub>	TiO <sub>2</sub>	Al <sub>2</sub> O <sub>3</sub>	Cr <sub>2</sub> O <sub>3</sub>	FeO	MnO	NiO	MgO	CaO	Na <sub>2</sub> O	K <sub>2</sub> O	Total	F.S./23	O	Si	Ti	Al	Cr	Fe <sup>2+</sup>	Mn	Ni	Mg	Ca	Na	K	Total	Mg%/ $Mg + Fe$	Fe%/ $Fe + Mg$
S1904-38	A4	51.95	0.21	4.88	0.94	3.85	0.08	21.67	10.91	1.02	0.15	95.66	7.36	0.02	0.82	0.11	0.46	0.01	0.00	4.58	1.66	0.28	0.03	15.31	90.76	9.05			
S1904-38	A4	53.84	0.07	4.65	1.23	3.03	0.05	21.13	12.14	0.80	0.03	96.97	7.49	0.01	0.76	0.14	0.35	0.01	0.00	4.38	1.81	0.22	0.01	15.16	92.44	7.44			
S1904-38	A4	53.64	0.19	3.94	0.71	4.22	0.15	21.77	10.70	0.63	0.08	96.03	7.54	0.02	0.65	0.08	0.50	0.02	0.00	4.56	1.61	0.17	0.01	15.17	89.87	9.78			
S1904-61	A3	44.89	0.60	11.07	1.77	3.90	0.00	0.09	18.79	12.91	1.94	0.05	96.01	6.48	0.06	1.88	0.20	0.47	0.00	0.01	4.04	2.00	0.54	0.01	15.69	89.57	10.43		
S1904-61	A3	45.72	0.53	10.68	1.72	3.94	0.06	0.11	19.16	13.09	1.83	0.05	96.90	6.53	0.06	1.80	0.19	0.47	0.01	0.01	4.08	2.00	0.51	0.01	15.67	89.52	10.32		
S1904-61	A3	44.91	0.68	10.46	1.54	3.74	0.02	0.09	18.57	12.97	1.88	0.04	94.89	6.55	0.07	1.80	0.18	0.46	0.00	0.01	4.03	2.03	0.53	0.01	15.66	89.80	10.14		
S1904-61	A3	45.04	0.57	9.92	1.16	3.66	0.04	0.08	19.07	13.20	1.87	0.00	94.60	6.58	0.06	1.71	0.13	0.45	0.00	0.01	4.15	2.07	0.53	0.00	15.70	90.19	9.71		
S1904-61	A3	46.80	0.66	11.10	1.79	3.68	0.00	0.12	18.86	13.07	1.89	0.01	97.97	6.59	0.07	1.84	0.20	0.43	0.00	0.01	3.95	1.97	0.51	0.00	15.58	90.12	9.88		
S1904-61	A3	45.81	0.58	10.61	1.42	3.66	0.04	0.11	18.82	12.70	1.85	0.02	95.63	6.60	0.06	1.80	0.16	0.44	0.01	0.01	4.04	1.96	0.52	0.00	15.61	90.05	9.83		
S1904-61	A3	46.51	0.59	10.85	1.50	3.79	0.06	0.05	18.78	13.05	1.97	0.02	97.16	6.60	0.06	1.81	0.17	0.45	0.01	0.01	3.97	1.99	0.54	0.00	15.61	89.70	10.15		
S1904-61	A3	45.46	0.57	9.62	1.45	4.02	0.02	0.09	19.90	12.11	1.64	0.00	94.86	6.61	0.06	1.65	0.17	0.49	0.00	0.01	4.31	1.89	0.46	0.00	15.65	89.76	10.18		
S1904-61	A3	47.35	0.57	11.09	1.58	3.84	0.00	0.12	18.83	13.06	1.95	0.00	98.39	6.63	0.06	1.83	0.17	0.45	0.00	0.01	3.93	1.96	0.53	0.00	15.57	89.73	10.27		
S1904-61	A3	47.04	0.55	10.91	1.44	3.94	0.00	0.04	18.98	12.68	1.86	0.03	97.46	6.64	0.06	1.82	0.16	0.46	0.00	0.00	3.99	1.92	0.51	0.01	15.57	89.58	10.42		
S1904-61	A3	46.61	0.61	10.37	1.54	3.93	0.06	0.09	18.06	12.95	1.73	0.02	95.97	6.69	0.07	1.75	0.17	0.47	0.01	0.01	3.87	1.99	0.48	0.00	15.52	88.96	10.87		
S1904-61	A3	46.62	0.56	8.78	1.12	3.67	0.01	0.11	19.74	13.14	1.58	0.03	95.37	6.74	0.06	1.50	0.13	0.44	0.00	0.01	4.25	2.03	0.44	0.01	15.61	90.53	9.45		
S1904-62	A4	48.60	0.47	10.20	1.73	3.54	0.01	0.08	18.95	13.03	1.10	0.00	97.71	6.80	0.05	1.68	0.19	0.41	0.00	0.01	3.95	1.96	0.30	0.00	15.36	90.49	9.49		
S1904-62	A4	48.42	0.57	9.79	1.70	3.23	0.00	0.09	18.91	13.14	1.09	0.01	96.94	6.83	0.06	1.63	0.19	0.38	0.00	0.01	3.97	1.98	0.30	0.00	15.35	91.25	8.74		
S1904-62	A4	48.70	0.43	9.98	1.61	3.24	0.00	0.08	18.86	13.30	1.05	0.02	97.26	6.84	0.05	1.65	0.18	0.38	0.00	0.01	3.95	2.00	0.29	0.00	15.34	91.22	8.78		
S1904-62	A4	49.17	0.40	9.31	1.37	3.54	0.00	0.06	19.51	13.33	1.07	0.03	97.80	6.88	0.04	1.54	0.15	0.41	0.00	0.01	4.07	2.00	0.29	0.00	15.39	90.75	9.25		
S1904-62	A4	49.67	0.31	8.69	1.23	3.00	0.07	0.17	19.58	13.29	0.94	0.00	96.95	6.98	0.03	1.44	0.14	0.35	0.01	0.02	4.10	2.00	0.26	0.00	15.33	91.92	7.90		
S1904-62	A4	50.51	0.31	8.48	1.31	3.36	0.06	0.08	19.75	13.12	0.88	0.03	97.88	7.03	0.03	1.39	0.14	0.39	0.01	0.01	4.10	1.96	0.24	0.01	15.29	91.15	8.70		
S1904-62	A4	50.64	0.33	8.63	1.44	3.31	0.00	0.09	19.42	13.29	0.87	0.00	98.02	7.03	0.03	1.41	0.16	0.38	0.00	0.01	4.02	1.98	0.23	0.00	15.26	91.28	8.72		
S1904-62	A4	50.68	0.27	8.04	1.32	3.14	0.00	0.03	19.73	13.09	0.91	0.03	97.24	7.08	0.03	1.32	0.15	0.37	0.00	0.00	4.11	1.96	0.25	0.00	15.28	91.80	8.20		
S1904-62	A4	51.21	0.27	8.11	1.30	3.15	0.02	0.03	19.77	12.76	0.83	0.00	97.46	7.12	0.03	1.33	0.14	0.37	0.00	0.00	4.10	1.90	0.22	0.00	15.22	91.73	8.21		
S1904-62	A4	51.87	0.34	7.31	0.93	3.06	0.05	0.16	20.41	13.33	0.79	0.01	98.27	7.17	0.04	1.19	0.10	0.35	0.01	0.02	4.20	1.97	0.21	0.00	15.26	92.10	7.76		
S1904-62	A4	54.01	0.20	5.19	0.57	2.64	0.00	0.15	20.92	13.14	0.49	0.04	97.34	7.47	0.02	0.85	0.06	0.31	0.00	0.02	4.31	1.95	0.13	0.01	15.12	93.39	6.61		

<sup>a</sup>Major element compositions are in wt %. Analyses are ordered by increasing sample number and Si content. Min. Ass., mineral assemblage.

**Table A1e.** Major Element Compositions of Amphiboles From VLS Ultramafic Mylonites Analyzed by Electron Microprobe: Site S1905<sup>a</sup>

Sample	Min.	Ass.	SiO <sub>2</sub>	TiO <sub>2</sub>	Al <sub>2</sub> O <sub>3</sub>	Cr <sub>2</sub> O <sub>3</sub>	FeO	MnO	NiO	MgO	CaO	Na <sub>2</sub> O	K <sub>2</sub> O	Total	F.S./23	O	Si	Ti	Al	Cr	Fe <sup>2+</sup>	Mn	Ni	Mg	Ca	Na	K	Total	Mg%/ <i>Mg</i> + Fe	Fe%/ <i>Mg</i> + Fe
S1905-83	A4	51.59	0.22	7.00	1.10	2.51	0.00	0.19	20.97	13.08	1.08	0.04	97.78	7.16	0.02	1.14	0.12	0.29	0.00	0.02	4.34	1.94	0.29	0.01	15.34	93.70	6.30			
S1905-83	A4	51.46	0.23	7.12	1.07	2.88	0.00	0.04	20.66	12.93	1.06	0.08	97.54	7.16	0.02	1.17	0.12	0.34	0.00	0.00	4.28	1.93	0.29	0.01	15.32	92.74	7.25			
S1905-83	A4	51.45	0.25	6.97	1.41	2.50	0.05	0.12	20.50	12.77	1.25	0.07	97.35	7.17	0.03	1.15	0.16	0.29	0.01	0.01	4.26	1.91	0.34	0.01	15.33	93.47	6.40			
S1905-83	A4	51.87	0.26	6.54	0.95	2.56	0.02	0.14	21.04	12.70	1.14	0.05	97.28	7.22	0.03	1.07	0.10	0.30	0.00	0.02	4.37	1.89	0.31	0.01	15.32	93.56	6.38			
S1905-83	A4	51.91	0.18	6.73	1.11	2.61	0.02	0.08	20.80	12.74	0.98	0.07	97.23	7.23	0.02	1.10	0.12	0.30	0.00	0.01	4.32	1.90	0.27	0.01	15.28	93.37	6.57			
S1905-83	A4	51.85	0.22	6.33	0.96	2.75	0.03	0.08	21.18	12.75	1.00	0.04	97.20	7.23	0.02	1.04	0.11	0.32	0.00	0.01	4.40	1.90	0.27	0.01	15.31	93.12	6.79			
S1905-83	A4	52.22	0.20	6.09	1.43	2.70	0.07	0.13	20.98	12.67	1.00	0.02	97.52	7.26	0.02	1.00	0.16	0.31	0.01	0.01	4.35	1.89	0.27	0.00	15.28	93.10	6.71			
S1905-83	A4	52.48	0.20	6.35	1.32	2.68	0.06	0.12	20.95	12.57	0.92	0.06	97.71	7.27	0.02	1.04	0.14	0.31	0.01	0.01	4.33	1.86	0.25	0.01	15.25	93.17	6.68			
S1905-83	A4	52.17	0.24	6.21	1.30	2.60	0.05	0.09	20.60	12.64	0.98	0.06	96.93	7.28	0.02	1.02	0.14	0.30	0.01	0.01	4.29	1.89	0.27	0.01	15.25	93.27	6.61			
S1905-85	A4	50.05	0.40	9.45	1.30	3.10	0.13	19.48	12.43	1.07	0.02	97.48	6.97	0.04	1.55	0.14	0.36	0.02	0.00	4.04	1.86	0.29	0.00	15.28	91.49	6.97				
S1905-85	A4	49.14	0.30	9.09	1.10	2.88	0.00	19.30	12.18	0.93	0.00	95.14	7.01	0.03	1.53	0.12	0.34	0.00	0.00	4.10	1.86	0.26	0.00	15.26	92.28	7.01				
S1905-85	A4	49.96	0.33	8.76	1.48	3.01	0.09	19.57	12.44	0.96	0.03	96.69	7.02	0.04	1.45	0.16	0.35	0.01	0.00	4.10	1.87	0.26	0.01	15.27	91.84	7.02				
S1905-85	A4	50.91	0.26	8.45	1.42	2.91	0.07	20.38	12.49	0.84	0.01	97.79	7.06	0.03	1.38	0.16	0.34	0.01	0.00	4.21	1.86	0.23	0.00	15.26	92.42	7.06				
S1905-85	A4	49.77	0.24	8.77	0.92	3.02	0.04	19.68	12.06	0.90	0.02	95.48	7.06	0.03	1.47	0.10	0.36	0.00	0.00	4.16	1.83	0.25	0.00	15.26	91.99	7.06				
S1905-85	A4	50.36	0.30	8.64	1.41	2.92	0.08	19.51	12.38	0.95	0.02	96.79	7.07	0.03	1.43	0.16	0.34	0.01	0.00	4.08	1.86	0.26	0.00	15.24	92.05	7.07				
S1905-85	A4	51.69	0.26	7.92	1.14	2.75	0.02	20.24	12.49	0.82	0.03	97.42	7.17	0.03	1.29	0.13	0.32	0.00	0.00	4.19	1.86	0.22	0.01	15.21	92.87	7.17				
S1905-87	A4	48.70	0.58	10.53	1.48	3.52	0.04	0.17	20.30	12.65	1.22	0.02	99.22	6.72	0.06	1.71	0.16	0.41	0.00	0.02	4.17	1.87	0.33	0.00	15.45	91.03	8.87			
S1905-87	A4	48.88	0.45	10.58	1.51	3.26	0.10	0.15	19.96	12.48	1.20	0.02	98.59	6.77	0.05	1.73	0.16	0.38	0.01	0.02	4.12	1.85	0.32	0.00	15.41	91.36	8.37			
S1905-87	A4	49.23	0.49	10.41	1.43	3.52	0.11	0.10	19.91	12.49	1.28	0.02	98.98	6.79	0.05	1.69	0.16	0.41	0.01	0.01	4.09	1.85	0.34	0.00	15.41	90.71	9.00			
S1905-87	A4	49.16	0.59	10.16	1.60	3.47	0.08	0.05	19.74	12.56	1.22	0.01	98.64	6.81	0.06	1.66	0.18	0.40	0.01	0.01	4.07	1.86	0.33	0.00	15.38	90.83	8.96			
S1905-87	A4	49.09	0.48	10.05	1.47	3.75	0.03	0.14	19.90	12.38	1.28	0.01	98.56	6.81	0.05	1.64	0.16	0.43	0.00	0.02	4.11	1.84	0.34	0.00	15.41	90.38	9.55			
S1905-87	A4	49.37	0.53	10.13	1.55	3.46	0.04	0.06	19.89	12.41	1.29	0.03	98.74	6.82	0.05	1.65	0.17	0.40	0.01	0.01	4.10	1.84	0.35	0.00	15.39	91.01	8.88			
S1905-87	A4	49.45	0.51	10.29	1.45	3.46	0.06	0.13	19.78	12.45	1.27	0.02	98.88	6.82	0.05	1.67	0.16	0.40	0.01	0.01	4.07	1.84	0.34	0.00	15.38	90.92	8.92			
S1905-87	A4	49.60	0.48	10.17	1.47	3.44	0.03	0.11	19.93	12.49	1.34	0.02	99.06	6.83	0.05	1.65	0.16	0.40	0.00	0.01	4.09	1.84	0.36	0.00	15.40	91.11	8.82			
S1905-87	A4	49.68	0.45	10.57	1.01	3.23	0.05	0.08	20.10	12.38	1.31	0.01	98.86	6.83	0.05	1.71	0.11	0.37	0.01	0.01	4.12	1.82	0.35	0.00	15.39	91.62	8.27			
S1905-87	A4	49.62	0.49	10.07	1.45	3.51	0.04	0.13	19.89	12.47	1.24	0.02	98.94	6.84	0.05	1.64	0.16	0.40	0.00	0.01	4.09	1.84	0.33	0.00	15.38	90.89	9.00			
S1905-87	A4	49.50	0.52	10.02	1.42	3.53	0.00	0.10	19.68	12.63	1.29	0.02	98.71	6.84	0.05	1.63	0.16	0.41	0.00	0.01	4.06	1.87	0.35	0.00	15.38	90.85	9.13			
S1905-87	A4	49.80	0.55	9.85	1.40	3.70	0.07	0.10	20.00	12.59	1.33	0.02	99.40	6.85	0.06	1.60	0.15	0.43	0.01	0.01	4.10	1.85	0.35	0.00	15.40	90.45	9.38			
S1905-87	A4	49.67	0.52	10.08	1.45	3.55	0.03	0.05	19.86	12.39	1.29	0.04	98.94	6.85	0.05	1.64	0.16	0.41	0.00	0.01	4.08	1.83	0.35	0.01	15.38	90.82	9.12			
S1905-87	A4	49.68	0.51	10.17	1.42	3.45	0.02	0.12	19.79	12.47	1.27	0.02	98.92	6.85	0.05	1.65	0.15	0.40	0.00	0.01	4.07	1.84	0.34	0.00	15.37	91.06	8.90			
S1905-87	A4	49.83	0.58	10.18	1.27	3.53	0.02	0.10	19.90	12.53	1.26	0.02	99.22	6.85	0.06	1.65	0.14	0.41	0.00	0.01	4.07	1.84	0.34	0.00	15.37	90.90	9.05			
S1905-87	A4	49.61	0.45	9.93	1.50	3.58	0.04	0.08	19.95	12.49	1.24	0.02	98.88	6.85	0.05	1.61	0.16	0.41	0.00	0.01	4.10	1.85	0.33	0.00	15.39	90.75	9.15			
S1905-87	A4	49.40	0.53	9.89	1.55	3.42	0.06	0.08	19.71	12.53	1.25	0.03	98.44	6.85	0.05	1.62	0.17	0.40	0.01	0.01	4.07	1.86	0.34	0.00	15.37	90.98	8.87			
S1905-87	A4	49.59	0.51	9.90	1.41	3.48	0.06	0.17	19.95	12.46	1.29	0.02	98.83	6.85	0.05	1.61	0.15	0.40	0.01	0.01	4.11	1.84	0.34	0.00	15.39	90.95	8.90			
S1905-87	A4	49.83	0.60	10.30	1.26	3.24	0.07	0.07	20.02	12.34	1.18	0.03	98.93	6.85	0.06	1.67	0.14	0.37	0.01	0.01	4.10	1.82	0.32	0.01	15.35	91.51	8.31			
S1905-87	A4	49.62	0.58	9.86	1.63	3.35	0.07	0.13	19.91	12.38	1.21	0.03	98.78	6.85	0.06	1.60	0.18	0.39	0.01	0.01	4.10	1.83	0.32	0.01	15.36	91.19	8.62			
S1905-87	A4	49.80	0.47	10.27	1.09	3.31	0.06	0.03	20.12	12.40	1.19	0.03	98.75	6.86	0.05	1.67	0.12	0.38	0.01	0.00	4.13	1.83	0.32	0.01	15.36	91.41	8.44			
S1905-87	A4	49.53	0.52	9.91	1.40	3.52	0.08	0.07	19.81	12.34	1.31	0.01	98.49	6.86	0.05	1.62	0.15	0.41	0.01	0.01	4.09	1.83	0.35	0.00	15.38	90.74	9.06			
S1905-87	A4	49.85	0.59	9.88	1.62	3.58	0.06	0.15	19.73	12.47	1.27	0.02	99.22	6.86	0.06	1.60	0.18	0.41	0.01	0.02	4.05	1.84	0.34	0.00	15.36	90.60	9.24			
S1905-87	A4	49.75	0.48	9.93	1.20	3.33	0.06	0.03	20.16	12.44	1.28	0.03	98.68	6.86	0.05	1.62	0.13	0.38	0.01	0.00	4.15	1.84	0.34	0.00	15.39					

Table A1e. (continued)

Sample	Min.	Ass.	SiO <sub>2</sub>	TiO <sub>2</sub>	Al <sub>2</sub> O <sub>3</sub>	Cr <sub>2</sub> O <sub>3</sub>	FeO	MnO	NiO	MgO	CaO	Na <sub>2</sub> O	K <sub>2</sub> O	Total	F.S./23 O	Si	Ti	Al	Cr	Fe <sup>2+</sup>	Mn	Ni	Mg	Ca	Na	K	Total	Mg <sup>0.9</sup> /Mg + Fe	Fe <sup>0.9</sup> /Fe + Mg
S1905-87	A4	49.96	0.48	9.90	1.32	3.38	0.04	0.07	20.17	12.54	1.17	0.02	99.05	6.87	0.05	1.60	0.14	0.39	0.00	0.01	4.13	1.85	0.31	0.00	15.37	91.30	8.59		
S1905-87	A4	50.00	0.48	10.02	1.25	3.36	0.02	0.07	20.17	12.44	1.21	0.02	99.06	6.87	0.05	1.62	0.14	0.39	0.00	0.01	4.13	1.83	0.32	0.00	15.36	91.40	8.55		
S1905-87	A4	49.82	0.53	9.84	1.46	3.32	0.05	0.10	19.87	12.59	1.22	0.02	98.82	6.87	0.06	1.60	0.16	0.38	0.01	0.01	4.08	1.86	0.33	0.00	15.36	91.30	8.56		
S1905-87	A4	49.87	0.58	9.73	1.22	3.39	0.03	0.09	20.00	12.54	1.25	0.03	98.71	6.88	0.06	1.58	0.13	0.39	0.00	0.01	4.11	1.85	0.33	0.00	15.37	91.25	8.69		
S1905-87	A4	50.09	0.53	9.88	1.41	3.23	0.05	0.09	20.04	12.46	1.21	0.03	99.01	6.88	0.06	1.60	0.15	0.37	0.01	0.01	4.11	1.83	0.32	0.01	15.35	91.59	8.29		
S1905-87	A4	50.06	0.44	9.81	1.40	3.42	0.04	0.09	19.91	12.57	1.20	0.02	98.96	6.89	0.05	1.59	0.15	0.39	0.00	0.01	4.08	1.85	0.32	0.00	15.35	91.12	8.77		
S1905-87	A4	50.06	0.59	9.55	1.51	3.39	0.05	0.11	20.02	12.47	1.23	0.03	99.00	6.89	0.06	1.55	0.16	0.39	0.01	0.01	4.11	1.84	0.33	0.01	15.36	91.21	8.67		
S1905-87	A4	50.32	0.44	9.82	1.29	3.43	0.07	0.13	20.17	12.56	1.18	0.02	99.43	6.89	0.05	1.59	0.14	0.39	0.01	0.01	4.12	1.84	0.31	0.00	15.36	91.13	8.70		
S1905-87	A4	49.87	0.52	9.58	1.28	3.40	0.12	0.04	20.00	12.40	1.27	0.01	98.49	6.90	0.05	1.56	0.14	0.39	0.01	0.00	4.12	1.84	0.34	0.00	15.37	91.00	8.69		
S1905-87	A4	49.91	0.63	9.51	1.17	3.45	0.04	0.06	19.93	12.49	1.22	0.02	98.42	6.91	0.07	1.55	0.13	0.40	0.00	0.01	4.11	1.85	0.33	0.00	15.35	91.05	8.85		
S1905-87	A4	50.62	0.60	9.72	1.06	3.48	0.08	0.08	20.32	12.46	1.11	0.02	99.54	6.92	0.06	1.57	0.11	0.40	0.01	0.01	4.14	1.82	0.29	0.00	15.33	91.06	8.75		
S1905-87	A4	50.34	0.52	9.43	1.19	3.37	0.08	0.07	20.22	12.39	1.15	0.02	98.78	6.93	0.05	1.53	0.13	0.39	0.01	0.01	4.15	1.83	0.31	0.00	15.34	91.24	8.54		
S1905-87	A4	50.71	0.52	9.51	1.18	3.29	0.03	0.09	20.34	12.43	1.17	0.03	99.30	6.94	0.05	1.53	0.13	0.38	0.00	0.01	4.15	1.82	0.31	0.00	15.33	91.60	8.32		
S1905-87	A4	50.45	0.53	9.34	1.19	3.35	0.06	0.14	20.04	12.51	1.21	0.03	98.84	6.95	0.06	1.52	0.13	0.39	0.01	0.02	4.11	1.85	0.32	0.01	15.34	91.30	8.56		
S1905-87	A4	49.88	0.43	9.55	1.26	3.48	0.04	19.40	12.26	1.24	0.00	97.54	6.95	0.05	1.57	0.14	0.41	0.00	0.04	4.03	1.83	0.34	0.00	15.31	90.76	9.14			
S1905-87	A4	50.53	0.47	9.34	0.96	3.62	0.04	0.14	20.13	12.45	1.14	0.02	98.85	6.96	0.05	1.52	0.10	0.42	0.00	0.02	4.13	1.84	0.30	0.00	15.34	90.73	9.16		
S1905-87	A4	49.72	0.49	9.37	0.96	3.35	0.07	19.55	12.14	1.11	0.04	96.80	6.97	0.05	1.55	0.11	0.39	0.01	0.00	4.09	1.82	0.30	0.01	15.30	91.06	8.76			
S1905-87	A4	51.08	0.28	9.56	0.88	3.22	0.09	0.10	20.41	12.64	1.15	0.01	99.43	6.97	0.03	1.54	0.09	0.37	0.01	0.01	4.15	1.85	0.30	0.00	15.33	91.65	8.11		
S1905-95	A4	46.98	0.06	11.90	3.21	3.62	0.07	20.37	11.69	1.19	0.08	99.15	6.51	0.01	1.94	0.35	0.42	0.01	0.00	4.20	1.73	0.32	0.01	15.51	90.78	9.05			
S1905-95	A4	46.40	0.11	10.32	1.43	3.14	0.05	23.62	9.83	1.00	0.04	95.96	6.57	0.01	1.72	0.16	0.37	0.01	0.00	4.99	1.49	0.28	0.01	15.61	92.95	6.93			
S1905-95	A4	47.75	0.19	10.89	1.45	3.70	0.07	20.61	11.88	1.26	0.08	97.88	6.67	0.02	1.79	0.16	0.43	0.01	0.00	4.29	1.78	0.34	0.01	15.51	90.67	9.14			
S1905-95	A4	48.55	0.13	11.03	0.96	2.97	0.08	20.10	12.85	1.48	0.06	98.21	6.74	0.01	1.81	0.10	0.34	0.01	0.00	4.16	1.91	0.40	0.01	15.50	92.16	7.63			
S1905-95	A4	48.07	0.00	10.31	1.31	3.29	0.03	20.61	12.08	1.22	0.08	96.98	6.76	0.00	1.71	0.15	0.39	0.00	0.00	4.32	1.82	0.33	0.01	15.49	91.71	8.21			
S1905-95	A4	48.67	0.06	10.28	1.49	3.05	0.09	20.33	12.55	1.34	0.10	97.96	6.78	0.01	1.69	0.16	0.36	0.01	0.00	4.22	1.87	0.36	0.02	15.48	92.01	7.75			
S1905-95	A4	48.66	0.11	10.43	1.35	2.98	0.03	20.15	12.63	1.38	0.11	97.82	6.78	0.01	1.71	0.15	0.35	0.00	0.00	4.19	1.89	0.37	0.02	15.47	92.26	7.66			
S1905-95	A4	49.31	0.09	11.01	1.20	3.13	0.03	20.14	12.62	1.33	0.08	98.92	6.78	0.01	1.79	0.13	0.36	0.00	0.00	4.13	1.86	0.35	0.01	15.43	91.92	8.00			
S1905-95	A4	48.98	0.19	10.58	1.61	2.82	0.07	20.09	12.68	1.12	0.08	98.22	6.79	0.02	1.73	0.18	0.33	0.01	0.00	4.15	1.88	0.30	0.01	15.40	92.54	7.28			
S1905-95	A4	49.01	0.14	10.44	1.50	2.81	0.06	20.15	12.58	1.33	0.09	98.11	6.80	0.01	1.71	0.16	0.33	0.01	0.00	4.17	1.87	0.36	0.02	15.43	92.58	7.25			
S1905-95	A4	49.06	0.16	10.12	1.46	2.96	0.04	20.47	12.71	1.22	0.07	98.28	6.80	0.02	1.65	0.16	0.34	0.00	0.00	4.23	1.89	0.33	0.01	15.44	92.40	7.50			
S1905-95	A4	49.99	0.14	10.42	1.34	2.95	0.09	20.19	12.52	1.33	0.08	98.06	6.80	0.01	1.71	0.15	0.34	0.01	0.00	4.18	1.86	0.36	0.02	15.44	92.20	7.57			
S1905-95	A4	49.44	0.16	10.72	1.65	2.82	0.02	20.12	12.48	1.29	0.10	98.78	6.81	0.02	1.74	0.18	0.32	0.00	0.00	4.13	1.84	0.34	0.02	15.40	92.68	7.28			
S1905-95	A4	49.16	0.10	10.53	1.40	2.91	0.06	20.14	12.59	1.33	0.10	98.33	6.81	0.01	1.72	0.15	0.34	0.01	0.00	4.16	1.87	0.36	0.02	15.43	92.35	7.49			
S1905-95	A4	49.54	0.10	10.67	1.27	3.12	0.01	20.20	12.59	1.39	0.08	98.97	6.81	0.01	1.73	0.14	0.36	0.00	0.00	4.14	1.86	0.37	0.01	15.43	92.00	7.97			
S1905-95	A4	48.63	0.10	10.51	1.35	2.92	0.09	19.64	12.49	1.36	0.09	97.16	6.81	0.01	1.74	0.15	0.34	0.01	0.00	4.10	1.88	0.37	0.02	15.42	92.08	7.68			
S1905-95	A4	49.21	0.22	10.33	1.55	2.85	0.10	20.13	12.49	1.36	0.10	98.34	6.82	0.02	1.69	0.17	0.33	0.01	0.00	4.15	1.85	0.37	0.02	15.43	92.39	7.35			
S1905-95	A4	49.51	0.04	10.88	1.39	2.92	0.13	20.02	12.51	1.27	0.10	98.77	6.82	0.00	1.77	0.15	0.34	0.02	0.00	4.11	1.85	0.34	0.02	15.40	92.10	7.55			
S1905-95	A4	48.97	0.16	10.19	1.39	2.87	0.05	20.27	12.51	1.32	0.08	97.80	6.82	0.02	1.67	0.15	0.33	0.01	0.00	4.20	1.87	0.36	0.01	15.44	92.53	7.35			
S1905-95	A4	49.40	0.14	10.49	1.35	3.07	0.07	20.07	12.69	1.35	0.09	98.71	6.82	0.01	1.71	0.15	0.35	0.01	0.00	4.13	1.88	0.36	0.02	15.43	91.94	7.88			
S1905-95	A4	49.24	0.11	10.44	1.43	2.83	0.07	20.15	12.51	1.36	0.09	98.23	6.82	0.01	1.71	0.16	0.33	0.01	0.00	4.16	1.86	0.36	0.02	15.43	92.52	7.30			
S1905-95	A4	49.10	0.20	10.26	1.44	2.74	0.09	20.18	12.54	1.32	0.08	97.95	6.82	0.02	1.68	0.16	0.32	0.01	0.00	4.18	1.87	0.36	0.01	15.42	92.69	7.06			
S1905-95	A4	48.97	0.15	10.01	1.67	2.85	0.07	20.33	12.41	1.20	0.07	97.72	6.82																

Table A1e. (continued)

Sample	Min. Ass.	SiO <sub>2</sub>	TiO <sub>2</sub>	Al <sub>2</sub> O <sub>3</sub>	Cr <sub>2</sub> O <sub>3</sub>	FeO	MnO	NiO	MgO	CaO	Na <sub>2</sub> O	K <sub>2</sub> O	Total	F.S./23 O	Si	Ti	Al	Cr	Fe <sup>2+</sup>	Mn	Ni	Mg	Ca	Na	K	Total	Mg%/ <sup>a</sup> Mg + Fe	Fe%/ <sup>a</sup> Mg + Fe
S1905-95	A4	49.64	0.13	10.35	1.48	2.99	0.11			20.31	12.67	1.28	0.09	99.05	6.83	0.01	1.68	0.16	0.34	0.01	0.00	4.16	1.87	0.34	0.02	15.42	92.11	7.60
S1905-95	A4	49.22	0.14	10.45	1.50	2.80	0.01	19.97	12.53	1.35	0.07	98.06	6.83	0.02	1.71	0.16	0.32	0.00	0.00	4.13	1.86	0.36	0.01	15.41	92.68	7.29		
S1905-95	A4	49.24	0.10	10.13	1.46	2.88	0.08			20.32	12.65	1.21	0.08	98.13	6.83	0.01	1.66	0.16	0.33	0.01	0.00	4.20	1.88	0.32	0.01	15.42	92.45	7.35
S1905-95	A4	49.50	0.07	10.68	1.43	2.85	0.02	19.95	12.60	1.28	0.09	98.47	6.83	0.01	1.74	0.16	0.33	0.00	0.00	4.10	1.86	0.34	0.02	15.39	92.53	7.43		
S1905-95	A4	49.39	0.07	10.29	1.53	2.97	0.05			20.08	12.66	1.29	0.09	98.40	6.84	0.01	1.68	0.17	0.34	0.01	0.00	4.14	1.88	0.35	0.02	15.42	92.23	7.65
S1905-95	A4	49.42	0.07	10.70	1.00	2.95	0.10			20.05	12.48	1.41	0.09	98.28	6.84	0.01	1.74	0.11	0.34	0.01	0.00	4.13	1.85	0.38	0.02	15.43	92.12	7.61
S1905-95	A4	49.67	0.19	10.36	1.58	2.71	0.05			20.23	12.58	1.35	0.07	98.78	6.84	0.02	1.68	0.17	0.31	0.01	0.00	4.15	1.85	0.36	0.01	15.40	92.89	6.97
S1905-95	A4	49.39	0.07	10.11	1.21	3.09	0.08			20.32	12.75	1.28	0.09	98.40	6.84	0.01	1.65	0.13	0.36	0.01	0.00	4.19	1.89	0.34	0.02	15.44	91.93	7.85
S1905-95	A4	49.20	0.13	10.06	1.46	2.93	0.07			20.24	12.44	1.24	0.09	97.87	6.84	0.01	1.65	0.16	0.34	0.01	0.00	4.19	1.85	0.33	0.02	15.41	92.31	7.51
S1905-95	A4	49.27	0.09	10.23	1.48	2.91	0.05			20.37	12.52	0.76	0.10	97.79	6.84	0.01	1.67	0.16	0.34	0.01	0.00	4.22	1.86	0.21	0.02	15.34	92.45	7.42
S1905-95	A4	49.30	0.07	9.95	1.40	2.88	0.09			20.41	12.61	1.26	0.10	98.08	6.84	0.01	1.63	0.15	0.33	0.01	0.00	4.22	1.88	0.34	0.02	15.44	92.44	7.32
S1905-95	A4	49.78	0.13	10.68	0.74	3.01	0.05			20.49	12.39	1.27	0.08	98.62	6.85	0.01	1.73	0.08	0.35	0.01	0.00	4.20	1.83	0.34	0.01	15.41	92.27	7.60
S1905-95	A4	49.79	0.12	10.37	1.40	3.03	0.04			20.34	12.40	1.22	0.09	98.79	6.85	0.01	1.68	0.15	0.35	0.00	0.00	4.17	1.83	0.32	0.02	15.39	92.20	7.70
S1905-95	A4	49.29	0.14	10.29	1.38	2.89	0.09			19.98	12.50	1.19	0.09	97.83	6.85	0.01	1.68	0.15	0.34	0.01	0.00	4.14	1.86	0.32	0.02	15.38	92.27	7.49
S1905-95	A4	50.00	0.35	10.36	1.28	2.87	0.01			20.31	12.54	1.30	0.06	99.07	6.86	0.04	1.67	0.14	0.33	0.00	0.00	4.15	1.84	0.35	0.01	15.38	92.63	7.34
S1905-95	A4	49.42	0.04	10.03	1.43	3.04	0.01			20.15	12.46	1.36	0.09	98.03	6.86	0.00	1.64	0.16	0.35	0.00	0.00	4.17	1.85	0.36	0.02	15.43	92.17	7.80
S1905-95	A4	50.24	0.12	10.39	1.37	2.85	0.09			20.44	12.50	1.36	0.08	99.44	6.86	0.01	1.67	0.15	0.33	0.01	0.00	4.16	1.83	0.36	0.01	15.40	92.52	7.25
S1905-95	A4	49.81	0.07	10.11	1.34	2.92	0.07			20.36	12.61	1.28	0.10	98.66	6.87	0.01	1.64	0.15	0.34	0.01	0.00	4.18	1.86	0.34	0.02	15.41	92.40	7.43
S1905-95	A4	49.68	0.12	10.46	1.44	2.96	0.07			20.17	12.68	0.42	0.09	98.09	6.87	0.01	1.70	0.16	0.34	0.01	0.00	4.16	1.88	0.11	0.02	15.25	92.21	7.60
S1905-95	A4	50.18	0.10	10.36	1.41	3.16	0.10			20.22	12.51	1.25	0.10	99.39	6.87	0.01	1.67	0.15	0.36	0.01	0.00	4.12	1.83	0.33	0.02	15.38	91.71	8.05
S1905-95	A4	49.75	0.10	10.14	1.18	2.81	0.08			20.54	12.40	1.26	0.06	98.33	6.87	0.01	1.65	0.13	0.32	0.01	0.00	4.23	1.84	0.34	0.01	15.40	92.69	7.12
S1905-95	A4	50.13	0.12	10.29	1.47	2.78	0.07			20.21	12.73	1.26	0.08	99.14	6.87	0.01	1.66	0.16	0.32	0.01	0.00	4.13	1.87	0.33	0.01	15.38	92.66	7.16
S1905-95	A4	49.54	0.14	10.07	1.16	2.83	0.05			20.30	12.52	1.22	0.08	97.89	6.87	0.01	1.65	0.13	0.33	0.01	0.00	4.20	1.86	0.33	0.01	15.40	92.63	7.24
S1905-95	A4	49.71	0.04	10.32	1.41	2.91	0.07			19.97	12.50	1.26	0.11	98.30	6.87	0.00	1.68	0.15	0.34	0.01	0.00	4.12	1.85	0.34	0.02	15.38	92.27	7.55
S1905-95	A4	49.90	0.25	10.53	1.49	2.86	0.06			19.83	12.42	1.07	0.08	98.48	6.88	0.03	1.71	0.16	0.33	0.01	0.00	4.07	1.83	0.29	0.01	15.31	92.37	7.48
S1905-95	A4	49.76	0.05	9.99	1.39	2.92	0.07			20.25	12.65	1.29	0.10	98.46	6.88	0.01	1.63	0.15	0.34	0.01	0.00	4.17	1.87	0.35	0.02	15.41	92.36	7.46
S1905-95	A4	50.23	0.14	10.03	1.43	2.91	0.03			20.43	12.77	1.33	0.09	99.38	6.88	0.01	1.62	0.16	0.33	0.00	0.00	4.17	1.87	0.35	0.02	15.41	92.54	7.39
S1905-95	A4	49.69	0.33	9.71	0.92	2.79	0.08			20.61	12.77	1.27	0.07	98.23	6.88	0.03	1.58	0.10	0.32	0.01	0.00	4.25	1.89	0.34	0.01	15.42	92.76	7.04
S1905-95	A4	50.27	0.10	10.13	1.25	2.95	0.08			20.69	12.51	1.17	0.09	99.24	6.88	0.01	1.63	0.14	0.34	0.01	0.00	4.22	1.83	0.31	0.02	15.39	92.40	7.39
S1905-95	A4	49.99	0.06	9.94	1.23	2.77	0.06			20.54	12.65	1.26	0.08	98.57	6.89	0.01	1.61	0.13	0.32	0.01	0.00	4.22	1.87	0.34	0.01	15.41	92.80	7.03
S1905-95	A4	50.19	0.09	10.35	1.33	2.88	0.10			20.00	12.61	1.30	0.08	98.92	6.89	0.01	1.68	0.14	0.33	0.01	0.00	4.09	1.86	0.35	0.01	15.37	92.27	7.46
S1905-95	A4	50.22	0.12	10.00	1.35	2.93	0.06			20.33	12.63	1.32	0.09	99.03	6.89	0.01	1.62	0.15	0.34	0.01	0.00	4.16	1.86	0.35	0.02	15.40	92.39	7.46
S1905-95	A4	49.84	0.13	10.15	1.32	2.71	0.03			20.05	12.46	1.17	0.07	97.93	6.90	0.01	1.66	0.14	0.31	0.00	0.00	4.14	1.85	0.31	0.01	15.35	92.89	7.04
S1905-95	A4	50.08	0.10	9.70	1.52	2.89	0.10			20.28	12.55	1.13	0.10	98.45	6.91	0.01	1.58	0.17	0.33	0.01	0.00	4.17	1.86	0.30	0.02	15.36	92.36	7.39
S1905-95	A4	50.22	0.13	9.67	0.88	2.98	0.07			20.74	12.74	1.15	0.08	98.66	6.91	0.01	1.57	0.10	0.34	0.01	0.00	4.26	1.88	0.31	0.01	15.40	92.38	7.45
S1905-95	A4	50.39	0.09	9.71	1.63	2.88	0.03			20.30	12.53	1.22	0.10	98.87	6.93	0.01	1.57	0.18	0.33	0.00	0.00	4.16	1.84	0.33	0.02	15.36	92.54	7.37
S1905-95	A4	50.53	0.10	10.01	1.57	2.89	0.10			19.96	12.58	1.25	0.08	99.08	6.93	0.01	1.62	0.17	0.33	0.01	0.00	4.08	1.85	0.33	0.01	15.34	92.25	7.49
S1905-95	A4	50.41	0.20	9.86	0.98	2.78	0.04			20.51	12.50	1.17	0.09	98.53	6.93	0.02	1.60	0.11	0.32	0.00	0.00	4.20	1.84	0.31	0.02	15.36	92.82	7.07
S1905-95	A4	50.44	0.08	9.57	1.36	2.84	0.07			20.58	12.53	1.20	0.06	98.75	6.94	0.01	1.55	0.15	0.33	0.01	0.00	4.22	1.85	0.32	0.01	15.37	92.63	7.18
S1905-95	A4	50.47	0.13	9.81	1.19	2.85	0.04			20.41	12.47	1.17	0.08	98.63	6.94	0.01	1.59	0.13	0.33	0.00	0.00	4.18	1.84	0.31	0.01	15.35	92.63	7.27
S1905-95																												

**Table Alf.** Major Element Compositions of Amphiboles From VLS Ultramafic Mylonites Analyzed by Electron Microprobe: Site S1907<sup>a</sup>

Sample	Min.	Ass.	SiO <sub>2</sub>	TiO <sub>2</sub>	Al <sub>2</sub> O <sub>3</sub>	Cr <sub>2</sub> O <sub>3</sub>	FeO	MnO	NiO	CaO	Na <sub>2</sub> O	K <sub>2</sub> O	Total F.S./23 O	Si	Ti	Al	Cr	Fe <sup>2+</sup>	Mn	Ni	Mg	Ca	Na	K	Total Mg <sup>o</sup> /Mg + Fe	Fe <sup>2+</sup> /Mg + Fe	
S1907-03	A4	48.40	1.17	10.65	0.67	4.25	0.05	0.13	19.61	12.29	1.55	0.05	98.81	6.71	0.12	1.74	0.07	0.49	0.01	0.01	4.05	1.83	0.42	0.01	15.47	89.04	10.82
S1907-03	A4	48.38	1.39	9.88	0.71	4.12	0.10	0.02	19.21	12.68	1.34	0.00	97.82	6.78	0.15	1.63	0.08	0.48	0.01	0.00	4.01	1.90	0.36	0.00	15.41	89.04	10.71
S1907-03	A4	48.75	1.36	10.11	0.56	4.30	0.04	0.08	19.10	12.62	1.44	0.04	98.39	6.79	0.14	1.66	0.06	0.50	0.00	0.01	3.96	1.88	0.39	0.01	15.41	88.69	11.21
S1907-03	A4	48.78	1.24	9.90	0.62	4.37	0.02	0.09	19.20	12.77	1.38	0.04	98.40	6.80	0.13	1.63	0.07	0.51	0.00	0.01	3.99	1.91	0.37	0.01	15.42	88.61	11.33
S1907-03	A4	48.60	1.40	9.68	0.53	4.27	0.02	0.15	19.17	12.54	1.35	0.01	97.70	6.81	0.15	1.60	0.06	0.50	0.00	0.02	4.01	1.88	0.37	0.00	15.39	88.84	11.10
S1907-03	A4	48.89	1.19	9.78	0.96	4.03	0.09	0.16	18.98	12.78	1.30	0.02	98.18	6.82	0.12	1.61	0.11	0.47	0.01	0.02	3.95	1.91	0.35	0.00	15.37	89.15	10.62
S1907-03	A4	48.65	0.91	9.76	0.63	4.18	0.05	0.07	19.18	12.73	1.34	0.03	97.53	6.83	0.10	1.62	0.07	0.49	0.01	0.01	4.01	1.91	0.37	0.01	15.42	88.98	10.89
S1907-03	A4	49.19	0.91	9.67	0.79	4.38	0.03	0.15	19.53	12.51	1.52	0.04	98.73	6.83	0.10	1.58	0.09	0.51	0.00	0.02	4.04	1.86	0.41	0.01	15.45	88.74	11.18
S1907-03	A4	48.80	1.30	9.35	0.55	4.30	0.04	0.09	19.42	12.55	1.26	0.02	97.67	6.84	0.14	1.54	0.06	0.50	0.00	0.01	4.06	1.89	0.34	0.00	15.39	88.87	11.03
S1907-03	A4	48.70	1.09	10.16	0.46	4.18	0.00	19.04	11.95	1.16	0.00	96.74	6.86	0.12	1.69	0.05	0.49	0.00	0.00	4.00	1.80	0.32	0.00	15.32	89.03	10.97	
S1907-03	A4	49.42	0.89	9.57	0.86	4.13	0.03	0.10	19.55	12.64	1.31	0.01	98.52	6.86	0.09	1.57	0.09	0.48	0.00	0.01	4.05	1.88	0.35	0.00	15.39	89.32	10.60
S1907-03	A4	49.19	0.79	9.43	0.56	4.22	0.10	0.02	19.32	12.91	1.30	0.05	97.91	6.88	0.08	1.56	0.06	0.49	0.01	0.00	4.03	1.93	0.35	0.01	15.41	88.85	10.89
S1907-03	A4	49.39	1.25	8.98	0.66	4.17	0.09	0.03	19.58	12.84	1.27	0.03	98.29	6.88	0.13	1.47	0.07	0.49	0.01	0.00	4.07	1.92	0.34	0.01	15.39	89.11	10.65
S1907-03	A4	49.05	1.22	9.66	0.57	4.15	0.10	19.22	11.72	1.46	0.03	97.18	6.88	0.13	1.60	0.06	0.49	0.01	0.00	4.02	1.76	0.40	0.01	15.36	88.96	10.78	
S1907-03	A4	49.94	0.79	9.32	0.60	4.24	0.07	0.11	19.63	12.99	1.40	0.05	99.13	6.90	0.08	1.52	0.07	0.49	0.01	0.01	4.04	1.92	0.37	0.01	15.42	89.04	10.79
S1907-03	A4	49.82	0.81	8.98	0.86	4.30	0.08	0.05	19.76	12.88	1.22	0.00	98.76	6.91	0.08	1.47	0.09	0.50	0.01	0.01	4.08	1.91	0.33	0.00	15.39	88.94	10.85
S1907-03	A4	49.83	0.74	9.28	0.70	4.04	0.00	0.09	19.84	12.62	1.35	0.03	98.50	6.91	0.08	1.52	0.08	0.47	0.00	0.01	4.10	1.87	0.36	0.01	15.40	89.75	10.25
S1907-03	A4	49.32	1.21	9.44	0.60	4.06	0.10	19.15	12.10	1.32	0.00	97.30	6.91	0.13	1.56	0.07	0.48	0.01	0.00	4.00	1.82	0.36	0.00	15.33	89.13	10.60	
S1907-03	A4	50.04	0.74	8.99	0.83	4.22	0.06	0.11	19.91	12.63	1.21	0.00	98.75	6.93	0.08	1.47	0.09	0.49	0.01	0.01	4.11	1.87	0.33	0.00	15.38	89.24	10.62
S1907-03	A4	49.67	0.81	9.44	0.52	4.15	0.07	0.03	19.30	12.50	1.34	0.00	97.85	6.93	0.09	1.55	0.06	0.48	0.01	0.00	4.01	1.87	0.36	0.00	15.36	89.07	10.76
S1907-03	A4	49.49	0.81	8.73	0.95	4.04	0.08	0.07	19.35	12.82	1.19	0.06	97.58	6.94	0.09	1.44	0.11	0.47	0.01	0.01	4.04	1.93	0.32	0.01	15.37	89.33	10.46
S1907-03	A4	49.68	0.89	8.75	0.67	4.00	0.02	0.04	19.62	12.66	1.30	0.01	97.65	6.95	0.09	1.44	0.07	0.47	0.00	0.01	4.09	1.90	0.35	0.00	15.38	89.67	10.27
S1907-03	A4	50.14	0.85	9.03	0.80	3.97	0.10	0.04	19.49	12.79	1.21	0.04	98.46	6.95	0.09	1.48	0.09	0.46	0.01	0.00	4.03	1.90	0.33	0.01	15.34	89.51	10.23
S1907-03	A4	49.99	0.80	8.74	0.57	4.06	0.08	0.03	19.65	12.52	1.34	0.04	97.81	6.98	0.08	1.44	0.06	0.47	0.01	0.00	4.09	1.87	0.36	0.01	15.37	89.42	10.36
S1907-03	A4	50.40	0.79	8.57	0.70	4.02	0.06	0.24	19.92	12.60	1.28	0.00	98.56	6.98	0.08	1.40	0.08	0.47	0.01	0.03	4.11	1.87	0.34	0.00	15.37	89.69	10.16
S1907-03	A4	49.14	1.16	9.58	0.78	4.29	0.10	0.05	17.58	11.90	1.19	0.00	95.76	6.99	0.12	1.61	0.09	0.51	0.01	0.01	3.73	1.81	0.33	0.00	15.20	87.72	12.01
S1907-03	A4	50.00	0.77	8.26	0.73	3.98	0.00	0.04	19.59	12.66	1.10	0.04	97.17	7.02	0.08	1.37	0.08	0.47	0.00	0.01	4.10	1.90	0.30	0.01	15.33	89.78	10.22
S1907-03	A4	50.19	0.76	8.26	0.62	4.05	0.05	0.06	19.65	12.65	1.11	0.04	97.45	7.03	0.08	1.36	0.07	0.47	0.01	0.01	4.10	1.90	0.30	0.01	15.33	89.53	10.35
S1907-03	A4	50.36	0.67	8.41	0.51	3.99	0.09	0.08	19.72	12.60	1.11	0.04	97.59	7.03	0.07	1.38	0.06	0.47	0.01	0.01	4.11	1.89	0.30	0.01	15.33	89.58	10.17
S1907-03	A4	50.59	0.74	8.14	0.49	3.89	0.12	0.04	20.12	12.55	1.07	0.03	97.79	7.04	0.08	1.34	0.05	0.45	0.01	0.00	4.18	1.87	0.29	0.01	15.33	89.93	9.75
S1907-03	A4	51.53	0.98	7.63	0.67	4.00	0.09	0.05	20.24	12.56	1.00	0.00	97.66	7.10	0.10	1.24	0.07	0.46	0.01	0.01	4.16	1.85	0.27	0.00	15.27	89.80	9.97
S1907-12	A5	57.68	0.19	1.02	0.00	1.83	0.00	23.14	13.13	0.24	0.03	97.26	7.91	0.02	0.16	0.00	0.21	0.00	0.00	4.73	1.93	0.06	0.01	15.03	95.75	4.25	
S1907-12	A5	58.14	0.00	0.47	0.00	1.65	0.07	23.76	12.65	0.11	0.00	96.85	7.98	0.00	0.08	0.00	0.19	0.01	0.00	4.86	1.86	0.36	0.00	15.00	96.09	3.74	
S1907-12	A5	58.45	0.04	0.34	0.10	2.04	0.05	23.00	13.01	0.06	0.00	97.09	8.02	0.00	0.05	0.01	0.23	0.01	0.00	4.70	1.91	0.02	0.00	14.95	95.15	4.74	
S1907-23	A4	49.72	0.36	9.59	0.46	3.94	0.08	20.53	12.09	1.50	0.07	98.34	6.89	0.04	1.57	0.05	0.46	0.01	0.00	4.24	1.80	0.40	0.01	15.47	90.10	9.70	
S1907-23	A4	50.30	0.34	8.93	0.31	3.39	0.08	20.27	12.00	1.35	0.05	97.02	7.03	0.04	1.47	0.03	0.40	0.01	0.00	4.22	1.80	0.37	0.01	15.37	91.23	8.56	
S1907-23	A4	50.67	0.40	8.54	0.72	3.85	0.07	20.44	11.82	1.37	0.03	97.91	7.04	0.04	1.40	0.08	0.45	0.01	0.00	4.23	1.76	0.37	0.01	15.37	90.28	9.54	
S1907-23	A4	52.02	0.20	6.40	0.84	3.32	0.12	21.08	11.68	1.14	0.04	96.84	7.27	0.02	1.05	0.09	0.39	0.01	0.00	4.39	1.75	0.31	0.01	15.29	91.61	8.10	
S1907-23	A4	53.67	0.22	5.76	0.48	3.16	0.13	21.78	12.04	0.94	0.02	98.20	7.37	0.02	0.93	0.05	0.36	0.02	0.00	4.46	1.77	0.25	0.00	15.24	92.18	7.51	
S1907-23	A4	53.82	0.10	4.55	0.62	2.85	0.05	22.23	12.53	0.80	0.02	97.57	7.44	0.01	0.74	0.07	0.33	0.01	0.00	4.58	1.86	0.21	0.00	15.25	93.18	6.70	
S1907-25	A4</																										

**Table A1f.** (continued)

Sample	Min.	Ass.	SiO <sub>2</sub>	TiO <sub>2</sub>	Al <sub>2</sub> O <sub>3</sub>	Cr <sub>2</sub> O <sub>3</sub>	FeO	MnO	NiO	Na <sub>2</sub> O	K <sub>2</sub> O	Total	F.S./23 O	Si	Ti	Al	Cr	Fe <sup>2+</sup>	Mn	Ni	Mg	Ca	Na	K	Total	Mg%/ <sup>o</sup> Mg + Fe	Fe%/ <sup>o</sup> Fe + Mg
S1907-25	A4	48.83	0.42	10.45	0.65	3.90	0.04	0.09	19.86	12.76	1.58	0.04	98.61	6.78	0.04	1.71	0.07	0.45	0.00	0.01	4.11	1.90	0.42	0.01	15.50	90.00	9.91
S1907-25	A4	48.56	0.37	9.99	1.47	3.51	0.00	0.11	19.73	12.71	1.48	0.00	97.94	6.79	0.04	1.65	0.16	0.41	0.00	0.01	4.11	1.90	0.40	0.00	15.47	90.93	9.07
S1907-25	A4	49.59	0.37	10.32	1.21	3.75	0.10	0.03	20.01	12.62	1.52	0.06	99.59	6.81	0.04	1.67	0.13	0.43	0.01	0.00	4.09	1.86	0.40	0.01	15.46	90.24	9.49
S1907-25	A4	48.36	0.45	9.90	0.79	3.69	0.00	0.09	19.82	12.53	1.36	0.02	97.00	6.81	0.05	1.64	0.09	0.43	0.00	0.01	4.16	1.89	0.37	0.00	15.46	90.55	9.45
S1907-25	A4	49.12	0.43	10.17	0.83	3.39	0.07	0.09	19.76	12.77	1.50	0.02	98.14	6.83	0.04	1.67	0.09	0.39	0.01	0.01	4.09	1.90	0.40	0.00	15.45	91.06	8.77
S1907-25	A4	49.49	0.44	10.00	1.06	3.56	0.07	0.01	19.89	12.83	1.50	0.06	98.91	6.84	0.05	1.63	0.12	0.41	0.01	0.00	4.09	1.90	0.40	0.01	15.45	90.71	9.12
S1907-25	A4	49.45	0.40	10.07	0.69	3.41	0.08	0.07	19.99	12.76	1.46	0.05	98.43	6.85	0.04	1.65	0.08	0.40	0.01	0.01	4.13	1.89	0.39	0.01	15.45	91.06	8.73
S1907-25	A4	49.46	0.46	9.83	0.74	3.50	0.08	0.13	19.93	12.64	1.49	0.03	98.29	6.87	0.05	1.61	0.08	0.41	0.01	0.01	4.12	1.88	0.40	0.01	15.44	90.84	8.95
S1907-25	A4	49.21	0.44	10.26	0.67	3.74	0.04	0.06	19.48	12.11	1.59	0.04	97.60	6.87	0.05	1.69	0.07	0.44	0.01	0.00	4.05	1.81	0.43	0.01	15.42	90.13	9.71
S1907-25	A4	49.37	0.42	9.24	0.70	3.51	0.00	0.16	20.29	12.94	1.51	0.05	98.20	6.87	0.04	1.52	0.08	0.41	0.00	0.02	4.21	1.93	0.41	0.01	15.49	91.16	8.84
S1907-25	A4	49.75	0.43	9.52	0.86	3.32	0.07	0.11	20.03	12.50	1.36	0.00	97.95	6.91	0.04	1.56	0.09	0.39	0.01	0.01	4.15	1.86	0.37	0.00	15.40	91.33	8.50
S1907-25	A4	49.66	0.39	9.33	0.80	3.25	0.10	0.08	19.78	12.55	1.36	0.02	97.34	6.94	0.04	1.54	0.09	0.38	0.01	0.01	4.12	1.88	0.37	0.00	15.39	91.31	8.43
S1907-25	A4	50.41	0.31	9.46	0.55	3.36	0.08	0.19	9.99	12.05	1.27	0.03	97.51	7.01	0.03	1.55	0.06	0.39	0.01	0.00	4.14	1.79	0.34	0.01	15.33	91.19	8.60
S1907-25	A4	50.74	0.42	8.21	0.96	3.36	0.04	0.10	20.72	12.78	1.17	0.00	98.50	7.01	0.04	1.34	0.11	0.39	0.00	0.01	4.27	1.89	0.31	0.00	15.38	91.58	8.32
S1907-32	see text	52.41	0.14	5.71	0.12	5.29	0.16	0.00	20.74	12.25	0.97	0.03	97.81	7.31	0.01	0.94	0.01	0.62	0.02	0.00	4.31	1.83	0.26	0.01	15.33	87.13	12.48
S1907-32	"	53.28	0.12	5.71	0.16	5.15	0.15	0.06	21.08	12.26	1.03	0.03	99.02	7.34	0.01	0.93	0.02	0.59	0.02	0.01	4.32	1.81	0.27	0.01	15.32	87.63	12.01
S1907-32	"	54.53	0.07	4.32	0.12	4.91	0.20	0.05	21.57	12.27	0.69	0.02	98.76	7.50	0.01	0.70	0.01	0.56	0.02	0.01	4.42	1.81	0.18	0.00	15.23	88.28	11.27
S1907-32	"	54.83	0.13	4.31	0.09	4.70	0.16	0.07	21.58	12.50	0.75	0.02	99.13	7.51	0.01	0.69	0.01	0.54	0.02	0.01	4.40	1.83	0.20	0.00	15.23	88.77	10.85
S1907-32	"	54.37	0.10	4.31	0.03	4.63	0.11	0.02	21.26	12.59	0.78	0.02	98.21	7.51	0.01	0.70	0.00	0.53	0.01	0.00	4.38	1.86	0.21	0.00	15.23	88.88	10.86
S1907-32	"	54.48	0.08	4.26	0.10	4.84	0.17	0.06	21.32	12.38	0.68	0.03	98.39	7.52	0.01	0.69	0.01	0.56	0.02	0.01	4.38	1.83	0.18	0.00	15.21	88.35	11.26
S1907-32	"	54.53	0.04	4.20	0.05	4.74	0.10	0.09	21.53	12.44	0.67	0.02	98.41	7.52	0.0	0.68	0.00	0.55	0.01	0.01	4.42	1.84	0.18	0.00	15.23	88.80	10.96
S1907-32	"	54.46	0.01	4.11	0.06	4.64	0.17	0.13	21.50	12.54	0.71	0.02	98.35	7.52	0.0	0.67	0.01	0.54	0.02	0.01	4.42	1.86	0.19	0.00	15.24	88.85	10.75
S1907-32	"	54.85	0.02	3.82	0.06	4.65	0.15	0.04	22.07	12.43	0.62	0.02	98.75	7.53	0.0	0.62	0.01	0.53	0.02	0.00	4.52	1.83	0.17	0.00	15.24	89.12	10.54
S1907-32	"	55.04	0.14	3.96	0.11	4.59	0.17	0.04	21.81	12.46	0.67	0.03	99.02	7.54	0.01	0.64	0.01	0.53	0.02	0.00	4.45	1.83	0.18	0.00	15.21	89.08	10.53
S1907-32	"	54.77	0.07	3.57	0.12	4.34	0.12	0.09	22.03	12.56	0.67	0.02	98.35	7.55	0.01	0.58	0.01	0.50	0.01	0.01	4.53	1.86	0.18	0.00	15.24	89.81	9.92
S1907-32	"	54.76	0.09	4.08	0.07	4.38	0.19	0.02	21.60	12.35	0.59	0.03	98.15	7.55	0.01	0.66	0.01	0.50	0.02	0.00	4.44	1.82	0.16	0.01	15.19	89.39	10.16
S1907-32	"	55.17	0.09	3.64	0.03	4.03	0.14	0.17	22.16	12.67	0.64	0.03	98.78	7.56	0.01	0.59	0.00	0.46	0.02	0.02	4.53	1.86	0.17	0.01	15.22	90.44	9.23
S1907-32	"	55.15	0.00	3.64	0.11	4.35	0.10	0.09	21.99	12.41	0.66	0.01	98.52	7.58	0.0	0.59	0.01	0.50	0.01	0.01	4.50	1.83	0.18	0.00	15.21	89.80	9.96
S1907-32	"	55.38	0.02	3.69	0.11	4.49	0.14	0.03	22.08	12.32	0.63	0.01	98.89	7.58	0.0	0.59	0.01	0.51	0.02	0.00	4.50	1.81	0.17	0.00	15.20	89.46	10.22
S1907-32	"	55.22	0.00	3.63	0.12	4.38	0.16	0.06	21.90	12.50	0.61	0.02	98.59	7.58	0.0	0.59	0.01	0.50	0.02	0.01	4.48	1.84	0.16	0.00	15.20	89.59	10.04
S1907-32	"	55.70	0.03	3.55	0.07	4.50	0.09	0.01	22.25	12.37	0.57	0.02	99.15	7.60	0.0	0.57	0.01	0.51	0.01	0.00	4.52	1.81	0.15	0.00	15.19	89.62	10.17
S1907-32	"	55.47	0.00	3.57	0.04	4.47	0.16	0.01	22.06	12.38	0.56	0.02	98.73	7.60	0	0.58	0.00	0.51	0.02	0.00	4.50	1.82	0.15	0.00	15.19	89.45	10.17
S1907-32	"	55.44	0.04	3.52	0.07	4.62	0.19	0.05	21.87	12.38	0.56	0.00	98.74	7.60	0	0.57	0.01	0.53	0.02	0.01	4.47	1.82	0.15	0.00	15.18	89.00	10.55
S1907-32	"	55.99	0.00	3.18	0.16	4.45	0.20	0.07	22.31	12.46	0.51	0.01	99.34	7.63	0	0.51	0.02	0.51	0.02	0.01	4.53	1.82	0.14	0.00	15.18	89.51	10.02
S1907-32	"	56.16	0.03	2.87	0.03	4.25	0.14	0.11	22.52	12.29	0.50	0.01	98.91	7.67	0	0.46	0.00	0.48	0.02	0.01	4.58	1.80	0.13	0.00	15.16	90.14	9.54
S1907-32	"	56.08	0.03	2.85	0.03	4.08	0.18	0.09	22.41	12.51	0.45	0.01	98.71	7.67	0	0.46	0.00	0.47	0.02	0.01	4.57	1.83	0.12	0.00	15.16	90.35	9.23
S1907-32	"	56.02	0.09	2.80	0.04	3.84	0.12	0.06	22.36	12.65	0.50	0.02	98.49	7.67	0	0.45	0.00	0.44	0.01	0.01	4.56	1.86	0.13	0.00	15.16	90.97	8.76
S1907-32	"	56.32	0.08	2.68	0.09	4.00	0.12	0.02	22.41	12.45	0.47	0.01	98.65	7.70	0	0.43	0.01	0.46	0.01	0.00	4.57	1.82	0.12	0.00	15.14	90.64	9.07
S1907-32	"	56.37	0.01	2.61	0.00	4.06	0.10	0.03	22.52	12.44	0.42	0.01	98.58	7.71	0	0.42	0.00	0.46	0.01	0.00	4.59	1.82	0.11	0.00	15.14	90.59	9.17
S1907-32	"	56.40	0.03	2.30	0.07	4.26	0.17	0.05	22.44	12.54	0.45	0.02	98.71	7.72	0	0.37	0.01	0.49	0.02	0.01	4.58	1.84	0.12	0.00	15.15	90.02	9.58
S1907-32	"	56.71	0.03</																								

**Table A1g.** Major Element Compositions of Amphiboles From VLS Ultramafic Mylonites Analyzed by Electron Microprobe: Site S1908<sup>a</sup>

Sample	Min. Ass.	SiO <sub>2</sub>	TiO <sub>2</sub>	Al <sub>2</sub> O <sub>3</sub>	Cr <sub>2</sub> O <sub>3</sub>	FeO	MnO	NiO	MgO	CaO	Na <sub>2</sub> O	K <sub>2</sub> O	Total	F.S./23 O	Si	Ti	Al	Cr	Fe <sup>2+</sup>	Mn	Ni	Mg	Ca	Na	K	Total	Mg%/ <sup>a</sup> Mg + Fe	Fe%/ <sup>a</sup> Fe + Mg
S1908-02	A4	48.59	0.70	10.36	1.61	3.43	0.00	0.05	19.34	12.68	1.28	0.05	98.09	6.77	0.07	1.70	0.18	0.40	0.00	0.01	4.02	1.89	0.35	0.01	15.39	90.95	9.05	
S1908-02	A4	48.89	0.74	10.24	1.61	3.36	0.07	0.10	19.56	12.82	1.29	0.04	98.72	6.77	0.08	1.67	0.18	0.39	0.01	0.01	4.04	1.90	0.35	0.01	15.40	91.05	8.78	
S1908-02	A4	49.06	0.68	10.32	1.58	3.43	0.07	0.09	19.29	12.79	1.30	0.04	98.65	6.80	0.07	1.68	0.17	0.40	0.01	0.01	3.98	1.90	0.35	0.01	15.38	90.75	9.06	
S1908-02	A4	49.15	0.63	10.31	1.70	3.23	0.04	0.09	19.39	12.76	1.22	0.03	98.52	6.81	0.07	1.68	0.19	0.37	0.00	0.01	4.00	1.89	0.33	0.00	15.36	91.36	8.54	
S1908-02	A4	48.91	0.60	10.48	1.26	3.30	0.00	19.12	12.40	1.22	0.04	97.33	6.84	0.06	1.73	0.14	0.39	0.00	0.00	3.98	1.86	0.33	0.01	15.33	91.17	8.83		
S1908-02	A4	49.03	0.57	9.69	1.66	3.15	0.08	19.07	12.51	1.15	0.06	96.97	6.89	0.06	1.60	0.18	0.37	0.01	0.00	3.99	1.88	0.31	0.01	15.32	91.32	8.46		
S1908-02	A4	54.22	0.24	5.58	0.24	2.65	0.07	21.58	12.99	0.52	0.00	98.09	7.43	0.02	0.90	0.03	0.30	0.01	0.00	4.41	1.91	0.14	0.00	15.15	93.39	6.44		
S1908-03	A4	50.42	0.39	8.48	0.61	2.65	0.04	0.04	20.63	12.73	1.11	0.07	97.16	7.03	0.04	1.39	0.07	0.31	0.00	0.00	4.29	1.90	0.30	0.01	15.35	93.19	6.71	
S1908-03	A4	51.47	0.30	7.95	0.53	2.59	0.00	0.15	20.67	12.87	1.05	0.04	97.63	7.13	0.03	1.30	0.06	0.30	0.00	0.02	4.27	1.91	0.28	0.01	15.30	93.43	6.57	
S1908-03	A4	51.64	0.32	7.68	0.71	2.82	0.05	0.12	20.94	12.75	0.99	0.06	98.09	7.13	0.03	1.25	0.08	0.33	0.01	0.01	4.31	1.89	0.27	0.01	15.31	92.84	7.02	
S1908-03	A4	51.58	0.31	7.50	0.59	2.42	0.00	0.12	20.75	12.67	1.00	0.02	96.96	7.18	0.03	1.23	0.07	0.28	0.00	0.01	4.31	1.89	0.27	0.00	15.27	93.85	6.15	
S1908-03	A4	51.88	0.24	6.82	0.62	2.44	0.16	0.00	21.34	12.72	0.91	0.05	97.18	7.21	0.02	1.12	0.07	0.28	0.02	0.00	4.42	1.89	0.25	0.01	15.30	93.60	6.01	
S1908-03	A4	52.42	0.30	6.82	0.64	2.66	0.01	0.06	21.70	12.38	0.93	0.04	97.95	7.22	0.03	1.11	0.07	0.31	0.00	0.01	4.46	1.83	0.25	0.01	15.28	93.56	6.42	
S1908-03	A4	52.24	0.25	6.71	0.69	2.49	0.03	0.01	21.32	12.88	0.96	0.05	97.62	7.23	0.03	1.09	0.08	0.29	0.00	0.00	4.40	1.91	0.26	0.01	15.29	93.78	6.14	
S1908-03	A4	52.60	0.20	6.89	0.60	2.79	0.08	0.04	21.24	12.58	0.90	0.05	97.97	7.25	0.02	1.12	0.06	0.32	0.01	0.00	4.36	1.86	0.24	0.01	15.26	92.94	6.86	
S1908-03	A4	52.72	0.25	6.31	0.53	2.79	0.00	0.10	21.54	12.82	0.84	0.04	97.95	7.27	0.03	1.03	0.06	0.32	0.00	0.01	4.43	1.89	0.22	0.01	15.27	93.22	6.78	
S1908-03	A4	53.07	0.22	6.17	0.36	2.58	0.08	0.16	21.84	12.90	0.80	0.06	98.21	7.30	0.02	1.00	0.04	0.30	0.01	0.02	4.47	1.90	0.21	0.01	15.28	93.62	6.20	
S1908-03	A4	53.97	0.28	6.19	0.73	2.86	0.00	0.25	20.91	12.70	0.67	0.03	98.59	7.38	0.03	1.00	0.08	0.33	0.00	0.03	4.26	1.86	0.18	0.01	15.14	92.87	7.13	
S1908-03	A4	53.68	0.18	4.82	0.51	2.50	0.11	0.14	21.99	12.87	0.60	0.04	97.44	7.43	0.02	0.79	0.06	0.29	0.01	0.02	4.54	1.91	0.16	0.01	15.22	93.76	5.98	

<sup>a</sup>Major element compositions are in wt %. Analyses are ordered by increasing sample number and Si content. Min. Ass., mineral assemblage.

**Table A1h.** Major Element Compositions of Amphiboles From VLS Ultramafic Mylonites Analyzed by Electron Microprobe: Site S1909<sup>a</sup>

Sample	Min. Ass.	$\text{SiO}_2$	$\text{TiO}_2$	$\text{Al}_2\text{O}_3$	$\text{Cr}_2\text{O}_3$	$\text{FeO}$	$\text{MnO}$	$\text{NiO}$	$\text{MgO}$	$\text{CaO}$	$\text{Na}_2\text{O}$	$\text{K}_2\text{O}$	Total	F.S./23 O	Si	Ti	Al	Cr	$\text{Fe}^{2+}$	Mn	Ni	Mg	Ca	Na	K	Total	$\text{Mg\%}/\text{Mg + Fe}$	$\text{Fe\%}/\text{Mg + Fe}$
S1909-01	A2	45.67	0.82	14.82	0.74	4.04	0.03		18.74	12.66	2.11	0.06	99.70		6.30	0.09	2.41	0.08	0.47	0.00	0.00	3.85	1.87	0.57	0.01	15.65	89.12	10.79
S1909-01	A2	46.05	0.73	14.36	0.56	4.15	0.03		19.11	12.53	2.12	0.05	99.70		6.35	0.08	2.33	0.06	0.48	0.00	0.00	3.93	1.85	0.57	0.01	15.66	89.07	10.85
S1909-01	A2	45.88	0.87	13.74	1.00	3.84	0.07		18.98	12.99	2.10	0.05	99.51		6.35	0.09	2.24	0.11	0.44	0.01	0.00	3.92	1.93	0.56	0.01	15.67	89.63	10.18
S1909-01	A2	45.67	0.67	13.51	1.21	4.00	0.03		19.14	12.77	2.09	0.06	99.13		6.35	0.07	2.22	0.13	0.46	0.00	0.00	3.97	1.90	0.56	0.01	15.69	89.43	10.48
S1909-01	A2	46.00	0.63	14.26	0.72	4.03	0.02		18.96	12.78	2.13	0.04	99.57		6.36	0.07	2.32	0.08	0.47	0.00	0.00	3.90	1.89	0.57	0.01	15.67	89.30	10.65
S1909-01	A2	45.86	0.83	13.91	0.65	4.19	0.01		18.72	12.88	2.13	0.05	99.22		6.37	0.09	2.28	0.07	0.49	0.00	0.00	3.87	1.92	0.57	0.01	15.66	88.83	11.15
S1909-01	A2	46.20	0.68	13.83	1.16	4.24	0.07		18.65	12.82	2.17	0.06	99.87		6.38	0.07	2.25	0.13	0.49	0.01	0.00	3.84	1.90	0.58	0.01	15.65	88.52	11.28
S1909-01	A2	45.93	0.95	13.43	1.27	3.80	0.06		18.89	12.71	1.98	0.05	99.06		6.38	0.10	2.20	0.14	0.44	0.01	0.00	3.91	1.89	0.53	0.01	15.62	89.71	10.12
S1909-01	A2	45.82	0.72	13.24	1.20	3.96	0.05		18.88	13.08	2.01	0.06	99.01		6.39	0.08	2.17	0.13	0.46	0.01	0.00	3.92	1.95	0.54	0.01	15.66	89.34	10.52
S1909-01	A2	46.48	0.04	14.95	0.00	4.21	0.01		19.00	12.87	2.19	0.04	99.78		6.39	0.00	2.42	0.00	0.48	0.00	0.00	3.89	1.90	0.58	0.01	15.69	88.92	11.06
S1909-01	A2	46.63	0.00	14.93	0.00	4.08	0.08		19.21	12.79	2.26	0.04	100.01		6.40	0.00	2.41	0.00	0.47	0.01	0.00	3.93	1.88	0.60	0.01	15.70	89.17	10.63
S1909-01	A2	46.31	0.78	13.65	1.05	3.88	0.07		18.87	12.84	2.03	0.05	99.52		6.40	0.08	2.23	0.11	0.45	0.01	0.00	3.89	1.90	0.54	0.01	15.62	89.49	10.33
S1909-01	A2	45.87	0.63	12.97	1.26	4.12	0.09		19.01	12.82	2.04	0.05	98.84		6.41	0.07	2.13	0.14	0.48	0.01	0.00	3.96	1.92	0.55	0.01	15.67	88.95	10.81
S1909-01	A2	46.07	0.61	13.18	1.05	4.08	0.04		19.24	12.71	1.97	0.05	98.99		6.41	0.06	2.16	0.12	0.47	0.01	0.00	3.99	1.90	0.53	0.01	15.66	89.27	10.61
S1909-01	A2	46.69	0.76	13.61	1.15	3.98	0.05		18.98	12.96	2.05	0.05	100.26		6.41	0.08	2.20	0.12	0.46	0.01	0.00	3.88	1.91	0.55	0.01	15.62	89.37	10.51
S1909-01	A2	46.23	0.59	12.51	1.09	4.38	0.10		20.39	12.18	1.90	0.05	99.41		6.41	0.06	2.04	0.12	0.51	0.01	0.00	4.21	1.81	0.51	0.01	15.70	89.02	10.74
S1909-01	A2	46.57	0.80	13.16	1.28	3.89	0.03		19.30	12.86	1.96	0.06	99.90		6.42	0.08	2.14	0.14	0.45	0.00	0.00	3.96	1.90	0.52	0.01	15.63	89.78	10.15
S1909-01	A2	46.05	0.71	12.91	1.33	3.69	0.03		19.12	12.92	1.99	0.05	98.80		6.42	0.07	2.12	0.15	0.43	0.00	0.00	3.97	1.93	0.54	0.01	15.65	90.15	9.77
S1909-01	A2	46.03	0.80	12.86	1.17	3.87	0.06		18.99	12.97	2.05	0.04	98.83		6.42	0.08	2.11	0.13	0.45	0.01	0.00	3.95	1.94	0.55	0.01	15.65	89.60	10.25
S1909-01	A2	46.46	0.82	12.81	1.24	3.97	0.06		19.38	12.97	1.92	0.06	99.68		6.42	0.09	2.09	0.14	0.46	0.01	0.00	3.99	1.92	0.52	0.01	15.64	89.55	10.29
S1909-01	A2	46.41	0.64	13.10	1.25	3.98	0.08		19.15	12.90	1.93	0.05	99.47		6.43	0.07	2.14	0.14	0.46	0.01	0.00	3.95	1.91	0.52	0.01	15.63	89.37	10.42
S1909-01	A2	46.46	0.64	13.35	1.00	4.10	0.04		19.00	12.80	2.04	0.05	99.49		6.43	0.07	2.18	0.11	0.47	0.00	0.00	3.92	1.90	0.55	0.01	15.64	89.10	10.79
S1909-01	A2	45.98	0.96	13.23	1.21	3.88	0.11		18.48	12.33	2.12	0.03	98.33		6.43	0.10	2.18	0.13	0.45	0.01	0.00	3.85	1.85	0.58	0.01	15.60	89.19	10.51
S1909-01	A2	46.77	1.11	13.71	0.10	4.18	0.10		19.02	12.76	2.07	0.05	99.86		6.43	0.11	2.22	0.01	0.48	0.01	0.00	3.90	1.88	0.55	0.01	15.62	88.80	10.95
S1909-01	A2	46.19	0.71	13.27	1.07	4.12	0.06		18.70	12.64	2.00	0.05	98.82		6.44	0.07	2.18	0.12	0.48	0.01	0.00	3.88	1.89	0.54	0.01	15.62	88.85	10.99
S1909-01	A2	46.97	0.80	13.52	0.96	3.97	0.07		19.03	12.91	2.04	0.05	100.33		6.44	0.08	2.18	0.10	0.46	0.01	0.00	3.89	1.90	0.54	0.01	15.61	89.35	10.46
S1909-01	A2	46.56	0.75	13.40	0.80	3.93	0.04		19.07	12.80	1.90	0.05	99.31		6.44	0.08	2.19	0.09	0.46	0.00	0.00	3.93	1.90	0.51	0.01	15.60	89.53	10.36
S1909-01	A2	46.42	0.73	13.24	0.91	4.25	0.03		18.78	12.68	2.18	0.05	99.27		6.44	0.08	2.17	0.10	0.49	0.00	0.00	3.88	1.89	0.59	0.01	15.65	88.66	11.26
S1909-01	A2	46.32	0.62	12.86	1.01	4.05	0.00		19.21	12.83	2.03	0.04	98.96		6.45	0.06	2.11	0.11	0.47	0.00	0.00	3.99	1.91	0.55	0.01	15.66	89.43	10.57
S1909-01	A2	47.01	1.03	13.31	0.54	3.82	0.04		19.44	12.80	1.98	0.05	100.02		6.45	0.11	2.15	0.06	0.44	0.00	0.00	3.97	1.88	0.53	0.01	15.60	89.97	9.91
S1909-01	A2	46.55	0.65	12.93	1.11	4.13	0.02		19.08	12.76	2.06	0.05	99.33		6.45	0.07	2.11	0.12	0.48	0.00	0.00	3.94	1.90	0.55	0.01	15.64	89.13	10.83
S1909-01	A2	46.47	0.65	12.92	1.07	3.87	0.01		19.14	12.85	2.02	0.05	99.06		6.46	0.07	2.12	0.12	0.45	0.00	0.00	3.96	1.91	0.54	0.01	15.64	89.78	10.20
S1909-01	A2	46.54	0.69	12.84	1.03	4.13	0.00		19.13	12.77	1.93	0.05	99.12		6.46	0.07	2.10	0.11	0.48	0.00	0.00	3.96	1.90	0.52	0.01	15.62	89.18	10.82
S1909-01	A2	47.02	0.58	13.05	1.21	3.86	0.07		19.36	12.86	1.99	0.05	100.04		6.46	0.06	2.11	0.13	0.44	0.01	0.00	3.97	1.89	0.53	0.01	15.62	89.77	10.05
S1909-01	A2	46.55	0.63	12.53	1.30	3.93	0.00		19.49	12.72	1.92	0.05	99.13		6.47	0.07	2.15	0.14	0.46	0.00	0.00	4.03	1.89	0.52	0.01	15.64	89.82	10.17
S1909-01	A2	46.93	0.88	13.03	1.14	3.68	0.04		19.21	12.87	1.87	0.04	99.68		6.47	0.09	2.12	0.12	0.42	0.00	0.00	3.94	1.90	0.50	0.01	15.58	90.20	9.69
S1909-01	A2	46.20	0.65	13.36	0.29	4.13	0.08		19.57	12.88	1.96	0.04	100.17		6.47	0.07	2.16	0.03	0.47	0.01	0.00	4.00	1.89	0.52	0.01	15.63	89.23	10.57
S1909-01	A2	46.74	0.67	12.81	1.22	3.80	0.05		19.08	12.95	1.95	0.05	99.31		6.48	0.07	2.09	0.13	0.44	0.01	0.00	3.94	1.92	0.52	0.01	15.61	89.82	10.03
S1909-01	A2	47.23	0.93	12.89	0.94	4.01	0.06		19.51	12.75	1.86	0.04	100.21		6.48	0.10	2.08	0.10	0.46	0.01	0.00	3.99	1.87	0.49	0.01	15.59	89.52	10.32
S1909-01	A2	46.80	0.65																									

**Table A1h.** (continued)

Sample	Min. Ass.	SiO <sub>2</sub>	TiO <sub>2</sub>	Al <sub>2</sub> O <sub>3</sub>	Cr <sub>2</sub> O <sub>3</sub>	FeO	MnO	NiO	MgO	CaO	Na <sub>2</sub> O	K <sub>2</sub> O	Total	F.S./23	O	Si	Ti	Al	Cr	Fe <sup>2+</sup>	Mn	Ni	Mg	Ca	Na	K	Total Mg <sup>2+</sup> /Mg + Fe Fe <sup>2+</sup> /Fe + Mg
S1909-01	A2	47.31	0.78	12.69	0.72	3.87	0.06	19.57	12.99	1.93	0.04	99.94		6.50	0.08	2.06	0.08	0.44	0.01	0.00	4.01	1.91	0.51	0.01	15.61	89.88	9.97
S1909-01	A2	46.92	0.61	12.38	1.18	4.12	0.05	19.43	12.68	1.88	0.04	99.29		6.50	0.06	2.02	0.13	0.48	0.01	0.00	4.01	1.88	0.51	0.01	15.61	89.26	10.61
S1909-01	A2	47.51	0.75	12.38	0.74	4.45	0.01	19.40	12.89	1.86	0.05	100.03		6.54	0.08	2.01	0.08	0.51	0.00	0.00	3.98	1.90	0.50	0.01	15.60	88.57	11.41
S1909-01	A2	46.72	0.54	12.91	1.13	3.83	0.04	18.51	12.17	2.07	0.05	97.97		6.54	0.06	2.13	0.13	0.45	0.00	0.00	3.86	1.83	0.56	0.01	15.56	89.50	10.39
S1909-01	A2	46.67	0.76	12.40	1.05	3.85	0.09	18.69	12.24	2.05	0.02	97.82		6.55	0.08	2.05	0.12	0.45	0.01	0.00	3.91	1.84	0.56	0.00	15.57	89.42	10.34
S1909-01	A2	46.78	0.73	12.57	1.08	3.68	0.06	18.63	12.38	1.88	0.03	97.82		6.55	0.08	2.08	0.12	0.43	0.01	0.00	3.89	1.86	0.51	0.01	15.53	89.87	9.96
S1909-01	A2	46.85	0.66	12.95	0.23	3.97	0.08	18.88	11.79	2.05	0.05	97.51		6.57	0.07	2.14	0.03	0.47	0.01	0.00	3.95	1.77	0.56	0.01	15.56	89.25	10.53
S1909-01	A2	47.80	0.55	12.11	0.53	3.82	0.10	19.72	12.93	1.83	0.03	99.42		6.59	0.06	1.97	0.06	0.44	0.01	0.00	4.05	1.91	0.49	0.01	15.59	89.95	9.79
S1909-01	A2	46.97	0.65	12.32	1.09	3.66	0.11	18.47	11.94	2.03	0.06	97.30		6.61	0.07	2.04	0.12	0.43	0.01	0.00	3.87	1.80	0.55	0.01	15.52	89.72	9.98
S1909-01	A2	47.79	0.36	13.06	0.08	3.87	0.06	18.92	11.81	2.01	0.05	98.01		6.64	0.04	2.14	0.01	0.45	0.01	0.00	3.92	1.76	0.54	0.01	15.52	89.56	10.28
S1909-01	A4	48.98	0.54	10.57	0.66	3.63	0.07	20.35	12.98	1.53	0.04	99.34		6.74	0.06	1.71	0.07	0.42	0.01	0.00	4.17	1.91	0.41	0.01	15.52	90.76	9.08
S1909-01	A4	50.30	0.53	9.39	0.52	3.60	0.07	21.06	12.97	1.35	0.04	99.83		6.87	0.05	1.51	0.06	0.41	0.01	0.00	4.29	1.90	0.36	0.01	15.47	91.09	8.74
S1909-01	A4	50.07	0.50	8.77	0.43	3.63	0.10	21.33	12.27	1.30	0.03	98.41		6.93	0.05	1.43	0.05	0.42	0.01	0.00	4.40	1.82	0.35	0.00	15.46	91.06	8.70
S1909-01	A4	51.32	0.40	8.31	0.52	3.43	0.08	21.53	13.02	1.22	0.03	99.86		7.00	0.04	1.33	0.06	0.39	0.01	0.00	4.37	1.90	0.32	0.01	15.43	91.61	8.19

<sup>a</sup>Major element compositions are in wt %. Analyses are ordered by increasing sample number and Si content. Min. Ass., mineral assemblage.

**Table A1i.** Major Element Compositions of Amphiboles From VLS Ultramafic Mylonites Analyzed by Electron Microprobe: Site S1910<sup>a</sup>

Sample	Min. Ass.	SiO <sub>2</sub>	TiO <sub>2</sub>	Al <sub>2</sub> O <sub>3</sub>	Cr <sub>2</sub> O <sub>3</sub>	FeO	MnO	NiO	MgO	CaO	Na <sub>2</sub> O	K <sub>2</sub> O	Total	F.S./23	O	Si	Ti	Al	Cr	Fe <sup>2+</sup>	Mn	Ni	Mg	Ca	Na	K	Total Mg%/ <sup>a</sup> Mg + Fe Fe%/ <sup>a</sup> Fe + Mg	
S1910-01	A4	49.61	0.55	9.30	1.39	2.36	0.12		20.03	11.92	1.39	0.05	96.72	6.95	0.06	1.54	0.15	0.28	0.01	0.00	4.18	1.79	0.38	0.01	15.34	93.50	6.18	
S1910-01	A4	50.00	0.74	9.21	1.39	2.29	0.06		20.11	11.95	1.36	0.06	97.17	6.96	0.08	1.51	0.15	0.27	0.01	0.00	4.17	1.78	0.37	0.01	15.32	93.84	6.00	
S1910-01	A4	51.33	0.58	8.24	1.17	2.48	0.00		20.67	12.14	1.32	0.07	98.00	7.08	0.06	1.34	0.13	0.29	0.00	0.00	4.25	1.79	0.35	0.01	15.31	93.69	6.31	
S1910-01	A4	50.87	0.58	8.34	1.12	2.14	0.04		20.45	11.82	1.29	0.03	96.68	7.09	0.06	1.37	0.12	0.25	0.00	0.00	4.25	1.77	0.35	0.01	15.27	94.35	5.54	
S1910-02	A4	47.03	0.22	12.36	1.91	2.53	0.00		18.53	12.53	2.29	0.03	97.43	6.60	0.02	2.04	0.21	0.30	0.00	0.00	3.88	1.88	0.62	0.01	15.56	92.88	7.12	
S1910-02	A4	52.60	0.05	6.59	0.39	2.25	0.02		24.87	11.13	0.60	0.02	98.53	7.16	0.01	1.06	0.04	0.26	0.00	0.00	5.05	1.62	0.16	0.00	15.36	95.12	4.83	
S1910-02	A4	52.69	0.17	7.45	0.53	2.09	0.00		21.03	12.34	1.25	0.00	97.55	7.26	0.02	1.21	0.06	0.24	0.00	0.00	4.32	1.82	0.33	0.00	15.26	94.72	5.28	
S1910-02	A4	52.16	0.04	4.03	0.45	2.52	0.00		25.69	11.11	0.71	0.03	96.73	7.27	0.00	0.66	0.05	0.29	0.00	0.00	5.34	1.66	0.19	0.00	15.47	94.78	5.22	
S1910-02	A4	53.57	0.13	5.37	0.53	2.30	0.06		22.39	13.11	1.02	0.01	98.48	7.34	0.01	0.87	0.06	0.26	0.01	0.00	4.57	1.92	0.27	0.00	15.32	94.43	5.44	
S1910-02	A4	53.94	0.08	5.21	0.34	2.23	0.07		22.57	13.18	0.89	0.01	98.50	7.38	0.01	0.84	0.04	0.26	0.01	0.00	4.60	1.93	0.23	0.00	15.29	94.58	5.25	
S1910-02	A4	53.53	0.08	4.43	1.09	2.52	0.03		22.88	12.65	0.74	0.01	97.96	7.38	0.01	0.72	0.12	0.29	0.00	0.00	4.70	1.87	0.20	0.00	15.29	94.11	5.82	
S1910-02	A4	53.62	0.06	3.78	0.39	2.60	0.06		24.73	11.39	0.64	0.01	97.30	7.41	0.01	0.62	0.04	0.30	0.01	0.00	5.09	1.69	0.17	0.00	15.34	94.30	5.57	
S1910-02	A4	54.99	0.04	4.66	0.63	2.32	0.10		23.02	12.96	0.75	0.01	99.48	7.44	0.00	0.74	0.07	0.26	0.01	0.00	4.64	1.88	0.20	0.00	15.25	94.41	5.35	
S1910-02	A4	53.84	0.06	3.96	0.41	2.18	0.06		23.21	12.78	0.68	0.02	97.18	7.46	0.01	0.65	0.04	0.25	0.01	0.00	4.79	1.90	0.18	0.00	15.28	94.87	4.99	
S1910-02	A4	54.80	0.07	3.99	0.44	2.17	0.05		23.39	13.00	0.72	0.02	98.63	7.47	0.01	0.64	0.05	0.25	0.01	0.00	4.75	1.90	0.19	0.00	15.27	94.96	4.93	
S1910-02	A4	55.24	0.05	4.21	0.41	2.19	0.05		23.33	12.99	0.73	0.01	99.22	7.48	0.01	0.67	0.04	0.25	0.01	0.00	4.71	1.89	0.19	0.00	15.25	94.87	5.01	
S1910-02	A4	55.31	0.05	4.13	0.48	2.60	0.07		23.34	12.50	0.76	0.02	99.25	7.50	0.00	0.66	0.05	0.29	0.01	0.00	4.71	1.82	0.20	0.00	15.25	93.97	5.88	
S1910-02	A4	55.07	0.06	3.93	0.53	2.51	0.03		23.12	12.91	0.76	0.01	98.93	7.50	0.01	0.63	0.06	0.29	0.00	0.00	4.69	1.88	0.20	0.00	15.26	94.20	5.73	
S1910-02	A4	55.50	0.07	4.22	0.36	2.20	0.07		22.93	13.25	0.69	0.01	99.30	7.51	0.01	0.67	0.04	0.25	0.01	0.00	4.63	1.92	0.18	0.00	15.22	94.73	5.10	
S1910-02	A5	56.06	0.05	3.25	0.35	2.09	0.07		22.74	12.33	0.47	0.00	97.41	7.69	0.01	0.53	0.04	0.24	0.01	0.00	4.65	1.81	0.12	0.00	15.09	94.94	4.90	
S1910-03	A4	53.62	0.03	4.74	0.64	2.35	0.08		21.99	12.92	0.65	0.03	97.05	7.44	0.00	0.78	0.07	0.27	0.01	0.00	4.55	1.92	0.17	0.01	15.22	94.16	5.65	
S1910-03	A4	55.43	0.02	4.78	0.59	2.09	0.08		21.90	12.78	0.73	0.02	98.42	7.55	0.00	0.77	0.06	0.24	0.01	0.00	4.44	1.86	0.19	0.00	15.13	94.73	5.07	
S1910-04	A4	52.75	0.07	6.48	1.21	2.55	0.00		0.16	21.00	13.02	0.94	0.03	98.20	7.27	0.01	1.05	0.13	0.29	0.00	0.02	4.31	1.92	0.25	0.01	15.26	93.62	6.38
S1910-04	A4	52.47	0.07	6.53	1.11	2.48	0.00		0.04	21.07	12.76	0.90	0.02	97.44	7.27	0.01	1.07	0.12	0.29	0.00	0.00	4.35	1.89	0.24	0.00	15.25	93.80	6.20
S1910-04	A4	52.63	0.04	6.38	0.97	2.49	0.01		0.06	21.51	12.69	0.90	0.04	97.72	7.27	0.00	1.04	0.11	0.29	0.00	0.01	4.43	1.88	0.24	0.01	15.27	93.87	6.10
S1910-04	A4	52.89	0.03	6.30	1.26	2.49	0.05		0.06	21.04	12.63	0.91	0.00	97.64	7.31	0.00	1.03	0.14	0.29	0.01	0.01	4.33	1.87	0.24	0.00	15.23	93.66	6.23
S1910-04	A4	52.38	0.01	6.09	1.02	2.35	0.11		0.10	20.94	12.71	0.85	0.04	96.59	7.32	0.00	1.00	0.11	0.27	0.01	0.01	4.36	1.90	0.23	0.01	15.24	93.82	5.91
S1910-04	A4	53.36	0.00	5.74	1.04	2.44	0.00		0.03	21.80	12.98	0.85	0.01	98.26	7.33	0.00	0.93	0.11	0.28	0.00	0.00	4.46	1.91	0.23	0.00	15.26	94.09	5.90
S1910-04	A4	52.87	0.01	5.52	1.02	2.42	0.04		0.09	21.71	12.75	0.85	0.00	97.30	7.34	0.00	0.90	0.11	0.28	0.00	0.01	4.49	1.90	0.23	0.00	15.27	94.03	5.87
S1910-04	A4	52.88	0.00	5.37	0.89	2.49	0.00		0.10	21.73	13.01	0.80	0.02	97.30	7.34	0.00	0.88	0.10	0.29	0.00	0.01	4.50	1.94	0.21	0.00	15.28	93.95	6.05
S1910-04	A4	53.54	0.03	5.99	1.05	2.32	0.00		0.13	21.40	12.99	0.77	0.02	98.24	7.35	0.00	0.97	0.11	0.27	0.00	0.01	4.38	1.91	0.20	0.00	15.21	94.27	5.73
S1910-04	A4	53.49	0.00	5.69	0.75	2.55	0.00		0.06	21.70	12.81	0.82	0.00	97.88	7.37	0.00	0.92	0.08	0.29	0.00	0.01	4.45	1.89	0.22	0.00	15.24	93.81	6.19
S1910-04	A4	53.20	0.01	5.48	0.89	2.44	0.07		0.06	21.51	12.84	0.74	0.00	97.24	7.38	0.00	0.90	0.10	0.28	0.01	0.01	4.45	1.91	0.20	0.00	15.22	93.85	5.98
S1910-04	A4	53.57	0.01	5.52	1.04	2.38	0.00		0.07	21.46	13.00	0.80	0.02	97.87	7.38	0.00	0.90	0.11	0.27	0.00	0.01	4.41	1.92	0.21	0.00	15.22	94.15	5.85
S1910-04	A4	53.58	0.03	5.40	1.01	2.39	0.02		0.13	21.32	13.06	0.74	0.00	97.69	7.40	0.00	0.88	0.11	0.28	0.00	0.01	4.39	1.93	0.20	0.00	15.20	94.02	5.92
S1910-04	A4	53.56	0.01	5.43	0.90	2.37	0.01		0.07	21.55	12.81	0.76	0.03	97.50	7.40	0.00	0.88	0.10	0.27	0.00	0.01	4.44	1.90	0.20	0.00	15.21	94.15	5.82
S1910-04	A4	53.74	0.02	5.21	0.90	2.39	0.00		0.01	21.81	13.00	0.72	0.01	97.80	7.40	0.00	0.85	0.10	0.27	0.00	0.00	4.48	1.92	0.19	0.00	15.22	94.22	5.78
S1910-04	A4	54.24	0.00	5.00	0.78	2.40	0.00		0.10	21.83	12.97	0.69	0.04	98.05	7.45	0.00	0.81	0.08	0.28	0.00	0.01	4.47	1.91	0.18	0.01	15.20	94.20	5.80
S1910-04	A4	54.57	0.00	4.49	0.42	2.34	0.00		0.07	22.07	12.90	0.54	0.00	97.40	7.52	0.00	0.73	0.05	0.27	0.00	0.01	4.53	1.91	0.14	0.00	15.16	94.38	5.61
S1910-04	A4	54.77	0.03	3.79	0.19	2.30	0.05		0.07	22.40	13.16	0.51	0.02	97.29	7.57	0.00	0.62	0.02	0.27	0.01	0.01	4.61	1.95	0.14	0.00	15.18	94.44	5.44

**Table A1j.** Major Element Compositions of Amphiboles From VLS Ultramafic Mylonites Analyzed by Electron Microprobe: Site S1911<sup>a</sup>

Sample	Min.	Ass.	SiO <sub>2</sub>	TiO <sub>2</sub>	Al <sub>2</sub> O <sub>3</sub>	Cr <sub>2</sub> O <sub>3</sub>	FeO	MnO	NiO	MgO	CaO	Na <sub>2</sub> O	K <sub>2</sub> O	Total	F.S./23	O	Si	Ti	Al	Cr	Fe <sup>2+</sup>	Mn	Ni	Mg	Ca	Na	K	Total	Mg%/ <sup>a</sup> Mg + Fe	Fe%/ <sup>a</sup> Fe + Mg
S1911-02	A4	49.08	0.11	12.59	0.03	3.25	0.08	20.14	12.10	2.23	0.03	99.64		6.70	0.01	2.02	0.00	0.37	0.01	0.00	4.10	1.77	0.59	0.01	15.58	91.51	8.29			
S1911-02	A4	48.76	0.42	10.22	0.40	3.09	0.05	20.24	12.08	1.80	0.05	97.11		6.83	0.04	1.69	0.04	0.36	0.01	0.00	4.23	1.81	0.49	0.01	15.51	91.99	7.88			
S1911-02	A4	51.18	0.26	8.84	0.65	2.78	0.10	20.84	12.44	1.59	0.02	98.70		7.03	0.03	1.43	0.07	0.32	0.01	0.00	4.26	1.83	0.42	0.00	15.41	92.80	6.95			
S1911-03	A4	47.65	0.12	13.66	0.00	3.13	0.07	18.83	12.04	2.35	0.05	97.90		6.62	0.01	2.24	0.00	0.36	0.01	0.00	3.90	1.79	0.63	0.01	15.57	91.29	8.52			
S1911-03	A4	51.12	0.21	9.34	0.96	2.71	0.10	20.43	12.36	1.44	0.04	98.71		7.01	0.02	1.51	0.10	0.31	0.01	0.00	4.18	1.82	0.38	0.01	15.35	92.83	6.91			
S1911-04	A2	45.21	0.39	13.41	0.25	4.39	0.11	0.14	18.28	12.33	2.47	0.10	97.08		6.43	0.04	2.25	0.03	0.52	0.01	0.02	3.87	1.88	0.68	0.02	15.74	87.87	11.84		
S1911-04	A4	47.19	0.39	12.01	0.30	4.27	0.01	0.09	18.77	12.62	2.04	0.04	97.74		6.63	0.04	1.99	0.03	0.50	0.00	0.01	3.93	1.90	0.56	0.01	15.60	88.65	11.32		
S1911-04	A4	47.81	0.04	12.61	0.03	3.92	0.07	19.19	12.14	2.14	0.00	97.95		6.66	0.00	2.07	0.00	0.46	0.01	0.00	3.99	1.81	0.58	0.00	15.58	89.55	10.27			
S1911-04	A4	48.64	0.57	9.33	0.77	3.70	0.11	0.00	19.87	12.48	1.68	0.03	97.18		6.85	0.06	1.55	0.09	0.44	0.01	0.00	4.17	1.88	0.46	0.00	15.51	90.28	9.43		
S1911-04	A4	48.82	0.38	9.78	0.45	3.42	0.06	0.12	19.70	12.56	1.78	0.04	97.11		6.86	0.04	1.62	0.05	0.40	0.01	0.01	4.13	1.89	0.49	0.01	15.51	90.97	8.87		
S1911-04	A4	50.30	0.25	9.42	0.24	3.35	0.05	0.07	20.76	12.50	1.75	0.04	98.74		6.93	0.03	1.53	0.03	0.39	0.01	0.01	4.26	1.85	0.47	0.01	15.50	91.58	8.29		
S1911-04	A4	49.72	0.58	7.87	2.00	3.01	0.08	0.08	20.02	12.25	1.54	0.05	97.20		6.98	0.06	1.30	0.22	0.35	0.01	0.01	4.19	1.84	0.42	0.01	15.41	92.04	7.76		
S1911-04	A4	50.97	0.10	8.93	0.04	2.89	0.11	0.13	20.96	12.66	1.46	0.04	98.30		7.03	0.01	1.45	0.00	0.33	0.01	0.01	4.31	1.87	0.39	0.01	15.43	92.56	7.16		
S1911-04	A4	50.69	0.39	7.79	1.22	3.20	0.06	0.06	20.18	12.30	1.46	0.05	97.40		7.08	0.04	1.28	0.14	0.37	0.01	0.01	4.20	1.84	0.40	0.01	15.37	91.68	8.17		
S1911-04	A4	51.48	0.18	8.23	0.19	3.57	0.15	0.05	20.69	12.18	1.54	0.03	98.24		7.11	0.02	1.34	0.02	0.41	0.02	0.00	4.26	1.80	0.41	0.01	15.40	90.83	8.79		
S1911-04	A4	52.14	0.17	6.61	0.47	2.42	0.14	0.05	21.03	13.21	1.18	0.09	97.51		7.24	0.02	1.08	0.05	0.28	0.02	0.01	4.35	1.96	0.32	0.02	15.34	93.61	6.05		
S1911-04	A5	54.98	0.23	3.41	0.49	2.73	0.04	0.13	22.14	12.58	0.66	0.01	97.39		7.60	0.02	1.56	0.05	0.32	0.00	0.01	4.56	1.86	0.18	0.00	15.16	93.44	6.46		
S1911-04	A5	55.59	0.17	2.86	0.66	2.66	0.00	0.08	22.35	13.08	0.43	0.02	97.90		7.64	0.02	1.46	0.07	0.31	0.00	0.01	4.58	1.93	0.11	0.00	15.13	93.74	6.25		
S1911-04	A5	56.08	0.30	2.45	0.83	2.16	0.07	0.11	22.47	13.38	0.52	0.04	98.41		7.67	0.03	1.39	0.09	0.25	0.01	0.01	4.58	1.96	0.14	0.01	15.13	94.72	5.11		
S1911-05	A2	44.78	1.50	12.74	1.88	3.84	0.07	0.07	18.19	12.24	2.88	0.00	98.12		6.32	0.16	2.12	0.21	0.45	0.01	0.00	3.83	1.85	0.79	0.00	15.75	89.23	10.57		
S1911-05	A2	45.35	1.52	13.35	1.59	3.64	0.01	0.11	18.33	12.63	2.28	0.01	98.81		6.33	0.16	2.20	0.18	0.43	0.00	0.01	3.81	1.89	0.62	0.00	15.63	89.94	10.03		
S1911-05	A2	45.75	1.41	12.59	1.78	3.71	0.04	0.12	18.35	12.63	2.54	0.01	98.94		6.39	0.15	2.07	0.20	0.43	0.00	0.01	3.82	1.89	0.69	0.00	15.67	89.73	10.17		
S1911-13	A4	52.32	0.25	7.20	0.62	2.38	0.05	0.05	21.33	12.36	0.94	0.00	97.45		7.23	0.03	1.17	0.07	0.28	0.01	0.00	4.39	1.83	0.25	0.00	15.25	93.99	5.89		
S1911-13	A4	52.44	0.13	5.94	0.64	2.45	0.08	0.05	21.30	12.28	0.95	0.00	96.21		7.34	0.01	0.98	0.07	0.29	0.01	0.00	4.44	1.84	0.26	0.00	15.25	93.75	6.05		
S1911-13	A4	52.76	0.17	6.07	0.34	2.54	0.10	0.11	21.17	12.20	0.87	0.01	96.33		7.37	0.02	1.00	0.04	0.30	0.01	0.01	4.41	1.83	0.24	0.00	15.21	93.46	6.30		
S1911-38	A3	46.17	0.83	12.19	1.78	3.68	0.10	0.13	18.83	12.75	2.11	0.02	98.57		6.46	0.09	2.01	0.20	0.43	0.01	0.01	3.93	1.91	0.57	0.00	15.63	89.89	9.85		
S1911-38	A3	46.49	0.84	12.37	1.93	3.72	0.01	0.08	18.87	12.58	2.25	0.03	99.17		6.47	0.09	2.03	0.21	0.43	0.00	0.01	3.91	1.87	0.61	0.00	15.63	90.02	9.95		
S1911-38	A3	45.87	0.90	12.29	1.78	3.73	0.06	0.05	18.32	12.19	2.11	0.03	97.28		6.49	0.10	2.05	0.20	0.44	0.01	0.00	3.86	1.85	0.58	0.01	15.58	89.60	10.24		
S1911-38	A3	46.38	0.80	12.20	1.66	3.92	0.05	0.05	18.60	12.51	2.36	0.04	98.52		6.49	0.08	2.01	0.18	0.46	0.01	0.00	3.88	1.88	0.64	0.01	15.65	89.30	10.56		
S1911-38	A3	46.84	0.70	12.09	1.76	3.72	0.05	0.12	18.84	12.79	2.22	0.02	99.15		6.51	0.07	1.98	0.19	0.43	0.01	0.01	3.90	1.91	0.60	0.00	15.63	89.92	9.96		
S1911-38	A3	46.53	0.80	12.28	1.65	3.78	0.04	0.05	18.51	12.46	2.17	0.03	98.25		6.52	0.08	2.03	0.18	0.44	0.00	0.00	3.86	1.87	0.59	0.01	15.59	89.62	10.27		
S1911-38	A3	46.69	0.69	11.82	1.73	3.65	0.00	0.13	18.85	12.81	2.04	0.03	98.44		6.53	0.07	1.95	0.19	0.43	0.00	0.01	3.93	1.92	0.55	0.00	15.60	90.19	9.81		
S1911-38	A3	47.05	0.86	11.21	1.72	3.39	0.08	0.08	18.72	12.37	2.05	0.00	97.45		6.63	0.09	1.86	0.19	0.40	0.01	0.00	3.93	1.87	0.56	0.00	15.54	90.58	9.20		
S1911-38	A3	49.20	0.68	9.82	1.16	3.40	0.09	0.09	20.19	12.87	1.67	0.02	99.19		6.79	0.07	1.60	0.13	0.39	0.01	0.01	4.15	1.90	0.45	0.00	15.50	91.17	8.61		
S1911-47	A2	45.39	0.98	12.75	2.03	3.92	0.04	0.03	18.56	12.35	2.66	0.02	98.72		6.36	0.10	2.11	0.22	0.46	0.01	0.00	3.88	1.85	0.72	0.00	15.73	89.31	10.57		
S1911-47	A2	45.32	0.96	12.59	2.12	4.00	0.03	0.08	18.36	12.45	2.69	0.04	98.63		6.37	0.10	2.09	0.24	0.47	0.00	0.01	3.85	1.88	0.73	0.01	15.74	89.04	10.88		
S1911-47	A2	45.59	1.03	12.81	2.07	3.96	0.05	0.10	18.40	12.34	2.74	0.02	99.09		6.37	0.11	2.11	0.23	0.46	0.01	0.01	3.83	1.85	0.74	0.00	15.72	89.11	10.76		



Table A1j. (continued)

Sample	Min.	Ass.	SiO <sub>2</sub>	TiO <sub>2</sub>	Al <sub>2</sub> O <sub>3</sub>	Cr <sub>2</sub> O <sub>3</sub>	FeO	MnO	NiO	MgO	CaO	Na <sub>2</sub> O	K <sub>2</sub> O	Total	F.S./23	O	Si	Ti	Al	Cr	Fe <sup>2+</sup>	Mn	Ni	Mg	Ca	Na	K	Total	Mg%/ $\text{Mg} + \text{Fe}$	Fe%/ $\text{Fe} + \text{Mg}$
S1911-47	A2	45.61	0.95	12.75	1.88	3.95	0.05	0.12	18.57	12.48	2.72	0.02	99.09	6.37	0.10	2.10	0.21	0.46	0.01	0.01	3.87	1.87	0.74	0.00	15.74	89.21	10.64			
S1911-47	A2	45.71	0.99	12.88	1.96	3.85	0.06	0.03	18.56	12.40	2.60	0.03	99.07	6.38	0.10	2.12	0.22	0.45	0.01	0.00	3.86	1.86	0.70	0.01	15.70	89.42	10.40			
S1911-47	A2	45.77	1.02	12.83	1.91	3.87	0.09	0.10	18.61	12.41	2.53	0.01	99.15	6.38	0.11	2.11	0.21	0.45	0.01	0.01	3.87	1.85	0.69	0.00	15.69	89.33	10.43			
S1911-47	A2	45.73	1.10	12.64	2.00	3.95	0.04	0.09	18.46	12.52	2.55	0.04	99.12	6.39	0.12	2.08	0.22	0.46	0.00	0.01	3.84	1.87	0.69	0.01	15.69	89.18	10.72			
S1911-47	A2	45.78	1.05	12.76	1.86	3.84	0.03	0.13	18.37	12.65	2.65	0.02	99.15	6.39	0.11	2.10	0.21	0.45	0.00	0.01	3.82	1.89	0.72	0.00	15.71	89.41	10.50			
S1911-47	A2	45.37	1.00	12.76	2.14	3.55	0.07	0.08	12.08	2.72	0.00	97.72	6.41	0.11	2.12	0.24	0.42	0.01	0.00	3.80	1.83	0.74	0.00	15.68	89.87	9.93				
S1911-47	A2	45.43	0.95	12.72	1.88	3.71	0.05	0.08	18.52	11.81	2.48	0.03	97.58	6.42	0.10	2.12	0.21	0.44	0.01	0.00	3.90	1.79	0.68	0.01	15.66	89.77	10.09			
S1911-47	A2	45.88	0.99	12.68	2.02	3.98	0.04	0.08	18.30	12.31	2.58	0.03	98.81	6.42	0.10	2.09	0.22	0.47	0.00	0.00	3.82	1.85	0.70	0.01	15.67	89.02	10.87			
S1911-47	A2	45.87	1.08	12.27	1.84	3.85	0.05	0.11	18.43	12.54	2.73	0.03	98.80	6.43	0.11	2.03	0.20	0.45	0.01	0.01	3.85	1.88	0.74	0.00	15.72	89.39	10.46			
S1911-47	A2	46.07	1.18	12.48	1.84	3.85	0.10	0.10	18.43	12.45	2.46	0.02	98.99	6.43	0.12	2.05	0.20	0.45	0.01	0.01	3.83	1.86	0.67	0.00	15.65	89.27	10.47			
S1911-58	A2	44.17	2.22	12.59	2.26	3.67	0.09	0.09	17.91	12.28	2.33	0.00	97.52	6.28	0.24	2.11	0.25	0.44	0.01	0.00	3.79	1.87	0.64	0.00	15.63	89.46	10.29			
S1911-58	A2	46.60	0.09	13.51	0.32	4.05	0.06	0.10	19.03	12.23	2.39	0.07	98.43	6.50	0.01	2.22	0.04	0.47	0.01	0.01	3.95	1.83	0.65	0.01	15.69	89.19	10.64			
S1911-58	A2	46.43	0.20	13.17	0.39	3.74	0.07	0.09	19.04	12.30	2.51	0.06	97.91	6.51	0.02	2.18	0.04	0.44	0.01	0.00	3.98	1.85	0.68	0.01	15.71	89.90	9.91			
S1911-58	A2	47.23	0.21	13.73	0.18	3.64	0.07	0.09	19.19	12.30	2.46	0.08	99.16	6.52	0.02	2.23	0.02	0.42	0.01	0.01	3.95	1.82	0.66	0.01	15.67	90.23	9.59			
S1911-58	A2	46.69	0.30	13.37	0.15	3.62	0.07	0.07	18.94	11.93	2.57	0.06	97.70	6.54	0.03	2.21	0.02	0.42	0.01	0.00	3.95	1.79	0.70	0.01	15.67	90.14	9.67			
S1911-58	A2	47.69	0.33	12.78	0.16	3.48	0.09	0.09	19.15	12.21	2.11	0.06	98.06	6.63	0.03	2.10	0.02	0.40	0.01	0.00	3.97	1.82	0.57	0.01	15.57	90.53	9.23			
S1911-58	A2	47.34	0.13	12.66	0.06	3.76	0.12	0.12	18.91	12.00	2.33	0.07	97.38	6.64	0.01	2.09	0.01	0.44	0.01	0.00	3.95	1.80	0.63	0.01	15.62	89.67	10.01			
S1911-58	A2	49.19	0.30	10.82	0.21	3.80	0.08	0.12	20.81	11.57	1.93	0.03	98.86	6.78	0.03	1.76	0.02	0.44	0.01	0.01	4.28	1.71	0.52	0.00	15.56	90.53	9.27			
S1911-58	A2	49.71	0.34	10.23	0.78	3.71	0.10	0.10	20.01	11.92	1.93	0.06	98.79	6.86	0.04	1.66	0.09	0.43	0.01	0.00	4.12	1.76	0.52	0.01	15.49	90.34	9.40			
S1911-58	A2	49.07	0.33	9.65	0.61	3.39	0.13	0.13	19.84	11.83	1.79	0.05	96.69	6.91	0.03	1.60	0.07	0.40	0.02	0.00	4.16	1.78	0.49	0.01	15.47	90.94	8.72			
S1911-58	A2	50.97	0.23	9.92	0.13	3.42	0.07	0.07	20.18	12.00	1.69	0.03	98.64	7.00	0.02	1.61	0.01	0.39	0.01	0.00	4.13	1.77	0.45	0.01	15.39	91.15	8.67			
S1911-58	A2	50.87	0.35	7.84	0.83	3.01	0.09	0.09	20.54	12.32	1.46	0.03	97.34	7.09	0.04	1.29	0.09	0.35	0.01	0.00	4.27	1.84	0.39	0.01	15.38	92.19	7.58			
S1911-63	A4	48.55	0.27	10.53	0.29	2.76	0.11	0.04	19.96	12.26	1.70	0.04	96.5	6.83	0.03	1.75	0.03	0.32	0.01	0.00	4.19	1.85	0.46	0.01	15.48	92.54	7.17			
S1911-63	A4	48.88	0.39	10.24	0.81	2.88	0.03	0.03	19.90	12.31	1.66	0.04	97.3	6.84	0.04	1.69	0.09	0.34	0.00	0.00	4.15	1.85	0.45	0.01	15.46	92.42	7.50			
S1911-63	A4	48.66	0.34	9.73	0.73	2.68	0.12	0.02	20.01	12.29	1.58	0.02	96.5	6.88	0.04	1.62	0.08	0.32	0.01	0.00	4.21	1.86	0.43	0.00	15.46	92.72	6.97			
S1911-63	A4	51.50	0.32	8.16	0.77	2.86	0.04	0.04	21.00	12.54	1.33	0.06	98.9	7.08	0.03	1.32	0.08	0.33	0.00	0.00	4.30	1.85	0.36	0.01	15.37	92.80	7.10			
S1911-63	A4	51.31	0.25	7.94	0.52	2.77	0.03	0.03	21.03	11.99	1.34	0.03	97.3	7.13	0.03	1.30	0.06	0.32	0.00	0.00	4.36	1.78	0.36	0.00	15.35	93.05	6.87			
S1911-63	A4	51.62	0.25	7.90	0.61	2.68	0.07	0.05	20.53	12.48	1.24	0.05	97.5	7.16	0.03	1.29	0.07	0.31	0.01	0.00	4.24	1.85	0.33	0.01	15.30	93.02	6.81			
S1911-64	A4	47.25	0.34	9.51	0.61	2.54	0.11	0.05	20.55	11.59	1.46	0.05	94.1	6.82	0.04	1.62	0.07	0.31	0.01	0.00	4.42	1.79	0.41	0.01	15.50	93.23	6.48			
S1911-64	A4	50.67	0.38	8.78	0.72	2.84	0.05	0.05	20.63	12.03	1.36	0.06	97.5	7.03	0.04	1.44	0.08	0.33	0.01	0.00	4.27	1.79	0.37	0.01	15.36	92.73	7.16			
S1911-64	A4	50.44	0.28	7.87	0.44	2.67	0.03	0.03	21.65	11.82	1.19	0.05	96.7	7.07	0.03	1.30	0.05	0.31	0.00	0.00	4.52	1.78	0.32	0.01	15.39	93.48	6.46			

<sup>a</sup> Major element compositions are in wt %. Analyses are ordered by increasing sample number and Si content. Min. Ass., mineral assemblage.

**Table A1k.** Major Element Compositions of Amphiboles From VLS Ultramafic Mylonites Analyzed by Electron Microprobe: Site S1915<sup>a</sup>

Sample	Min.	Ass.	Spot	SiO <sub>2</sub>	TiO <sub>2</sub>	Al <sub>2</sub> O <sub>3</sub>	Cr <sub>2</sub> O <sub>3</sub>	FeO	MnO	NiO	MgO	CaO	Na <sub>2</sub> O	K <sub>2</sub> O	Total	F.S./23	O	Si	Ti	Al	Cr	Fe <sup>2+</sup>	Mn	Ni	Mg	Ca	Na	K	Total	Mg%/ <sup>b</sup> Mg	Fe%/ <sup>b</sup> Fe	Mg%/ <sup>b</sup> Mg + Fe + Mg
S1915-20	A4	50.50	0.12	8.18	0.40	3.54	0.04	20.31	12.56	1.74	0.07	97.46	7.06	0.01	1.35	0.04	0.41	0.00	0.00	4.23	1.88	0.47	0.01	15.48	91.00	8.90	11.75					
S1915-20	A4	54.55	0.28	4.29	0.18	2.35	0.00	22.14	12.98	0.90	0.04	97.71	7.51	0.03	0.70	0.02	0.27	0.00	0.00	4.54	1.91	0.24	0.01	15.23	94.38	5.62	14.03					
S1915-20	A4	55.30	0.09	3.77	0.07	2.59	0.07	22.41	13.08	0.67	0.00	98.05	7.58	0.01	0.61	0.01	0.30	0.01	0.00	4.58	1.92	0.18	0.00	15.19	93.75	6.08	12.20					
S1915-20	A4	56.60	0.10	2.51	0.00	1.85	0.00	23.19	12.99	0.39	0.00	97.63	7.74	0.01	0.40	0.00	0.21	0.00	0.00	4.73	1.90	0.10	0.00	15.10	95.72	4.28	14.66					
S1915-37	A2	core	41.02	1.69	15.01	1.85	4.35	0.03	18.32	12.73	2.59	0.08	97.67	5.88	0.18	2.54	0.21	0.52	0.00	0.00	3.91	1.95	0.72	0.01	15.93	88.18	11.75	11.75				
S1915-37	A2	core	41.08	1.74	13.67	1.89	5.09	0.02	0.08	17.51	12.49	3.29	0.09	96.96	5.97	0.19	2.34	0.22	0.62	0.00	0.01	3.79	1.95	0.93	0.02	16.03	85.91	14.03	14.03			
S1915-37	A2	core	42.40	1.63	15.13	1.75	4.36	0.02	17.62	12.40	2.74	0.08	98.12	6.02	0.17	2.53	0.20	0.52	0.00	0.00	3.73	1.89	0.76	0.01	15.83	87.76	12.20	12.20				
S1915-37	A2	core	42.94	2.04	14.36	1.17	5.29	0.00	17.27	13.27	2.89	0.14	99.37	6.06	0.22	2.39	0.13	0.62	0.00	0.00	3.63	2.01	0.79	0.03	15.87	85.33	14.66	14.66				
S1915-37	A2	core	43.67	1.62	13.88	2.05	4.39	0.10	17.50	12.58	3.05	0.08	98.93	6.16	0.17	2.31	0.23	0.52	0.01	0.00	3.68	1.90	0.83	0.01	15.83	87.41	12.31	12.31				
S1915-37	A2	core	43.87	1.67	13.71	2.00	4.63	0.07	17.75	12.56	3.10	0.06	99.42	6.16	0.18	2.27	0.22	0.54	0.01	0.00	3.72	1.89	0.84	0.01	15.84	87.07	12.74	12.74				
S1915-37	A2	core	43.84	1.63	13.90	2.07	4.51	0.08	17.51	12.49	3.17	0.07	99.27	6.16	0.17	2.30	0.23	0.53	0.01	0.00	3.67	1.88	0.86	0.01	15.84	87.17	12.61	12.61				
S1915-37	A2	core	43.79	1.57	12.78	1.58	4.54	0.02	19.60	12.20	2.88	0.07	99.04	6.17	0.17	2.12	0.18	0.53	0.00	0.00	4.11	1.84	0.79	0.01	15.92	88.44	11.50	11.50				
S1915-37	A2	core	44.05	1.62	13.57	1.88	4.65	0.05	17.97	12.64	3.14	0.08	99.66	6.17	0.17	2.24	0.21	0.55	0.01	0.00	3.75	1.90	0.85	0.01	15.86	87.19	12.67	12.67				
S1915-37	A2	core	43.95	1.60	13.67	2.01	4.57	0.01	17.91	12.33	3.19	0.07	99.31	6.17	0.17	2.26	0.22	0.54	0.00	0.00	3.75	1.86	0.87	0.01	15.85	87.45	12.53	12.53				
S1915-37	A2	core	43.94	1.60	13.65	1.90	4.73	0.03	17.51	12.62	3.23	0.07	99.28	6.18	0.17	2.26	0.21	0.56	0.00	0.00	3.67	1.90	0.88	0.01	15.86	86.77	13.14	13.14				
S1915-37	A2	core	43.93	1.69	13.64	1.99	4.40	0.05	17.68	12.35	3.15	0.08	98.95	6.19	0.18	2.26	0.22	0.52	0.01	0.00	3.71	1.86	0.86	0.01	15.83	87.60	12.25	12.25				
S1915-37	A2	core	44.20	1.67	13.59	1.96	4.60	0.04	17.59	12.56	3.24	0.07	99.51	6.20	0.18	2.25	0.22	0.54	0.00	0.00	3.68	1.89	0.88	0.01	15.84	87.11	12.78	12.78				
S1915-37	A2	core	43.17	1.71	13.06	1.87	4.52	0.03	0.12	17.03	12.39	3.25	0.04	97.19	6.21	0.19	2.21	0.21	0.54	0.00	0.01	3.65	1.91	0.91	0.01	15.85	86.96	12.95	12.95			
S1915-37	A2	core	43.56	1.62	13.46	1.74	4.59	0.08	17.55	11.84	3.10	0.08	97.62	6.21	0.17	2.26	0.20	0.55	0.01	0.00	3.73	1.81	0.86	0.01	15.82	87.01	12.77	12.77				
S1915-37	A2	core	44.22	1.44	13.48	1.66	4.46	0.07	18.65	12.36	2.46	0.07	98.85	6.21	0.15	2.23	0.18	0.52	0.01	0.00	3.91	1.86	0.67	0.01	15.77	87.99	11.81	11.81				
S1915-37	A2	core	44.65	1.68	13.30	1.73	4.34	0.00	18.56	12.60	2.79	0.08	99.74	6.23	0.18	2.19	0.19	0.51	0.00	0.00	3.86	1.88	0.75	0.01	15.79	88.40	11.59	11.59				
S1915-37	A2	core	43.50	1.98	12.54	1.75	4.50	0.00	0.04	17.51	12.76	2.93	0.07	97.57	6.23	0.21	2.12	0.20	0.54	0.00	0.00	3.74	1.96	0.81	0.01	15.82	87.40	12.60	12.60			
S1915-37	A2	core	43.49	1.69	12.37	1.66	4.49	0.03	0.11	17.75	12.62	3.05	0.06	97.33	6.24	0.18	2.09	0.19	0.54	0.00	0.01	3.80	1.94	0.85	0.01	15.86	87.48	12.43	12.43			
S1915-37	A2	core	44.55	1.70	13.00	1.74	4.32	0.06	18.22	12.73	2.96	0.07	99.34	6.25	0.18	2.15	0.19	0.51	0.01	0.00	3.81	1.91	0.80	0.01	15.81	88.12	11.72	11.72				
S1915-37	A2	core	43.62	1.67	12.34	2.13	4.49	0.00	0.06	17.46	12.73	3.14	0.04	97.69	6.25	0.18	2.08	0.24	0.54	0.00	0.01	3.72	1.95	0.87	0.01	15.85	87.38	12.62	12.62			
S1915-37	A2	core	43.85	1.69	12.60	1.78	4.36	0.00	0.07	17.66	12.52	3.09	0.08	97.71	6.26	0.18	2.12	0.20	0.52	0.00	0.01	3.76	1.92	0.85	0.01	15.83	87.84	12.16	12.16			
S1915-37	A2	core	43.72	1.60	12.51	1.84	4.41	0.01	0.12	17.56	12.48	3.08	0.06	97.40	6.26	0.17	2.11	0.21	0.53	0.00	0.01	3.75	1.92	0.86	0.01	15.84	87.62	12.36	12.36			
S1915-37	A2	core	43.97	1.72	12.34	1.86	4.63	0.00	0.10	17.76	12.58	2.98	0.08	98.03	6.27	0.18	2.07	0.21	0.55	0.00	0.01	3.77	1.92	0.82	0.01	15.83	87.23	12.77	12.77			
S1915-37	A2	core	44.41	2.04	12.67	1.63	4.09	0.05	0.16	17.78	13.10	2.64	0.06	98.62	6.27	0.22	2.11	0.18	0.48	0.01	0.02	3.74	1.98	0.72	0.01	15.74	88.44	11.43	11.43			
S1915-37	A2	core	44.13	1.61	12.86	1.98	4.17	0.09	17.83	12.04	3.10	0.07	97.88	6.27	0.17	2.15	0.22	0.50	0.01	0.00	3.78	1.83	0.85	0.01	15.80	88.17	11.57	11.57				
S1915-37	A2	core	44.00	1.70	12.72	1.85	4.30	0.02	0.12	17.52	12.41	3.07	0.06	97.76	6.27	0.18	2.14	0.21	0.51	0.00	0.01	3.72	1.89	0.85	0.01	15.80	87.86	12.10	12.10			
S1915-37	A2	core	44.87	1.56	12.88	1.95	4.51	0.07	18.07	12.55	3.09	0.08	99.63	6.28	0.16	2.12	0.22	0.53	0.01	0.00	3.77	1.88	0.84	0.01	15.82	87.55	12.26	12.26				
S1915-37	A2	core	44.29	1.62	12.54	2.06	4.42	0.00	0.18	17.77	12.38	3.17	0.04	98.46	6.28	0.17	2.09	0.23	0.52	0.00	0.02	3.75	1.88	0.87	0.01	15.83	87.76	12.24	12.24			
S1915-37	A2	core	43.77	1.71	12.20	1.85	4.46	0.00	0.07	17.68	12.46	2.97	0.13	97.30	6.28	0.18	2.06	0.21	0.54	0.00	0.01	3.78	1.91	0.83	0.02	15.82	87.60	12.40	12.40			
S1915-37	A2	core	44.21	1.71	12.49	2.00	4.33	0.00	0.12	17.44	12.79	3.08	0.10	98.27	6.28	0.18	2.09	0.23	0.51	0.00	0.01	3.69	1.95	0.85	0.02	15.81	87.77	12.23	12.23			
S1915-37	A2	core	43.83	1.89	12.34	1.88	4.25	0.00	0.04	17.43	12.59	2.94	0.06	97.24	6.28	0.20	2.08	0.21	0.51	0.00	0.01	3.72	1.93	0.82	0.01	15.78	87.97	12.03	12.03			
S1915-37	A2	core	44.86	1.65	12.87	1.65	4.31	0.07	18.14	12.78	2.93	0.07	99.34	6.28	0.17	2.12	0.18	0.50	0.01	0.00	3.79	1.92	0.80	0.01	15.79	88.06	11.74	11.74				
S1915-37	A2	core	43.97	1.71	12.38	1.87	4.45	0.02	0.08	17.55	12.45	2.99	0.08	97.56	6.29	0.18	2.09	0.21	0.53	0.00	0.01	3.74	1.91	0.83	0.02	15.80	87					



Table A1k. (continued)

	Min.	Ass.	Spot	SiO <sub>2</sub>	TiO <sub>2</sub>	Al <sub>2</sub> O <sub>3</sub>	Cr <sub>2</sub> O <sub>3</sub>	FeO	MnO	NiO	MgO	CaO	Na <sub>2</sub> O	K <sub>2</sub> O	Total	F.S./23	O	Si	Ti	Al	Cr	Fe <sup>2+</sup>	Mn	Ni	Mg	Ca	Na	K	Total	Mg <sup>0.9</sup> /Mg	Fe <sup>0.9</sup> /Fe + Mg
S1915-37	A2	core	44.34	1.71	12.22	1.88	4.39	0.02	0.00	17.83	3.00	0.09	97.87			6.31	0.18	2.05	0.21	0.52	0.00	0.00	3.78	1.89	0.83	0.02	15.80	87.82	12.13		
S1915-37	A2	core	44.70	1.71	12.15	1.94	4.24	0.00	0.08	17.85	12.73	3.14	0.07	98.61			6.32	0.18	2.03	0.22	0.50	0.00	0.01	3.76	1.93	0.86	0.01	15.82	88.23	11.77	
S1915-37	A2	core	44.70	1.65	12.64	1.73	4.28	0.08		18.02	12.11	2.91	0.08	98.20			6.32	0.18	2.11	0.19	0.51	0.01	0.00	3.80	1.84	0.80	0.01	15.76	88.04	11.73	
S1915-37	A2	core	44.91	1.64	12.74	1.78	4.06	0.04		17.84	12.25	3.20	0.09	98.55			6.33	0.17	2.12	0.20	0.48	0.00	0.00	3.75	1.85	0.87	0.02	15.79	88.58	11.31	
S1915-37	A2	core	44.44	1.66	11.97	1.99	4.39	0.00	0.04	17.72	12.45	2.90	0.08	97.64			6.34	0.18	2.01	0.22	0.52	0.00	0.00	3.77	1.90	0.80	0.02	15.77	87.80	12.19	
S1915-37	A2	core	44.88	1.61	12.60	1.75	4.31	0.06		18.05	11.90	2.90	0.08	98.14			6.34	0.17	2.10	0.20	0.51	0.01	0.00	3.80	1.80	0.79	0.01	15.74	88.04	11.80	
S1915-37	A2	core	44.57	1.57	11.98	1.69	4.24	0.00	0.06	17.87	12.62	2.80	0.06	97.47			6.36	0.17	2.02	0.19	0.51	0.00	0.01	3.80	1.93	0.77	0.01	15.76	88.25	11.75	
S1915-37	A2	core	45.90	1.62	12.46	1.62	4.06	0.00		18.53	12.99	2.52	0.10	99.80			6.37	0.17	2.04	0.18	0.47	0.00	0.00	3.83	1.93	0.68	0.02	15.70	89.04	10.96	
S1915-37	A2	core	44.52	1.56	11.65	1.59	4.32	0.03	0.08	18.04	12.53	2.76	0.07	97.13			6.38	0.17	1.97	0.18	0.52	0.00	0.01	3.85	1.92	0.77	0.01	15.77	88.09	11.83	
S1915-37	A2	core	44.55	1.62	11.67	1.71	4.17	0.12	0.01	17.92	12.43	2.89	0.08	97.16			6.38	0.17	1.97	0.19	0.50	0.01	0.00	3.82	1.91	0.80	0.02	15.78	88.15	11.52	
S1915-37	A2	core	45.02	1.62	11.70	1.29	4.43	0.15	0.11	18.41	12.72	2.63	0.03	98.10			6.38	0.17	1.95	0.14	0.53	0.02	0.01	3.89	1.93	0.72	0.01	15.76	87.74	11.85	
S1915-37	A2	core	45.65	1.49	11.80	1.33	4.23	0.02		19.03	12.78	2.64	0.05	99.02			6.40	0.16	1.95	0.15	0.50	0.00	0.00	3.97	1.92	0.72	0.01	15.76	88.88	11.07	
S1915-37	A2	core	45.46	1.64	11.26	0.93	4.04	0.00	0.03	18.51	12.88	2.68	0.09	97.53			6.46	0.18	1.89	0.10	0.48	0.00	0.00	3.92	1.96	0.74	0.02	15.75	89.09	10.91	
S1915-37	A4	rim	49.85	0.03	8.91	0.00	4.31	0.01	0.01	19.47	13.46	1.24	0.17	97.47			7.00	0.00	1.47	0.00	0.51	0.00	0.00	4.07	2.02	0.34	0.03	15.45	88.93	11.04	
S1915-37	A4	rim	52.92	0.08	5.89	0.04	3.33	0.00	0.00	21.42	13.67	0.81	0.00	98.25			7.30	0.01	0.96	0.00	0.38	0.01	0.00	4.40	2.02	0.22	0.00	15.31	91.78	8.01	
S1915-37	A4	rim	52.95	0.00	5.24	0.09	3.82	0.05	0.02	21.09	13.68	0.79	0.08	97.80			7.36	0.00	0.86	0.01	0.44	0.01	0.00	4.37	2.04	0.21	0.01	15.32	90.68	9.21	
S1915-37	A4	rim	54.66	0.08	4.98	0.02	3.21	0.04		22.67	13.97	0.61	0.03	100.27			7.38	0.01	0.79	0.00	0.36	0.00	0.00	4.56	2.02	0.16	0.00	15.30	92.55	7.35	
S1915-37	A4	rim	54.52	0.03	4.20	0.00	2.75	0.05	0.05	22.05	13.61	0.62	0.07	97.94			7.51	0.00	0.68	0.00	0.32	0.01	0.01	4.53	2.01	0.17	0.01	15.24	93.34	6.54	
S1915-37	A4	rim	56.47	0.00	2.71	0.00	2.80	0.00		22.29	13.32	0.30	0.05	97.94			7.74	0.00	0.44	0.00	0.32	0.00	0.00	4.55	1.96	0.08	0.01	15.09	93.41	6.59	
S1915-40	A4		47.69	0.66	10.28	0.57	3.41	0.00	0.13	19.64	13.11	2.04	0.06	97.60			6.71	0.07	1.70	0.06	0.40	0.00	0.02	4.12	1.98	0.56	0.01	15.62	91.12	8.88	
S1915-40	A4		48.00	0.43	9.80	1.20	4.42	0.05		19.34	12.79	1.88	0.08	97.99			6.75	0.05	1.62	0.13	0.52	0.01	0.00	4.05	1.93	0.51	0.01	15.59	88.52	11.35	
S1915-40	A4		49.89	0.38	8.04	0.89	4.07	0.09		19.68	12.64	1.27	0.07	97.02			7.03	0.04	1.34	0.10	0.48	0.01	0.00	4.13	1.91	0.35	0.01	15.39	89.39	10.37	
S1915-40	A4		52.16	0.49	4.75	0.69	2.81	0.16	0.07	21.03	13.48	1.08	0.04	96.78			7.33	0.05	0.79	0.08	0.33	0.02	0.01	4.40	2.03	0.30	0.01	15.34	92.65	6.95	
S1915-40	A4		56.20	0.04	2.78	0.00	2.07	0.00	0.03	23.24	13.65	0.60	0.00	98.61			7.65	0.00	0.45	0.00	0.24	0.00	0.00	4.71	1.99	0.16	0.00	15.20	95.25	4.75	
S1915-44	A2		43.99	1.25	13.71	1.87	3.97	0.02		17.50	12.16	3.00	0.04	97.51			6.26	0.13	2.30	0.21	0.47	0.00	0.00	3.71	1.85	0.83	0.01	15.77	88.66	11.29	
S1915-44	A2		44.40	1.10	12.92	1.82	4.03	0.00		17.87	12.44	2.91	0.06	97.55			6.32	0.12	2.17	0.20	0.48	0.00	0.00	3.79	1.90	0.80	0.01	15.79	88.77	11.23	
S1915-44	A2		45.66	1.16	12.66	1.94	4.03	0.08		18.47	12.24	2.88	0.10	99.22			6.38	0.12	2.08	0.21	0.47	0.01	0.00	3.84	1.83	0.78	0.02	15.75	88.90	10.88	

<sup>a</sup> Major element compositions are in wt %. Analyses are ordered by increasing sample number and Si content. Min. Ass., mineral assemblage.

**Table A11.** Major Element Compositions of Amphiboles From VLS Ultramafic Mylonites Analyzed by Electron Microprobe: Site S2201<sup>a</sup>

Sample <sup>b</sup>	Spot	SiO <sub>2</sub>	TiO <sub>2</sub>	Al <sub>2</sub> O <sub>3</sub>	Cr <sub>2</sub> O <sub>3</sub>	FeO	MnO	NiO	MgO	CaO	Na <sub>2</sub> O	K <sub>2</sub> O	Total	F.S./23	O	Si	Ti	Al	Cr	Fe <sup>2+</sup>	Mn	Ni	Mg	Ca	Na	K	Total	Mg <sup>0.5</sup> /Mg + Fe	Fe <sup>0.5</sup> /Fe + Mg
S2201-01V	core 46.39	0.16	7.70	0.84	4.57	0.10	0.10	20.06	11.53	2.21	0.05	93.71	6.84	0.02	1.34	0.10	0.56	0.01	0.01	4.41	1.82	0.63	0.01	15.75	88.43	11.31			
S2201-01V	core 48.01	0.17	8.20	0.99	4.68	0.05	0.08	20.16	11.55	2.30	0.03	96.22	6.87	0.02	1.38	0.11	0.56	0.01	0.01	4.30	1.77	0.64	0.01	15.68	88.36	11.52			
S2201-01V	core 46.54	0.19	7.27	0.65	4.51	0.07	0.06	20.51	11.35	2.03	0.04	93.23	6.88	0.02	1.27	0.08	0.56	0.01	0.01	4.52	1.80	0.58	0.01	15.72	88.86	10.97			
S2201-01V	core 46.75	0.12	7.00	0.61	4.45	0.06	0.11	20.63	11.40	1.99	0.04	93.15	6.91	0.01	1.22	0.07	0.55	0.01	0.01	4.55	1.81	0.57	0.01	15.72	89.08	10.79			
S2201-01V	core 47.91	0.10	7.65	0.75	4.29	0.12	0.10	20.59	11.50	2.04	0.04	95.08	6.92	0.01	1.30	0.09	0.52	0.01	0.01	4.43	1.78	0.57	0.01	15.66	89.28	10.43			
S2201-01V	core 48.59	0.12	7.83	0.85	4.33	0.01	0.10	20.30	11.54	2.18	0.04	95.89	6.96	0.01	1.32	0.10	0.52	0.00	0.01	4.33	1.77	0.61	0.01	15.63	89.29	10.69			
S2201-01V	core 47.85	0.15	7.11	0.89	4.63	0.07	0.09	20.02	11.54	1.96	0.04	94.33	6.98	0.02	1.22	0.10	0.56	0.01	0.01	4.35	1.80	0.55	0.01	15.62	88.37	11.46			
S2201-01V	core 50.01	0.15	6.74	0.75	4.08	0.12	0.13	20.96	11.42	1.99	0.03	96.37	7.10	0.02	1.13	0.08	0.48	0.01	0.01	4.43	1.74	0.55	0.01	15.56	89.89	9.82			
S2201-01V	core 50.21	0.15	6.39	0.61	4.34	0.11	0.11	21.19	11.44	1.95	0.04	96.54	7.12	0.02	1.07	0.07	0.51	0.01	0.01	4.48	1.74	0.54	0.01	15.57	89.46	10.28			
S2201-01V	core 50.20	0.16	6.22	0.51	4.40	0.02	0.09	20.90	11.66	1.97	0.02	96.15	7.15	0.02	1.04	0.06	0.52	0.00	0.01	4.43	1.78	0.54	0.00	15.56	89.41	10.55			
S2201-01V	core 50.94	0.10	5.22	0.57	3.88	0.04	0.10	21.59	11.47	1.32	0.03	95.25	7.27	0.01	0.88	0.06	0.46	0.00	0.01	4.60	1.76	0.37	0.00	15.43	90.76	9.15			

<sup>a</sup>Major element compositions are in wt %. Analyses are ordered by increasing sample number and Si content. Min. Ass., mineral assemblage.  
<sup>b</sup>V, amphib in vein.

## Acknowledgments

[79] We are grateful to the Captain, officers, crew, and technicians of R/V *Strakhov* and R/V *Logachev*. M.S. thanks Philippe Recourt (University of Lille) for his valuable help with the SEM. We thank A. von der Handt and an anonymous reviewer for their thoughtful reviews. Work supported by the U.S. National Science Foundation (OCE-03-28217 and OCE-05-51288) and the Italian Consiglio Nazionale delle Ricerche (Progetto Strategico Dorsali). This is LDEO contribution 7292.

## References

- Anders, E., and N. Grevesse (1989), Abundances of the elements: Meteoritic and solar, *Geochim. Cosmochim. Acta*, 53, 197–214, doi:10.1016/0016-7037(89)90286-X.
- Auzende, J. M., D. Bideau, E. Bonatti, M. Cannat, J. Honnorez, Y. Lagabrielle, J. Malavieille, V. Mamaloukas-Frangoulis, and C. Mevel (1989), Direct observation of a section through slow-spreading oceanic crust, *Nature*, 337(6209), 726–729, doi:10.1038/337726a0.
- Bach, W., C. J. Garrido, H. Paulick, J. Harvey, and M. Rosner (2004), Seawater-peridotite interactions: First insights from ODP Leg 209, MAR 15°N, *Geochem. Geophys. Geosyst.*, 5, Q09F26, doi:10.1029/2004GC000744.
- Bence, A. E., and A. L. Albee (1968), Empirical correction factors for the electron microanalyses of silicates and oxides, *J. Geol.*, 76, 382–403.
- Blackman, D. K., J. R. Cann, B. Janssen, and D. K. Smith (1998), Origin of extensional core complexes: Evidence from the Mid-Atlantic Ridge at the Atlantic Fracture Zone, *J. Geophys. Res.*, 103, 21,315–21,333, doi:10.1029/98JB01756.
- Bonatti, E. (1968), Ultramafic rocks from the Mid-Atlantic Ridge, *Nature*, 219, 363–365, doi:10.1038/219363a0.
- Bonatti, E., M. Ligi, D. Brunelli, A. Cipriani, P. Fabretti, V. Ferrante, L. Gasperini, and L. Ottolini (2003), Mantle thermal pulses below the Mid-Atlantic Ridge and temporal variation in the formation of oceanic lithosphere, *Nature*, 423, 499–505, doi:10.1038/nature01594.
- Bonatti, E., D. Brunelli, R. W. Buck, A. Cipriani, P. Fabretti, V. Ferrante, L. Gasperini, and M. Ligi (2005), Flexural uplift of a lithospheric slab near the Vema Transform (central Atlantic): Timing and mechanisms, *Earth Planet. Sci. Lett.*, 240, 642–655, doi:10.1016/j.epsl.2005.10.010.
- Bottazzi, P., L. Ottolini, R. Vannucci, and A. Zanetti (1994), An accurate procedure for the quantification of rare earth elements in silicates, in *IX International Conference on Secondary Ion Mass Spectrometry, Yokohama (Japan)*, Nov. 7–12 (1993), edited by A. Benninghoven et al., pp. 927–930, John Wiley, Chichester, New York.
- Brunelli, D., M. Seyler, A. Cipriani, L. Ottolini, and E. Bonatti (2006), Discontinuous melt extraction and refertilization of mantle peridotites from the Vema Lithospheric Section (Mid-Atlantic Ridge), *J. Petrol.*, 47(4), 745–771, doi:10.1093/petrology/egi092.
- Cande, S. C., and D. Kent (1995), Revised calibration of the geomagnetic polarity timescale for the late Cretaceous and Cenozoic, *J. Geophys. Res.*, 100, 6093–6095, doi:10.1029/94JB03098.
- Cande, S. C., J. L. LaBreque, and W. F. Haxby (1988), Plate kinematics of the south Atlantic, chron C34 to the present, *J. Geophys. Res.*, 93, 13,479–13,492, doi:10.1029/JB093iB11p13479.

- Cannat, M. (1993), Emplacement of mantle rocks in the sea-floor at mid-ocean ridges, *J. Geophys. Res.*, 98, 4163–4172, doi:10.1029/92JB02221.
- Cannat, M., and M. Seyler (1995), Transform tectonics, metamorphic plagioclase and amphibolitization in ultramafic rocks of the Vema transform fault (Atlantic Ocean), *Earth Planet. Sci. Lett.*, 133(3–4), 283–298, doi:10.1016/0012-821X(95)00078-Q.
- Cannat, M., et al. (1995), Thin crust, ultramafic exposures, and rugged faulting patterns at the Mid-Atlantic Ridge (22–24°N), *Geology*, 23, 49–52, doi:10.1130/0091-7613(1995)023<0049:TCUEAR>2.3.CO;2.
- Cannat, M., T. Juteau, and E. Berger (1990), Petrostructural analysis of the Leg 109 serpentinized peridotites, *Proc. Ocean Drill. Program Sci. Results*, 106/109, 47–56, doi:10.2973/odp.proc.sr.106109.118.1990.
- Ceuleneer, G., and M. Cannat (1997), High-temperature ductile deformation of Site 920 peridotites, *Proc. Ocean Drill. Program Sci. Results*, 153, 23–34.
- Cipriani, A., H. K. Brueckner, E. Bonatti, and D. Brunelli (2004), Oceanic crust generated by elusive parents: Sr and Nd isotopes in basalt-peridotite pairs from the Mid-Atlantic ridge, *Geology*, 32, 657–660, doi:10.1130/G20560.1.
- Cipriani, A., E. Bonatti, D. Brunelli, and M. Ligi (2009), 26 million years of mantle upwelling below the Mid-Atlantic Ridge: The Vema Lithospheric Section revisited, *Earth Planet. Sci. Lett.*, 285, 87–95, doi:10.1016/j.epsl.2009.05.046.
- Cordier, P. (2002), Dislocations and slip systems of mantle minerals, in *Plastic Deformation of Minerals and Rocks*, *Rev. Mineral. Geochem.*, vol. 51, edited by S. I. Karato and H. R. Wenk, pp. 137–179, Mineral. Soc. of Am., Washington, D. C.
- Dalrymple, G. B., and M. A. Lanphere (1969), *Potassium-Argon Dating—Principles, Techniques, and Applications to Geochronology*, W. H. Freeman, San Francisco, Calif.
- Dalrymple, G. B., and M. A. Lanphere (1974),  $^{40}\text{Ar}/^{39}\text{Ar}$  age spectra of some undisturbed terrestrial samples, *Geochim. Cosmochim. Acta*, 38, 715–738, doi:10.1016/0016-7037(74)90146-X.
- Dick, H. J. B., W. B. Bryan, and G. Thompson (1981), Low-angle faulting and steady-state emplacement of plutonic rocks at ridge-transform intersections, *Eos Trans. AGU*, 62, 406.
- Dick, H. J. B., et al. (2000), A long in situ section of the lower ocean crust: Results of ODP Leg 176 drilling at the Southwest Indian Ridge, *Earth Planet. Sci. Lett.*, 179, 31–51, doi:10.1016/S0012-821X(00)0102-3.
- Drury, M. R., R. L. M. Vissers, D. Van der Wal, and E. H. Hoogerdijk Strating (1991), Shear localisation in upper mantle peridotites, *Pure Appl. Geophys.*, 137(4), 439–460, doi:10.1007/BF00879044.
- Durham, W. B., C. Goetze, and B. Blake (1977), Plastic flow of oriented single crystals of olivine: 2. Observations and interpretation of the dislocation structures, *J. Geophys. Res.*, 82, 5755–5770, doi:10.1029/JB082i036p05755.
- Eiler, J. M. (2001), Oxygen isotope variations of basaltic lavas and upper mantle rocks, in *Stable Isotope Geochemistry*, *Rev. Mineral. Geochem.*, vol. 43, pp. 319–364, Mineral. Soc. of Am., Washington, D. C., doi:10.2138/gsrmg.43.1.319.
- Ernst, W. G., and J. Liu (1998), Experimental phase-equilibrium study of Al- and Ti-contents of calcic amphibole in MORB—A semiquantitative thermobarometer, *Am. Mineral.*, 83, 952–969.
- Escartín, J., C. Mével, C. J. MacLeod, and A. M. McCaig (2003), Constraints on deformation conditions and the origin of oceanic detachments: The Mid-Atlantic Ridge core complex at 15°45'N, *Geochem. Geophys. Geosyst.*, 4(8), 1067, doi:10.1029/2002GC000472.
- Escartín, J., D. K. Smith, J. R. Cann, H. Schouten, C. H. Langmuir, and S. Escrig (2008), Central role of detachment faults in accretion of slow-spreading oceanic lithosphere, *Nature*, 455, 790–794, doi:10.1038/nature07333.
- Evans, B. W., and B. R. Frost (1975), Chrome spinel in progressive metamorphism—A preliminary analysis, *Geochim. Cosmochim. Acta*, 39, 959–972, doi:10.1016/0016-7037(75)90041-1.
- Evans, W. E. (1982), Amphiboles in metamorphosed ultramafic rocks, in *Amphiboles: Petrology and Experimental Phase Relations*, *Rev. Mineral.*, vol. 9B, edited by D. R. Veblen and P. H. Ribbe, pp. 98–112, Mineral. Soc. of Am., Washington, D. C.
- Fleck, R. J., J. F. Sutter, and D. H. Elliot (1977), Interpretation of discordant  $^{40}\text{Ar}/^{39}\text{Ar}$  age-spectra of Mesozoic tholeiites from Antarctica, *Geochim. Cosmochim. Acta*, 41, 15–32, doi:10.1016/0016-7037(77)90184-3.
- Früh-Green, G. L., D. S. Kelley, S. M. Bernasconi, J. A. Karson, K. A. Ludwig, D. A. Butterfield, C. Boschi, and G. Proskurowski (2003), 30,000 years of hydrothermal activity at the Lost City vent field, *Science*, 301, 495–498.
- Gilbert, M. C., R. T. Helz, R. K. Popp, and F. S. Spear (1982), Experimental studies of amphibole stability, in *Amphiboles: Petrology and Experimental Phase Relations*, *Rev. Mineral. Geochim.*, vol. 9B, pp. 229–354, Mineral. Soc. of Am., Washington, D. C.
- Gregory, R. T., and H. P. Taylor (1981), An oxygen isotope profile in a section of Cretaceous oceanic crust, Samail ophiolite, Oman: Evidence for  $\delta^{18}\text{O}$  buffering of oceans by deep (>5 km) seawater–hydrothermal circulation at mid-ocean ridges, *J. Geophys. Res.*, 86, 2737–2755, doi:10.1029/JB086iB04p02737.
- Harmon, R. S., and J. Hoefs (1995), Oxygen isotope heterogeneity of the mantle deduced from global  $^{18}\text{O}$  systematics of basalts from different geotectonic settings, *Contrib. Mineral. Petrol.*, 120, 95–114, doi:10.1007/BF00311010.
- Hellebrand, E., E. J. Snow, H. J. B. Dick, and A. W. Hofman (2001), Coupled major and trace element melting indicators in mid-ocean ridge peridotites, *Nature*, 410, 677–681, doi:10.1038/35070546.
- Hobbs, B. E., H. B. Muhlhaus, and A. Ord (1990), Instability, softening and localization of deformation, in *Deformation Mechanisms, Rheology, and Tectonics*, edited by R. Knipe and E. H. Rutter, *Geol. Soc. Spec. Publ.*, 54, 143–165.
- Honnorez, J., C. Mevel, and R. Montigny (1984), Geotectonic significance of gneissic amphibolites from the Vema Fracture Zone, equatorial Mid-Atlantic Ridge, *J. Geophys. Res.*, 89(B13), 11,379–11,400, doi:10.1029/JB089iB13p11379.
- Hoogerdijk Strating, E. H., E. Rampone, G. B. Piccardo, M. R. Drury, and R. L. M. Vissers (1993), Subsolidus emplacement of mantle peridotites during incipient oceanic rifting and opening of the Mesozoic Tethys (Voltri Massif, NW Italy), *J. Petrol.*, 34(5), 901–927.
- Ildefonse, B., D. K. Blackman, B. E. John, Y. Ohara, D. J. Miller, C. J. Macleod, and IODP Expeditions 304/305 Science Party (2007), Oceanic core complexes and crustal accretion at slow-spreading ridges, *Geology*, 35, 623–625, doi:10.1130/G23531A.1.
- Jaroslav, G. E., G. Hirth, and H. J. B. Dick (1996), Abyssal peridotite mylonites: Implications for grain-size sensitive flow and strain localization in the oceanic lithosphere, *Tectonophysics*, 256(1–4), 17–37, doi:10.1016/0040-1951(95)00163-8.
- Johnson, K. T. M., H. J. B. Dick, and N. Shimizu (1990), Melting in the oceanic upper mantle: An ion microprobe

- study of diopsides in abyssal peridotites, *J. Geophys. Res.*, 95, 2661–2678, doi:10.1029/JB095iB03p02661.
- Kappel, E. S., and W. B. E. Ryan (1986), Volcanic episodicity and a non-steady state rift valley along northeast Pacific spreading centers: Evidence from Sea MARC 1, *J. Geophys. Res.*, 91, 13,925–13,940, doi:10.1029/JB091iB14p13925.
- Karato, S. I., M. S. Paterson, and J. D. Fitzgerald (1986), Rheology of synthetic olivine aggregates: Influence of grain size and water, *J. Geophys. Res.*, 91, 8151–8176, doi:10.1029/JB091iB08p08151.
- Karson, J. (1999), Geological investigation of a lineated massif at the Kane Transform: Implications for oceanic core complexes, *Philos. Trans. R. Soc. London, Ser. A*, 357, 713–740, doi:10.1098/rsta.1999.0350.
- Kelemen, P. B., E. Kikawa, D. J. Miller, and the Shipboard Scientific Party (2004), *Proceedings of the Ocean Drilling Program, Initial Reports*, vol. 209, Ocean Drill. Program, College Station, Tex., doi:10.2973/odp.proc.ir.209.2004.
- Kelemen, P. B., E. Kikawa, D. J. Miller, and the Shipboard Scientific Party (2007), Leg 209 summary: Processes in a 20-km-thick conductive boundary layer beneath the Mid-Atlantic Ridge, 14°–16°N, *Proc. Ocean Drill. Program Sci. Results*, 209, 1–33, doi:10.2973/odp.proc.sr.209.001.2007.
- Kohlstedt, D. L., B. Evans, and S. J. Mackwell (1995), Strength of the lithosphere: Constraints imposed by laboratory experiments, *J. Geophys. Res.*, 100, 17,587–17,602, doi:10.1029/95JB01460.
- Lacan, F., and C. Jeandel (2004), Neodymium isotopic composition and rare earth element concentrations in the deep and intermediate Nordic Seas: Constraints on the Iceland–Scotland Overflow Water signature, *Geochem. Geophys. Geosyst.*, 5(11), Q11006, doi:10.1029/2004GC000742.
- Leake, B. E., et al. (1997), Nomenclature of amphiboles: Report of the Subcommittee on Amphiboles of the International Mineralogical Commission on New Minerals and Mineral Names, *Mineral. Mag.*, 61, 295–321, doi:10.1180/minmag.1997.061.405.13.
- Lissenberg, C. J., M. Rioux, S. Nobumichi, S. A. Bowring, and C. Mevel (2009), Zircon dating of oceanic crustal accretion, *Science*, 323, 1048–1050, doi:10.1126/science.1167330.
- Mattey, D., D. Lowry, and C. Macpherson (1994), Oxygen isotope composition of mantle peridotite, *Earth Planet. Sci. Lett.*, 128, 231–241, doi:10.1016/0012-821X(94)90147-3.
- Newman, J., W. M. Lamb, M. R. Drury, and R. L. M. Vissers (1999), Deformation processes in a peridotite shear zone: Reaction-softening by an H<sub>2</sub>O-deficient, continuous net transfer reaction, *Tectonophysics*, 303(1–4), 193–222.
- Nicolas, A., F. Boudier, and A. Meshi (1999), Slow-spreading accretion and mantle denudation in the Mirdita ophiolite (Albania), *J. Geophys. Res.*, 104(B7), 15,155–15,168, doi:10.1029/1999JB900126.
- Nimis, P., and W. R. Taylor (2000), Single clinopyroxene thermobarometry for garnet peridotites. Part I. Calibration and testing of a Cr-in-Cpx barometer and an enstatite-in-Cpx thermometer, *Contrib. Mineral. Petrol.*, 139, 541–544, doi:10.1007/s004100000156.
- Pockalny, R. A., R. S. Detrick, and P. J. Fox (1988), Morphology and tectonics of the Kane Transform from SeaBeam bathymetry data, *J. Geophys. Res.*, 93(B4), 3179–3193, doi:10.1029/JB093iB04p03179.
- Salter, V. J. M., and H. J. B. Dick (2002), Mineralogy of the mid-ocean-ridge basalt source from neodymium isotopic composition of abyssal peridotites, *Nature*, 418, 68–72, doi:10.1038/nature00798.
- Scribano, V., M. Viccaro, R. Cristofolini, and L. Ottolini (2009), Metasomatic events recorded in ultramafic xenoliths from the Hyblean area (southeastern Sicily, Italy), *Mineral. Petrol.*, 95, 235–250, doi:10.1007/s00710-008-0031-4.
- Sharp, Z. D. (1990), A laser-based microanalytical method for the in situ determination of oxygen isotope ratios of silicates and oxides, *Geochim. Cosmochim. Acta*, 54, 1353–1357, doi:10.1016/0016-7037(90)90160-M.
- Sharp, Z. D. (1995), Oxygen isotope geochemistry of the Al<sub>2</sub>SiO<sub>5</sub> polymorphs, *Am. J. Sci.*, 295, 1058–1076.
- Shaw, W. J., and J. Lin (1996), Models of ocean ridge lithospheric deformation: Dependence on crustal thickness, spreading rate, and segmentation, *J. Geophys. Res.*, 101(B8), 17,977–17,993, doi:10.1029/96JB00949.
- Shimizu, N., M. P. Semet, and C. J. Allegre (1978), Geochemical applications of quantitative ion-microprobe analyses, *Geochim. Cosmochim. Acta*, 42, 1321–1334, doi:10.1016/0016-7037(78)90037-6.
- Smith, D. K., J. Cann, and J. Escartín (2006), Widespread active detachment faulting and core complex formation near 13°N at the Mid-Atlantic Ridge, *Nature*, 442, 440–443, doi:10.1038/nature04950.
- Smith, D. K., J. Escartín, H. Schouten, and J. Cann (2008), Fault rotation and core complex formation: Significant processes in seafloor formation at slow spreading mid-ocean ridges, *Geochim. Geophys. Geosyst.*, 9, Q03003, doi:10.1029/2007GC001699.
- Snow, J. E., S. R. Hart, and H. J. B. Dick (1993), Orphan Sr-87 in abyssal peridotites—Daddy was a granite, *Science*, 262, 1861–1863, doi:10.1126/science.262.5141.1861.
- Snow, J. E., S. R. Hart, and H. J. B. Dick (1994), Nd and Sr isotope evidence linking mid-ocean-ridge basalts and abyssal peridotites, *Nature*, 371, 57–60, doi:10.1038/371057a0.
- Spear, F. S. (1993), *Metamorphic Phase Equilibria and Pressure-Temperature-Time Paths*, Mineral. Soc. of Am., Washington, D. C.
- Talbi, E. L. H., J. Honnorez, N. Clauer, F. Gauthier-Lafaye, and P. Stille (1999), Petrology, isotope geochemistry and chemical budgets of oceanic gabbros-seawater interactions in the equatorial Atlantic, *Contrib. Mineral. Petrol.*, 137(3), 246–266, doi:10.1007/s004100050549.
- Taylor, W. R. (1998), An experimental test of some geothermometer and geobarometer formulations for upper mantle peridotites with application to the thermobarometry of fertile lherzolite and garnet websterite, *Neues Jahrb. Mineral. Abh.*, 172, 381–408.
- Tribuzio, R., M. F. Thirlwall, and B. Messiga (1999), Petrology, mineral and isotope geochemistry of the Sondalo gabbroic complex (central Alps, northern Italy): Implications for the origin of post-Variscan magmatism, *Contrib. Mineral. Petrol.*, 136, 48–62, doi:10.1007/s004100050523.
- Tucholke, B. E., and J. Lin (1994), A geological model for the structure of ridge segments in slow-spreading ocean crust, *J. Geophys. Res.*, 99(B6), 11,937–11,958.
- Tucholke, B. E., J. Lin, M. C. Kleinrock, and M. A. Tivey (1997), Segmentation and crustal structure of the western Mid-Atlantic Ridge flank, 12°25'–27°10' and 0–29 m.y., *J. Geophys. Res.*, 102, 10,203–10,223, doi:10.1029/96JB03896.
- Tucholke, B. E., J. Lin, and M. C. Kleinrock (1998), Megamullions and mullion structure defining oceanic metamorphic core complexes on the Mid-Atlantic Ridge, *J. Geophys. Res.*, 103, 9857–9866, doi:10.1029/98JB00167.
- Tucholke, B. E., M. D. Behn, W. R. Buck, and J. Lin (2008), Role of melt supply in oceanic detachment faulting and formation of megamullions, *Geology*, 36(6), 455–458.
- Turpin, B. D., R. L. Christiansen, M. A. Clyne, D. E. Champion, W. J. Gerstel, L. J. P. Muffler, and D. A. Trimble (1998),

Age of Lassen Peak, California, and implications for the ages of late Pleistocene glaciations in the southern Cascade Range, *Geol. Soc. Am. Bull.*, 110, 931–945, doi:10.1130/0016-7606(1998)110<0931:AOLPCA>2.3.CO;2.

Turpin, B. D., L. J. P. Muffler, M. A. Clyne, and D. E. Champion (2007), Robust  $24 \pm 6$  ka  $^{40}\text{Ar}/^{39}\text{Ar}$  age of a low-potassium tholeiitic basalt in the Lassen region of NE California, *Quat. Res.*, 68(1), 96–110.

Vissers, R. L. M., M. R. Drury, E. H. Hoogerduijn Strating, and D. Van der Wal (1991), Shear zones in the upper mantle: A case study in an Alpine type lherzolite massif, *Geology*, 19, 990–993, doi:10.1130/0091-7613(1991)019<0990:SZITUM>2.3.CO;2.

Wells, P. R. A. (1977), Pyroxene thermometry in simple and complex systems, *Contrib. Mineral. Petrol.*, 62, 129–139, doi:10.1007/BF00372872.